Monitoring tuberculosis treatment response using molecular techniques

Eoghan Farmer

A thesis submitted for the degree of PhD
at the
University of St Andrews

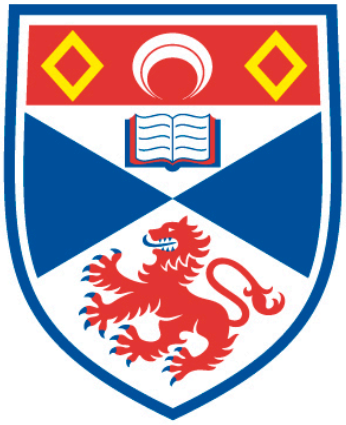

2019

Identifier to use to cite or link to this thesis:
DOI: https://doi.org/10.17630/sta/138

Candidate's declaration

I, Eoghan Farmer, do hereby certify that this thesis, submitted for the degree of MD, which is approximately 33,000 words in length, has been written by me, and that it is the record of work carried out by me, or principally by myself in collaboration with others as acknowledged, and that it has not been submitted in any previous application for any degree.

I was admitted as a research student at the University of St Andrews in August 2013.

I received funding from an organisation or institution and have acknowledged the funder(s) in the full text of my thesis.

Date Signature of candidate

Supervisor's declaration

I hereby certify that the candidate has fulfilled the conditions of the Resolution and Regulations appropriate for the degree of MD in the University of St Andrews and that the candidate is qualified to submit this thesis in application for that degree.

Date Signature of supervisor

Permission for publication

In submitting this thesis to the University of St Andrews we understand that we are giving permission for it to be made available for use in accordance with the regulations of the University Library for the time being in force, subject to any copyright vested in the work not being affected thereby. We also understand, unless exempt by an award of an embargo as requested below, that the title and the abstract will be published, and that a copy of the work may be made and supplied to any bona fide library or research worker, that this thesis will be electronically accessible for personal or research use and that the library has the right to migrate this thesis into new electronic forms as required to ensure continued access to the thesis.

I, Eoghan Farmer, confirm that my thesis does not contain any third-party material that requires copyright clearance.

The following is an agreed request by candidate and supervisor regarding the publication of this thesis:

Printed copy

Embargo on all of print copy for a period of 2 years on the following ground(s):

- Publication would preclude future publication

Supporting statement for printed embargo request

Primer sequences remain unpublished

Electronic copy

Embargo on all of electronic copy for a period of 2 years on the following ground(s):

- Publication would preclude future publication

Supporting statement for electronic embargo request

primer sequences remain unpublished

Title and Abstract

- I agree to the title and abstract being published.

Date Signature of candidate

Date Signature of supervisor

Underpinning Research Data or Digital Outputs

Candidate's declaration

I, Eoghan Farmer, hereby certify that no requirements to deposit original research data or digital outputs apply to this thesis and that, where appropriate, secondary data used have been referenced in the full text of my thesis.

Date Signature of candidate

ABSTRACT

This study looks to monitor tuberculosis treatment response using molecular techniques. An assay for the detection and enumeration of *Mycobacterium tuberculosis* already existed in the form of the Mycobacterial Load Assay (MBL). This utilised reverse transcriptase quantitative polymerase chain reaction (RT-qPCR) to detect *M. tuberculosis* 16S ribosomal RNA (rRNA) and thereby quantify bacillary loads in patient sputa. By measuring labile RNA the assay was thought to only measure viable bacilli.

However, unpublished data from the Gillespie lab suggested that 16S rRNA remains stable even once cell are non-viable. Two new markers were sought to represent the viable bacilli: *M. tuberculosis* precursor 16S rRNA (pre-16S rRNA) and transfer-messenger RNA (tm-RNA).

Both of these novel biomarkers were chosen because of their complex secondary structures giving them increased stability allowing for their detection in adverse environments.

Development and of a multiplex assay using the same messenger RNA (mRNA) *phyB* internal control utilised by the MBL assay, then the fielding testing of these multiplex assays was performed with the subsequent failure of the *phyB* control.

The internal control was then redesigned to be more robust and reproducible utilising a novel *M. marinum* control. The new multiplex assays with 16S rRNA, pre-16S rRNA and tm-RNA with the *M. marinum* internal control were then tested on 520 patient samples to demonstrate that the assays could be used for monitoring treatment response.

ACKNOWLEDGEMENTS

I would like to acknowledge the University of St Andrews for allowing me to undertake this degree.

I cannot thank my supervisor Professor Stephen H Gillespie enough. First, for giving me this opportunity and then for the unending support to allow the completion of this thesis.

I would like to thank the Gillespie lab: Dr Wilber Sabitii, Dr Katarina Oravcova, Dr Han Xiao, Dr Ruth Bowness, Dr Robert Hammond, Mr Vincent Baron, Mr John Kennedy, Mr Prince Agyirey-Kwakye and Mrs Souad Alateah.

Also, the whole team at KCRI but particularly Mr Davis Kuchaka whom I worked closely with and taught me a little Tanzanian culture.

LIST OF ABBREVIATIONS

AUC	Area under the curve
BCG	Bacillus Calmette–Guérin
BMRC	British Medical Research Council
BTS	British Thoracic Society
CL3	Containment level 3
Ct	Cycle threshold
DNA	Deoxyribonucleic acid
E	Ethambutol
EDCTP	European & Developing Countries Clinical Trials Partnership
GTC	Guanidine thiocyanate
H	Isoniazid
HIV	Human immunodeficiency virus
IC	Internal control
LJ	Löwenstein–Jensen Medium
LAM	Lipoarabinomannan
KCRI	Kilimanjaro Christian Research Institute
MAMS-TB-01	A multiple arm, multiple stage (MAMS), phase 2, open label, randomized, controlled clinical trial to evaluate four treatment

	regimens including SQ109, two increased doses of rifampicin, and moxifloxacin in adult subjects with newly diagnosed, smear positive pulmonary tuberculosis
MBL	Mycobacterial Load
MGIT	Mycobacterial Growth Indicator tube
MIC	Minimum Inhibitory Concentration
PanACEA	Pan-African Consortium for the Evaluation of Anti-tuberculosis Antibiotics
PanBiome	Pan-African Consortium for the Evaluation of Anti-tuberculosis Antibiotics Biomarker Extension
PBS	Phosphate buffered saline
PD	Pharmacodynamics
PK	Pharmacokinetics
Pre-16S	Precursor 16S
R	Rifampicin
RNA	Ribonucleic acid
RT	Reverse transcriptase
RT-qPCR	Real time quantitative polymerase chain reaction
S	Streptomycin
TB	Tuberculosis

Tm-RNA	Transfer messenger RNA
USPHS	United States Public Health Service
WHO	World Health Organisation
Z	Pyrazinamide

1. Chapter 1: General Introduction

1.1 Introduction

Tuberculosis research has changed over the last two decades since the World Health Organisation, WHO, declared the disease a global health emergency (Ma et al. 2010). There has been a vast increase in drug discovery; meaning there are now a large number of lead compounds awaiting drug development and clinical trials (Zumla et al. 2013). At present, this is a very expensive process costing hundreds of millions of pounds per compound (Ma et al. 2010). This is in part because the currently used endpoints of clinical trials are infrequent and occur up to two years after the initiation of treatment. Therefore trials must last a minimum of two years and are required to enroll large numbers of patients in order to be sufficiently powered. Now, the search is for surrogate endpoints for clinical trials and in particular biomarkers.

A biomarker is a measure of a physiological or pathological response to therapy. This means, simply, that they would allow treatment response to be monitored. In some cases, such as plasma HIV RNA, the biomarker has such a strong predictive value that it can replace the clinical outcomes in trials and becomes a surrogate endpoint (O'Brien et al. 1996; O'Brien et al. 1997; Murray et al. 1999). If this can be achieved for tuberculosis then drug development can be hastened and money and manpower can be saved. This is not the only use of biomarkers. They can provide information about disease progression, risk of treatment failure or toxicity. The purpose of this MD is to evaluate and investigate potential molecular biomarkers for the detection and enumeration of *Mycobacterium tuberculosis* in the context of clinical trials and clinical practice.

1.2 Tuberculosis

1.2.1 History

Tuberculosis has been present throughout recorded history and it has likely afflicted humanity since pre-history. Characteristic osteological lesions of tuberculosis and *M. tuberculosis* DNA have been found in remains in the Eastern Mediterranean from up to 9,000 years ago (Hershkovitz et al. 2008). Indeed, it is likely the disease has existed for far longer. Molecular phylogenetics puts forward that an early progenitor may have infected hominids three million years ago (Gutierrez et al. 2005).

Our current understanding of tuberculosis began in the late 19th Century. In 1865, Jean-Antoine Villemin demonstrated the infectious nature of tuberculosis by inoculating a healthy rabbit with ‘‘a small amount of purulent liquid from a tuberculous cavity’’ and then found lesions of tuberculosis on autopsy (Daniel 2015). This was swiftly followed by Koch’s seminal work: ‘Die Aetiologie der Tuberculose’, presented to the Berlin Physiological Society in 1882 (Sakula 1979). This revealed that mycobacteria were the causative agent for tuberculosis. He went on to receive the Noble Prize for his work on tuberculosis, cholera and microbial pathogenesis. After these discoveries tuberculosis began to decline, a full century before the development of chemotherapy and decades before the sanatorium(Grigg 1958).

The introduction of successful combinational chemotherapy in the 1940s saw a further and more rapid decline in tuberculosis rates with hopes in the early 1980s that tuberculosis could be eradicated. Inopportunely, the combination of the rise of HIV, drug resistance and a lack of additional research saw an upsurge in incidence. This led the WHO in 1993 to declare tuberculosis a global health emergency. Although, the upsurge has since been reversed; drug resistant strains continue to become more prevalent.

1.2.2 Epidemiology

1.2.2.1 World

There has been significant progress in reducing the global burden of tuberculosis since 1993 when there were an estimated 7-8 million cases and 1.3-1.6 million TB deaths per year. The prevalence has declined and continues by 2.2% between 2011 and 2012. Despite this the mortality remains high with an estimated 1 million lives lost annually, making it the most important infectious cause of death. Incidence is estimated to be 10.3 million, a relative decline per population(World Health Organization 2016). Despite these developments multidrug resistant and extensively drug resistant strains are on the rise worldwide. This puts added urgency on the development of new therapeutics.

1.2.2.2 UK

The incidence in Scotland is low; the Enhanced Surveillance of Mycobacterial Infections reported 315 cases of TB with an incidence of 5.9 cases per 100,000 population (95% CI 0.7-0.8)" in 2015. (Scotland 2016) The UK incidence is more than 15 times higher estimated to be around 45.4 per 100,000. This is primarily accounted for by the higher prevalence in London. Mortality from tuberculosis is 0.46 per 100,000.

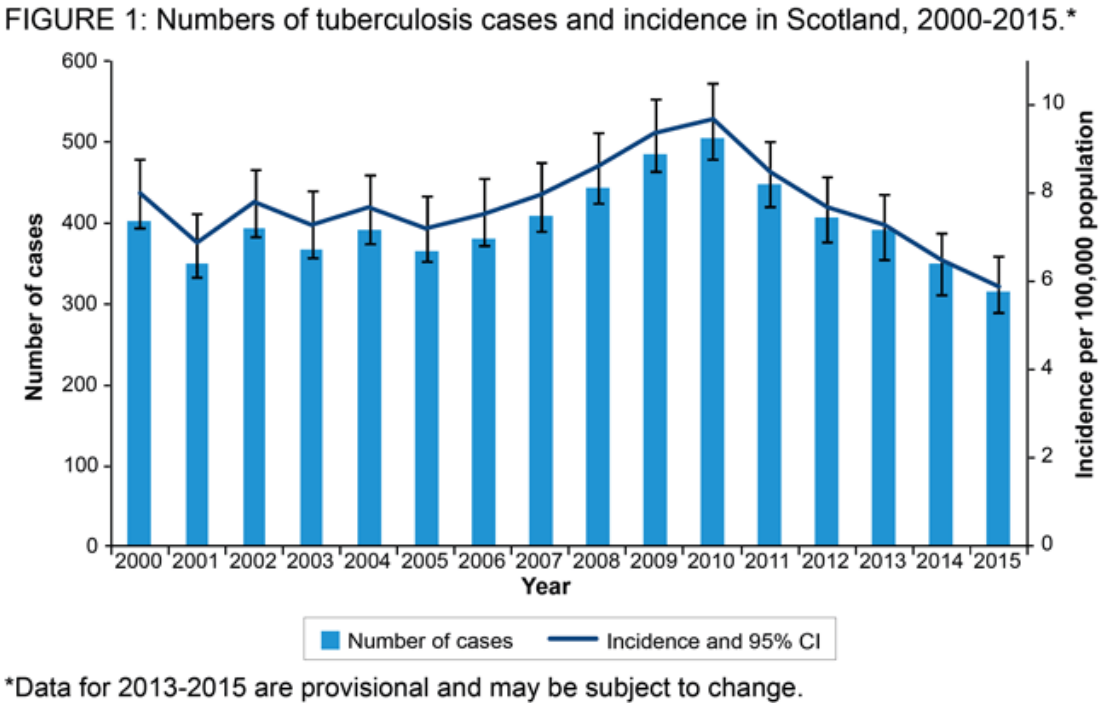

Figure 1.1: Numbers of tuberculosis cases and incidence in Scotland, 2000-2015

1.2.2.3 Tanzania

Tanzania is one of the 16 high prevalence countries for TB. The incidence in 2014 was 327 per 100,000 per population. Mortality is 100 times higher than UK at 53 (World Health Organization 2016).

1.2.3 Taxonomy

The causative organisms of tuberculosis are members of the genus *Mycobacteriaceae*. *Mycobacteria* belong to the phylum *Actinobacteria* that includes genus such as *Streptomyces* and *Corynebacterium*. The name *Mycobacterium* derives from the Greek meaning 'fungus-bacterium' alluding to the characteristic fungus-like pellicle found in liquid cultures. The first recording of the genus *Mycobacterium* was in an "Atlas of Bacteriology" and contained two members: *Mycobacterium leprae* observed by Hansen in 1874 and *M. tuberculosis* by Koch in 1882 (Forbes 2017). In 1898, Smith divided Koch's bacillus into human and bovine types based upon slight but consistent cultural differences (Smith 1898). A third member was added in 1946, the vole bacillus, by Wells (WELLS 1949). These are named *M. tuberculosis, M. bovis and M. microtti* respectively. They were thought of as three separate species; however, based on both antigenic structure and whole genome sequencing, they are likely to be a heterogeneous

species with *M. africanumi* (Tortoli 2012). The term *M. tuberculosis* complex is often used to negate this issue. There are now recognised to be greater than 170 differing species of *Mycobacteria*. The increase in the number of species is down to the discriminatory power of whole genome sequencing to that of culture traits and phenotypic analysis (Forbes 2017).

1.2.4 Microbiology

Mycobacteria are fastidious, aerobic, rod-shaped bacteria with thick mycolic acid cell walls, making them resistant to gram staining and resilient to both acid and alcohol. This property is utilised when staining with auramine or hot carbolfuchsin pigments as they are not discoloured by acid-alcohol solvents. Mycobacteria are slow growing organisms taking 1-6 weeks to grow on solid media. The methodology used for identifying mycobacteria has changed very little since the time of Koch. Growth is on a selective media such as Löwenstein–Jensen (LJ) medium which contains malachite green in order to inhibit more rapidly growing organisms. *M. tuberculosis* is a readily transmissible pathogen capable of causing severe and debilitating disease and as such must be handled in a laboratory containment level 3 (CL3).

1.2.5 Pathogenesis

Tuberculosis transmission usually occurs through the inhalation of droplet nuclei; about 5um across containing 1-3 tubercle bacilli. Ten to two hundred of these droplets must reach the alveoli for infection to take place. It is estimated that only 30%-50% of people with heavy exposure to tuberculosis will become infected (RATCLIFFE & MERRICK 1957).

Figure 1.2: Droplet nuclei generated by sneezing, coughing and talking from the CDC website

Initially, bacilli lodge in the lung and are taken up by alveolar macrophages leading to a small focus of inflammation causing recruitment of lymphocytes and monocytes(Philips & Ernst 2012). Many host cells can phagocytose *M. tuberculosis* including dendritic cells, monocytes and lymphocytes; however, they are primarily engulfed by alveolar macrophages(Philips & Ernst 2012; Ernst 2012). The cells aggregate around the infected macrophage and forms the sine qua non of tuberculosis; the granuloma. This pathological hallmark is very heterogeneous; it ranges from cellular to caseous to fibrotic and can even vary within an individual (Lenaerts et al. 2015). When this process occurs in the lung it is known as a Ghon focus. Subsequently, regional lymphadenopathy develops as the bacilli are carried by the lymphatics and this is known as the primary Ghon complex. The overall pathological process is known as primary tuberculosis and is often asymptomatic; and in 95% of cases heals but may

calcify. In 5% of cases the bacilli spread either locally or haematogenously leading to disease.

Post-primary or secondary tuberculosis involves the reactivation of tuberculosis years after the initial infective episode. It is thought that 80% of clinical disease is secondary tuberculosis (de Steenwinkel, de Knegt, et al. 2013). Whether this is a separate pathological process or reinfection is widely debated and as yet there is no consensus.

1.2.6 Signs & Symptoms

The clinical presentation of tuberculosis is dependent on the organ affected. Tuberculosis is classically divided into two forms: pulmonary tuberculosis and the heterogeneous extra-pulmonary tuberculosis. In 2014 in the UK there were 3000 cases of extra-pulmonary and 3500 of pulmonary. The presentations of pulmonary tuberculosis the most common form of tuberculosis is outlined in brief below.

1.2.7 Pulmonary Tuberculosis

Tuberculosis presents with the usual tetrad of: fever, night sweats, anorexia and weight loss. Cough is typical of pulmonary tuberculosis and is often productive; it may be purulent or blood streaked. A minority of patients produce minimal sputum and paediatric patients rarely expectorate as they tend to swallow their sputum. On examination there may be cachexia or localising signs- bronchial breathing, dullness to percussion or crepitations. Chest X-ray can reveal a number of changes consistent with the diagnosis of active TB. These range form: consolidation, cavities, nodules, lymph nodes, military nodules and pleural effusions. Clinical diagnosis hangs upon the sub-acute time course and risk of exposure.

1.2.8 Diagnosis

Positive microbiological culture is the gold standard for the diagnosis of tuberculosis. The advantage of smear microscopy is that it is cheap, rapid and widely available. The disadvantage is the low sensitivity, requiring 10,000 cells per ml. In the past solid culture, typically on LJ slants, was the norm; however, liquid culture is becoming more common. These utilise either radiometric or fluorometric methods to detect respiration through changes in CO_2 or O_2 in the headspace above liquid cultures. In comparison to microscopy, culture is a slower methodology and can take over a month to reveal a positive result. This leads to delay in diagnosis and subsequent initiation of treatment.

Most guidelines recommend acquiring multiple samples for culture in order to successfully grow *M. tuberculosis*. This can prove difficult, particularly in children, therefore expectoration can be induced or more invasive procedures such as broncho-alveolar lavage or gastric lavage may be performed.

Extra-pulmonary biopsies can be taken from the affected site and this can be sent for culture or to histology for staining. Differing imaging modalities can demonstrate the typical changes of tuberculosis and all patients with suspected tuberculosis should have a chest X-ray.

1.2.9 Treatment

Standard treatment consists of four oral medications: rifampicin (R), isoniazid (H), pyrazinamide (Z) and ethambutol (E). There are two phases of treatment; the initial or intensive phase where all four drugs are given, usually lasting two months. Then the continuation phase where only rifampicin and isoniazid continue for a further 4 months. This is abbreviated to 2RHZE/4RH or 2RHZS/4RH. It has been found to successfully treat 95% of drug sensitive patients. In clinical practice the success rate is lower with around 90% if new cases in the UK and close to 85% of cases in Tanzania successfully treated.

1.2.10Monitoring Chemotherapy

The WHO has published guidelines on monitoring tuberculosis chemotherapy. These along with the British Thoracic Society and American Thoracic Society suggest that patients should be followed up for the six months of treatment and define treatment outcomes below (World Health Organization 2010).

Table 4.1 DEFINITIONS OF TREATMENT OUTCOMES[a]

Outcome	Definition
Cure	A patient whose sputum smear or culture was positive at the beginning of the treatment but who was smear- or culture-negative in the last month of treatment and on at least one previous occasion.
Treatment completed	A patient who completed treatment but who does not have a negative sputum smear or culture result in the last month of treatment and on at least one previous occasion[b]
Treatment failure	A patient whose sputum smear or culture is positive at 5 months or later during treatment. Also included in this definition are patients found to harbour a multidrug-resistant (MDR) strain at any point of time during the treatment, whether they are smear-negative or -positive.
Died	A patient who dies for any reason during the course of treatment.
Default	A patient whose treatment was interrupted for 2 consecutive months or more.
Transfer out	A patient who has been transferred to another recording and reporting unit and whose treatment outcome is unknown.
Treatment success	A sum of cured and completed treatment[c]

[a] These definitions apply to pulmonary smear-positive and smear-negative patients, and to patients with extrapulmonary disease. Outcomes in these patients need to be evaluated separately.
[b] The sputum examination may not have been done or the results may not be available.
[c] For smear- or culture-positive patients only.

Figure 1.3: WHO Definitions of Treatment Outcomes

The notable exception is relapse which is defined as a previously declared patient cured or having completed treatment and is diagnosed with bacteriologically positive (sputum smear or culture).

1.2.10.1 Regimen Development

According to the World Health Organisation (WHO), the current tuberculosis treatment has a "strong evidence base" (World Health Organization 2016). This evidence is founded on a series of clinical trials produced by two separate research groups: the British Medical Research Council (BMRC) and the United States Public Health Service (USPHS). These were supplemented by a number of other trials in the literature, particularly from the British Thoracic Society (BTS).

In 1948, the BMRC's first controlled trial on tuberculosis meningitis was published (Anon 1948). The paper claimed a 33% reduction in mortality with streptomycin. Later

that year, a second paper, often quoted as the first ever randomised controlled trial was published on the effect of streptomycin on pulmonary tuberculosis in addition to bed rest (Fox et al. 1954). Initially it was thought to be a success, as it demonstrated the ability of streptomycin to reduce the bacillary burden and six month mortality. However, at the end of the five year follow up, the streptomycin arm was found to have the same mortality as the control arm, due mainly to the emergence of drug resistance (Fox et al. 1999). To overcome the resistance problem, the BMRC went on to explore combination therapy with para-aminosalicylic acid, isoniazid and thiocetazone as well as isoniazid monotherapy and in the process revolutionised tuberculosis treatment. A comprehensive review of the BMRC trials has been published(Grosset 1980; Grosset 1978). Although cure rates at the time were high in comparison with previous standard of care, which was bed-rest, compliance was low. Most regimens lasted 9-24 months, which meant there was a perceived need to reduce treatment duration.

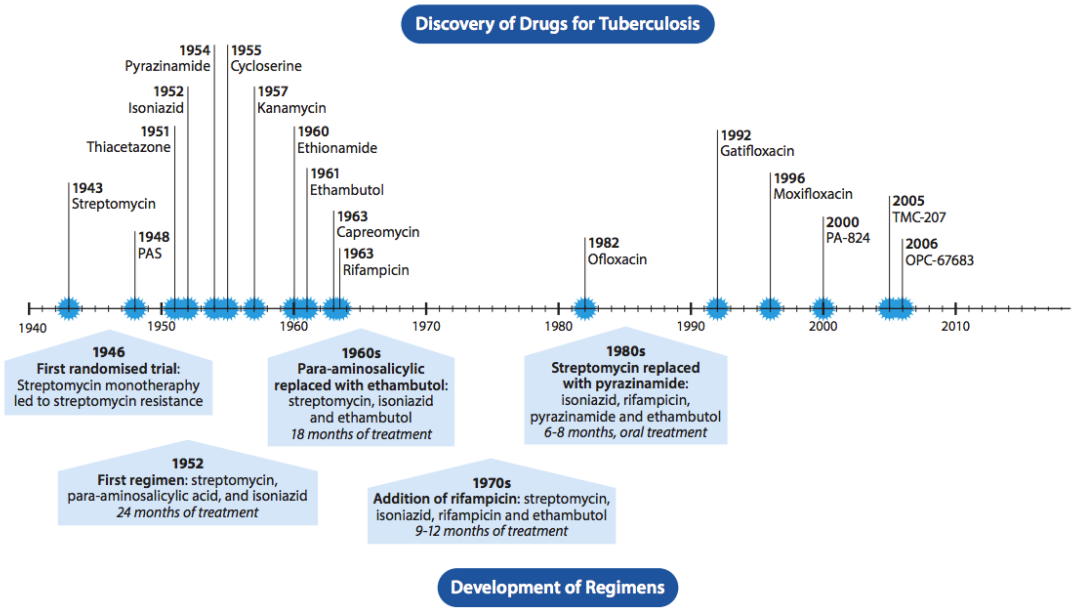

Figure 1.4: Time line of tuberculosis drug discovery from the initial isolation of streptomycin detailing the emergence of multidrug regimens

1.3 Rifampicin

Rifampicin is a semi synthetic antibiotic used in the first line treatment of *M. tuberculosis*. It is both a bacteriostatic and bactericidal drug which acts in the cytoplasm; the target site is bacterial DNA dependant RNA polymerase involved in transcription. RNA polymerase consists of 4 polypeptide units; the drug inhibits bacterial RNA polymerase by binding to the β-subunit (rpoB) close to the Mg^{2+} active site. This enables it to directly block the path of elongating RNA transcription at the 5' end when it becomes 2 or 3 nucleotides in length, thus preventing mycobacterial transcription and causing cessation of growth or cell death (Campbell et al. 2001)

1.3.1 Clinical Development

Rifampicin is a highly effective drug that dramatically improved treatment outcomes and in particular relapse. The reasons behind the selection of the current dose of rifampicin have been reviewed previously(van Ingen et al. 2011). Three main arguments were identified: pharmacokinetic/pharmacodynamic (PK/PD) considerations, cost and toxicity. Early PK/PD studies in the 1960s established that a dose of 10mg/kg achieved a high peak serum concentration, which was assumed to be sufficient to maintain serum values greater than the MIC throughout the 24 hour dosing interval(Pallanza et al. 1967; Furesz et al. 1967; Arioli et al. 1967). These data were interpreted by investigators to mean that there would be little benefit in increasing the current dose.

Despite the early PK/PD data, thirteen trials up to 2011 evaluated the concept of a higher dose of rifampicin (Ruslami et al. 2007; Long et al. 1979). These trials evaluated regimens with doses of rifampicin up to 1200 mg (20 mg/kg) and different dosing intervals (once, twice, thrice, six times a week, and daily). The largest study to compare rifampicin doses, USPSHS Study 19, demonstrated no statistical difference between 600mg and 750mg(Long et al. 1979). It has been suggested that the potential therapeutic difference was too minor to be discerned but of note there was no difference

in toxicity. In contrast, a more recent systematic review of several trials suggested an advantage in terms of likelihood of culture conversion among patients receiving at least 900 mg of rifampicin(Steingart et al. 2011). Opinion at the time, however, suggested that doses greater than 600mg would produce intolerable side effects. This supposition was based on high intermittent dosing producing rifampicin sensitisation and antibody formation, resulting in the so called 'flu-like syndrome'(Poole et al. 1971).

1.3.2 PK-PD

There is a substantial body of evidence on the PD of rifampicin emerging from *in vitro*, mice and even human studies. Hollow-fibre systems used to create PK/PD data suggest that microbial kill due to rifampicin is based on $AUC_{0\text{-}24}$/MIC killing closely followed by $C_{max/}$ /MIC, but not by C_{min}>MIC, whereas resistance suppression and post-antibiotic effect were closely linked to the $C_{max/}$ /MIC ratio (Ruslami et al. 2007). Murine experiments have shown that the current dose of rifampicin (10 mg/kg) is low and that an increase in the dose leads to enhanced sterilizing activity and a decrease in treatment duration for pulmonary TB(Jayaram et al. 2003; de Steenwinkel, Aarnoutse, et al. 2013).

There are several studies that evaluate the effectiveness of antimicrobials in reducing bacillary load in the first 2-14 days(Boeree et al. 2015). These supported the conclusions of the PK/PD data and showed that increasing the dose beyond 10mg/kg showed enhanced early bacterial activity.

Using efficacy cut-off data from the hollow-fibre system and murine data combined with human pharmacokinetic data, PK/PD mathematical models suggested that intrapulmonary target attainment at 20mg/kg may be superior to 10mg/kg (Goutelle et al. 2009) .

Van Ingen et al., concluded that: "The 600-mg dose is at the lower end of the dose-response curve, and the nonlinear pharmacokinetics and dose-dependent activity of

rifampicin mean that studies of higher dosages within the multidrug anti-tuberculosis treatment regimens are urgently required." This is currently being pursued by three trials or trial series of high dose rifampicin (PanACEA-MAMS, HIGHRIF, Rifatox and the HIRIF study in Peru).

The recently published PanACEA HIGHRIF paper was an ascending dose study that showed no excess in toxicity with doses up to 35mg/kg(Boeree et al. 2015). There was a trend to increased bacterial killing associated with the higher doses. The mechanism was suggested by Bowness et al. that showed that the higher doses of rifampicin were killing critical sub-populations that did not grow on solid medium(Bowness et al. 2015). Of note, the average systemic exposure of 35mg/kg dose was tenfold higher than the exposure to the currently used 10mg/kg dose, without severe toxicities during two weeks of administration[23].

The enhanced dose has now been tested in the MAMS-TB trial which demonstrated that the heightened dose of rifampicin was associated with a greater possibility of being culture negative at two and three months in comparison with the standard regimen, again with only limited severe adverse effects during three months of combined administration with the other TB drugs(Boeree et al. 2017).

1.4 Isoniazid

Isoniazid acts by blocking the synthesis of the cell wall; it targets long-chain enoyl-acyl carrier protein reductase (InhA) which acts during fatty acid synthesis. Under normal conditions this enzyme reduces long chain substrates (>16C) and the products are used to create mycolic acid. Isoniazid is a pro-drug requiring activation by catalase-peroxidase enzyme which is encoded by the *katG* gene. Once activated it forms an adduct with NAD which disrupts the synthesis of essential mycolic acids by inhibiting the NADH-dependant enoyl-ACP reductase leading to cell wall disruption (Rozwarski et al. 1998).

1.4.1 Clinical Development

Isoniazid was first synthesised in 1912 and its effect on *Mycobacterium tuberculosis* was discovered in three laboratories independently in 1952(Benson et al. 1952; Domagk et al. 1952; Bernstein et al. 1952). The first clinical trial describing isoniazid effect, *in vivo*, was published later that year(Selikoff et al. 1952). This was followed by the first MRC drug trial to evaluate 200mg of isoniazid with and without the established chemotherapy of streptomycin 1g and para-aminosalicylic acid 20g(Anon 1953). With limited phase I and no phase II trials, the maximum tolerated dose was never established in humans and was thus instead estimated primarily from animal models(Wolinsky et al. 1956; Elmendorf et al. 1952). American physicians decided on 5mg/kg whereas, in the UK the British chose a more conservative dose of 200mg daily, equating to 3-4mg/kg.

The reason the BTS, now, recommend 300mg of isoniazid is because in 1963 the standard dose of isoniazid used in trials by the BMRC changed from 200mg to 300mg following a study that combined the two doses with thiocetazone(Anon 1970). In the study the 200mg did not produce the same outcomes as 300mg. Subsequently the BMRC stopped using 200mg and started using 300mg instead(Fox et al. 1999). The current dose is not based on PK/PD analysis but rather an extrapolation from a small trial using a combination of isoniazid and a largely untested agent.

1.4.2 PK-PD

In vitro, murine, guinea-pig and clinical data for isoniazid all suggest an $AUC_{0\text{-}24}$/MIC killing ratio(Pasipanodya & Gumbo 2011). Suppression of resistant populations in hollow fibre studies is reported to be driven by both $AUC_{0\text{-}24}$/MIC and $C_{max/}$ /MIC(Gumbo et al. 2007). Donald *et al.*, showed only 18.75mg was required to produce an bactericidal effect(Donald et al. 2004; Donald et al. 1997). They also suggested no difference between 300mg and 600mg in monotherapy EBA. As correlated clinical

evidence, they quoted the thiocetazone trials that there is no discernible difference between 300mg to 400mg. This is not in keeping with monotherapy trials that showed an optimum dose of near 400mg(Fox et al. 1999). This may be related to resistance and an MIC creep, highlighting an inadequacy of small early phase clinical studies. In Donald *et al*. each arm had roughly 20 patients. This makes it hard to gain statistical significance let alone project the results into future trials or treatments.

Isoniazid is different from the other anti-tuberculosis agents as its elimination shows a tri-modal distribution, resulting in homozygous fast, heterozygous fast (or intermediate) and slow metabolisers(Parkin et al. 1997). These genotypes reflect in two phenotypes (fast and slow acetylators) in clinical practice. This difference in elimination and thus in exposures achieved is caused by the polymorphism in the N-acetyltransferase enzyme that is critical in the metabolism of isoniazid. The impact of acetylator status has been widely discussed before, particularly an influential review by Ellard *et al*. that stated that there was modest effect on both toxicity and outcome by acetylator status(Ellard 1984). This was based on large but heterogeneous clinical trial data sets. More recently, evidence has been presented suggesting reduced efficacy among fast acetylators and increased toxicity in slow acetylators. A meta-analysis of 26 trials by Pasipanodya *et al*. showed that rapid-acetylators were more likely than slow acetylators to have microbiological failure and acquired drug resistance, with a trend for more relapse TB (Pasipanodya et al. 2012). The trials analysed were heterogeneous using different dosing regimens; in particular, once and twice weekly dosing. The short half-life of isoniazid means that and the effect of acetylator status is particularly susceptible to weekly dosing and indeed the sub group analysis of dosing regimen showed that largest effect size was in the weekly dosing regimens. The sub group analysis of daily dosing regimens (n=6) showed a relative risk of 1.2 with the 95% CI crossing through 1 for positive two-month culture status. In addition to this meta-

analysis, the majority of genotyping studies suggest that slow acetylators are at an increased risk for isoniazid-induced hepatotoxicity(Donald & van Helden 2011).

More evidence of this trend comes from an interesting 'pharmaco-genetic' trial, whereby they adjusted doses based on NAT2 genotype(Azuma et al. 2013). The sample size in this study was small with only 16 patients in the slow acetylator arms. Trends were again seen in surrogate end points for both efficacy and toxicity and the association of acetylator status is clearest when lower thresholds for liver injury are used (1.5x). The clinical benefit for testing for acetylator status remains uncertain as does dosing based on acetylator status. The optimal dose for slow acetylators has been suggested to be 2.5 mg/kg/day, for intermediate 5 mg/kg and for fast acetylators 7.5 mg/kg/day, whereas others have suggested 3 mg/kg in slow acetylators and at least 6 mg/kg in fast acetylator phenotypes (Kinzig-Schippers et al. 2005; Seifart et al. 2001). Without pre-emptive genotyping, the 5 mg/kg is the compromise dose, but it disadvantages the fast acetylator and slow acetylator subgroups in terms of efficacy and toxicity, respectively.

1.5 Pyrazinamide

The complete molecular mechanism of pyrazinamide is unknown; however, it is a pro-drug converted by bacterial nicotinamidase/pyrazinamidase to pyrazonic acid. The pyrazonic acid decreases the membrane potential by decreasing the pH within the cell. This inhibits proton-ATPase, NADH dehydrogenase and cytochrome *c* oxidase therefore reducing the transport function of the cell membrane leading to cell death (Zhang et al. 2011).

1.5.1 Clinical Development

Pyrazinamide was first synthesised in 1940 but it was not until 1948 that McKenzie *et al*., identified its effect against mycobacteria in mice (Kushner & Dalalian 1948; Erickson & Spoerri 1946; McKenzie & Malone 1948). The first animal models required very high doses to achieve bactericidal concentrations, particularly in guinea-pigs (4g/kg) were pyrazinamide is less effective. Consequently, the first human studies used high doses as well, up to 200mg/kg (Yeager et al. 1952). These were associated with an unacceptable adverse event profile. Pyrazinamide was, for many years relegated to the position of a second line agent. No ascending dose studies were performed and no other doses were investigated in a clinical trial setting. The first clinical studies were performed with concomitant medications that were, in themselves, hepatotoxic.

Once the mechanism of action of pyrazinamide was thought to be better understood, a hypothesis was put forward that streptomycin and pyrazinamide would form a highly effective drug combination. Investigators postulated that lower doses, 15-35mg/kg could be effective and these were evaluated in a series of trials that resulted in reduction of the duration of therapy to six months (Grosset 1980).

1.5.2 PK-PD

Pyrazinamide is difficult drug to work with *in vitro*. Its MIC varies depending on the conditions used and of note shows no effect at physiological pH. Pyrazinamide has little early bacterial activity (Gillespie et al. 2002). Hollow fibre studies have had limited success with evaluating PK parameters. In the first week of treatment bacillary loads remained static and then in the second and third weeks there was a slight decay, 0.1 $\log_{10}$ CFU/mL/day. After the third week the bacterial counts rose as resistant clones predominated. Based on the results obtained from the second and third weeks the microbial killing parameter was AUC/MIC and the resistance suppression was related to

time above MIC (%t>MIC), similar to those obtained from the *in vivo* pyrazinamide monotherapy trials(Gumbo et al. 2015).

A paper published in 2009 by Gumbo *et al*. used Monte Carlo model of hollow fibre systems to replicate human PK/PD data showed that bacilli respond best to >60mg/kg (Gumbo et al. 2009). In addition, a range of pyrazinamide doses were evaluated against intracellular and extracellular *M. tuberculosis* in chronically infected mice and guinea pigs (Ahmad et al. 2011). This showed doubling the human-equivalent dose of pyrazinamide reduced the lung bacillary burden by 1.7 and 3.0 log in mice and guinea pigs respectively (Ahmad et al. 2011).

In humans, a recent PK-PD study in South-African TB patients also suggested that the currently used dose of pyrazinamide is at the lower end of the dose-response curve (Pasipanodya et al. 2013). For example, the cut-off AUC value for favourable responses was similar to average exposures in TB patients, meaning that half of the patients would be under-dosed. A literature review on clinical data concluded that increasing the dose was not associated with an increase in the risk of toxicity, although the descriptive data with overlapping confidence intervals seemed to show a trend: the frequencies of hepatotoxicity were 4.2% for 30 mg/kg, 5.5% at 40 mg/kg and 9.8% at 60 mg/kg (Pasipanodya & Gumbo 2010). The overall conclusion is nevertheless compounded by the work of Sahota *et al*; who assessed the feasibility of a fixed dose of pyrazinamide (Sahota & Pasqua 2012). They showed that the current weight bandings produce a skewed distribution of AUC/MIC and a fixed dose could produce more efficacious dosing with minimal increased risk of hepatotoxicity.

These data suggest that there is still work to do to optimise the dose of pyrazinamide and trials of higher doses should be performed.

1.6 Ethambutol

Ethambutol targets the synthesis of arabinogalactan. It specifically targets the *emb operon* which codes for the enzymes; arabinosyltransferase embA/B/C (Escuyer et al. 2001). These are responsible for the polymerisation of arabinose into the arabinan of the arabinogalact (Belanger et al. 1996). Ethambutol acts particularly on the *embB* gene of the operon which forms the 3,5-α-Ara*f* in the Ara6 motif found in the arabinogalactan. Under normal conditions arabinogalactan is covalently linked to long-chain alpha-alkyl-beta-hydroxy mycolic acids but with *embB* inhibited, mycolic acid builds up resulting in cell death (Besra et al. 1995).

1.6.1 Drug Development

In 1961, the Lederle Company published a report describing the finding of a new agent for treating tuberculosis: ethambutol(Thomas et al. 1961). It showed good efficacy *in vitro* and for treating infected guinea pigs but to achieve these results in patients, doses of 60-100mg/kg would have to be used(Carr & Henkind 1962). At such high doses the ocular side effects were intolerable. Thus, ethambutol is now primarily used at lower doses to prevent rifampicin resistance in the event of pre-existing isoniazid resistance.

1.6.2 PK-PD

PK/PD data suggests a mix between AUC/MIC and C_{max}/MIC for efficacy of ethambutol (Donald et al. 2006; Dickinson et al. 1968; Srivastava et al. 2010). The challenge of ethambutol therapy, however, is its ocular toxicity. At all therapeutic levels ocular toxicity is a risk to be considered, although this adverse effect is dose related with minimal risk at a daily dose of 15 mg/kg (Doster et al. 1973; Leibold 1966). Therefore, a balance must be struck between toxicity and efficacy. This has meant that initial dosages of 40-100mg/kg were discarded and changed to 15-25mg/kg (Bobrowitz & Gokulanathan 1965).

Of note, early bactericidal activity studies show a significant improvement in efficacy between 15mg/kg and 20mg/kg without a substantial increase in risk of ocular toxicity in Monte-Carlo modelling studies (Srivastava et al. 2010).

1.7 Biomarkers

The rise of drug resistant strains has led to the acknowledgement that new drugs are required to prevent the escalation of the tuberculosis pandemic. Biomarkers and surrogate endpoints are required to support the development of these lead compounds. A biomarker is a measurable characteristic that indicates either a normal biological process; pathogenic process or a pharmacological response to a therapeutic intervention. The most valuable biomarkers measure an event that is directly involved in the pathogenesis and that change in early treatment and is associated with the PK/PD.

Biomarkers and diagnostics overlap, some biomarkers can diagnose and some diagnostics can be biomarkers. At present, tuberculosis diagnostics have been unsuccessful at being biomarkers. Measures such as baseline bacterial load or cavitatory disease on chest x-ray can accurately prognosticate but have less success in monitoring response to treatment responding to treatment(Perrin et al. 2010; Perrin et al. 2007).

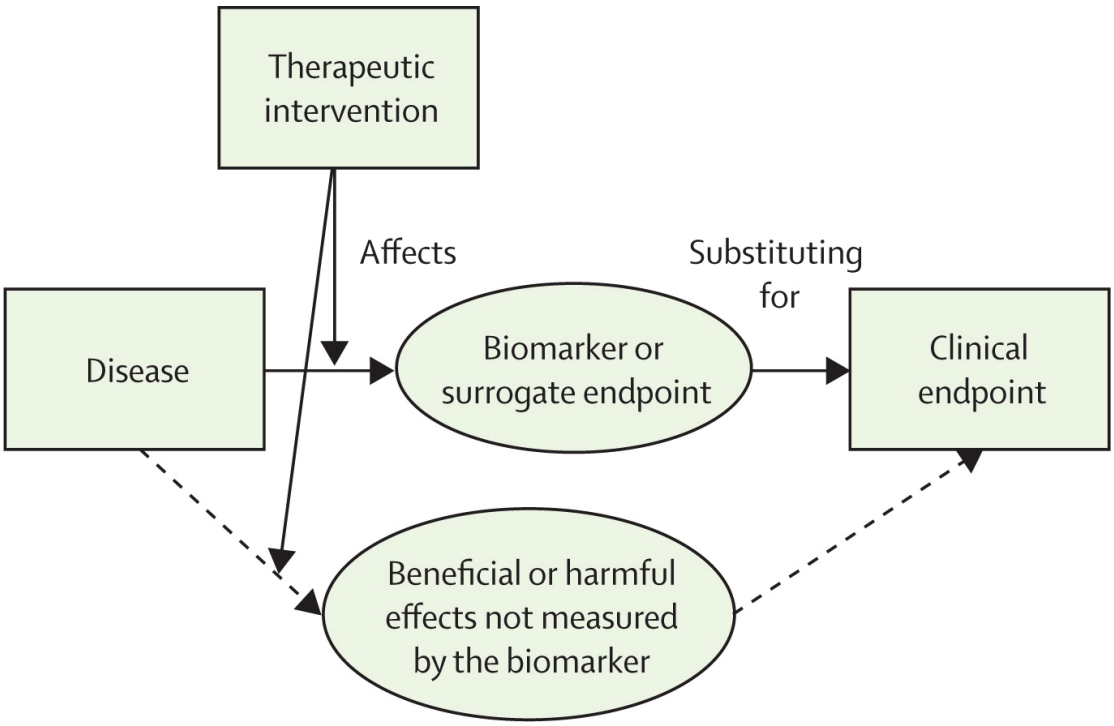

Figure 1.5: Biomarker flow diagram from FM Perrin et al 2010.

The issue with generating - identifying biomarkers is the low incidence of tuberculosis relapse and treatment failure rates as well as the long duration of chemotherapy. This combined with the low predictive value of early bacterial studies means that a small and heterogeneous data set exists for predicting poor outcomes despite the large number of sizable trials that have been conducted.

1.7.1 Current Biomarkers for Tuberculosis

A number of biomarkers have been developed based on either *M. tuberculosis* or the human inflammatory response. Below is a table summarising the biomarkers that so far been evaluated excluding molecular markers that will be outlined in more detail in the next section.

Biomarker	Outcome	Patients (Outcomes)
Two Month culture/smear Status	Duration of Rx Relapse	2450 (187)
Serial Sputum Colony Counts	Treatment effect	75 (0)
Serial MGIT or Bactec TTP	Treatment effect, failure and recurrence	26 (13) 42 (2)
CRP	Treatment effect, death	105, 100, 18
Sputum Ag85	Treatment effect, recurrence	18, 42 (4) 40
Urine tuberculosis DNA	Treatment effect	20 (0)
Anti-alanine dehydrogenase	Treatment failure	168 (10)
PET/CT Imaging	Treatment effect	20 (0)
Antiphospholipid Antibody	Treatment effect	40 (0)
Urine Lipoarabinomannan	Treatment effect	32 (8)
Neoneptrin	Treatment effect, Recurrence	39 (11) 31
sICAM-1	Treatment effect	30 (0)
sTNF receptor, granzyme B	2 Month Culture Status	36 (18)
Sputum Interferon-γ	Treatment Effect	15 (5)
Soluble urokinase plasminogen activator receptor	Death	47 (13)
Interferon-γ release assay	Treatment Effect	14 (7)
Soluble interleukin-2R	Treatment Effect	44 (0)

Table 1.1: Summary of Current Biomarkers adapted from Wallis et al.

Both the FDA and EMA recommend two biomarkers for use in drug developemt. First, through either MGIT TTD or serial decline of CFU measure through Miles-Misra up to the first 8 weeks of treatment. Second, sustained culture conversion that can be measured with proportion of patients that were culture negative at two and six months or sustained culture conversion.

1.7.1.1 Culture Methods

1.7.1.1.1 Two month Culture

The marker most widely used as a predictor of durable eradication is two-month culture status. This has been shown in meta-analysis to be inversely proportional to

relapse but with the caveat that the relationship is dependent on a single study arm (6SH) that had an atypical relapse rate (29%). This relationship improves when analysed within studies, however, the positive predictive value for individual patients remains very low(Wallis et al. 2012). The methodology of this meta-analysis has been questioned.[i] This meta-regression analysis has recently been updated by Wallis *et al.* to include the data sets from REMox, OFLOTUB and RIFAQUIN.(Wallis et al. 2015) The inclusion of the further data sets resulted in "minimal changes to its predictions".

Micro	Relapse Sensitivity	Relapse Specificity	Failure Sensitivity	Failure Specificity
Smear	24% [95% CI 12–42%], six studies	85% [95% CI 72–90%]	57% [95% CI 41–73%]	81% [95% CI 72–87%]
Culture	40% [95% CI 25–56%], four studies	85% [95% CI 77–91%]	Insufficient Data Available	Insufficient Data Available

Table 1.2: Two Month Culture and Smear predicting relapse and treatment failure adapted from Horne et al

1.7.1.2 Serial Sputum Colony Counts

Serial sputum colony counts have been undertaken to try and quantify the decline in bacterial load. They are performed by plating series dilutions on agar and inferring back the number of colony forming units in the sputum expressed as $\log_{10}$ colony forming units per ml (CFU/ml). This has been used to assess the decline in bacterial load over the first couple of weeks and up to one month. It has revealed the varying ability of different agents and combinations to reduce bacillary load. There has been no trial that has shown any correlation between the results of colony counts, during initial treatment and long term outcomes. It has been postulated that the correlation is unlikely to exist because the drugs that appear to have a strong effect on long-term outcomes have little effect on reducing the colony count.

1.7.1.3 Serial Mycobacterial Growth Indicator Tube (MGIT) or Bactec Time to Positivity (TTP)

Automated liquid culture instruments measure CO2 production or O2 consumption in the headspace above culture tubes. It has been inferred that the time for the culture to 'flag' as positive would inversely proportional to the concentration of the inoculum; the bacterial load. Increasingly MGIT TTP is replacing colony counting as the treatment-monitoring tool in clinical trials.

As early as 1998 MGIT TTP has been shown to be correlated with treatment effect, failure and recurrence in a small number of patients (Epstein et al. 1998). Indeed in 1999 it was established that TTP was inversely correlated with duration of sputum culture positivity. (Wallis et al. 1999)

In 2008 Pheiffer et al. showed that there was an inverse correlation between MGIT TTP and CFU during the first two weeks of treatment. (Pheiffer et al. 2008) Using multiple logistic regression Hesseling et al. demonstrated that TTP predicts 2-month culture status and relapse. (Hesseling et al. 2010) This was further developed by Weiner et al. used mixed-model analysis of covariance of TTP to show it was a better discriminator of treatment failure and relapse than 2-month culture status. (Weiner et al. 2010)

Diacon et al. showed that increase in TTP closely followed the decline in CFU over the first 7 days and went on to suggest that MGIT TTP could replace CFU. (Diacon et al. 2010) The close correlation was shown to continue out till 60 days by Bark et al. Spearman correlation (rho) equaled -0.91. (Bark et al. 2011) Most recently Sloan et al. showed that the change in TTP over the first 8 weeks of treatment was associated with both treatment failure and relapse. (Sloan et al. 2015)

1.7.2 Serological Markers

1.7.2.1 CRP

C-Reactive Protein, named after the serovar of pneumococcus it was discovered in, is an acute phase reactant produced by hepatocytes. It is commonly used in monitoring bacterial infections such as pneumonia and does decline with chemotherapy and will prognosticate. Its decline has not found to strongly associate with clinical outcomes (Bajaj et al. 1989; Scott et al. 1990; Mzinza et al. 2015; Djoba Siawaya et al. 2008; Jin Hwa Lee 2003).

1.7.2.2 Neopterin

Neopterin is a biochemical marker produced by monocytes by the stimulation of TNF-γ. This correlates with signs of disease activity such as fever, anaemia and weight loss. Persistently elevated levels were found to be associated with relapse (Hosp et al. 1997; O'Brien et al. 1996; Immanuel et al. 2001).

1.7.2.3 sICAM-1

Soluble Intracellular adhesion molecule-1 is a glycoprotein associated with inflammation. One study showed it declined more severely than in other lung diseases. Its specificity is likely to be low as not only is it raised in other inflammatory conditions but also some chronic diseases such as type II diabetes (Djoba Siawaya et al. 2008; Demir et al. 2002).

1.7.2.4 Antigen 85

Antigen 85 complex consists of three 30-32-kDa related proteins and is induced in mycobacteria by isoniazid. The expression is thought to be an attempt by damaged mycobacteria to maintain the integrity of the partially compromised cell wall. Two studies looked at its magnitude and decline by ELISA and found that it was associated with relapse in 4 of the 42 patients studied (Wallis et al. 1998). One study looked at PCR for 85B RNA and found it could not distinguish the one patient that relapsed (DESJARDIN et al. 2012).

1.7.2.5 Antibody to M. tuberculosis alanine dehydrogenase

Various antibodies to mycobacterial antigens have been found to be raised at diagnosis and subsequently modulated during treatment. Antibody to alanine dehydrogenase has been found to be higher in those who failed treatment. However, it was not elevated in patients compared with control; and did not decline during therapy (Azzurri et al. 2006).

1.7.2.6 Anti-phospholipid antibodies

Anti-phospholipid antibodies against various *M. tuberculosis* phospholipids have been evaluated for monitoring. They decline in non-cavitatory disease but were unable to detect treatment failure (Goodridge et al. 2012).

1.7.2.7 Interferon-γ Release assay (IGRA)

Interferon-γ Release assay is an in vitro assay that detects T cell–mediated interferon-γ response to selected peptides of *M. tuberculosis* and is used in the diagnosis of latent tuberculosis infection. In a study of 18 patients it did not decline in the 5 patients that had not improved either clinically or microbiologically after three months (Mzinza et al. 2015).

1.7.2.8 Sputum Interferon-γ

One study looked at the change in cytokine profile over time in 15 patients found that Sputum Interferon-γ correlated with bacterial load and declined during treatment (Ribeiro-Rodrigues et al. 2002).

1.7.3 Other Markers

1.7.3.1 Positron Emission Tomography (PET) CT

The combination of PET and CT allows superposition of two types of data: structural from CT and functional from PET, particularly FDG PET that shows metabolic activity. This has shown to change in response to treatment in one study of 21 patients (Martinez et al. 2012). PET CT was combined with mRNA in a study of 99 patients and again failed to show significant differences between patients successfully treated and those that were not (Malherbe et al. 2016).

1.7.3.2 Trans renal-DNA

Trans renal DNA has been used both as a biomarker and a diagnostic. One study found that of 20 patients that tested positive for trans renal-DNA IS6110 were still positive after two months of treatment (Cannas et al. 2008). The copy number is very low and some studies have quoted the sensitivity as 6% (Rebollo et al. 2006; Sechi et al. 1997). The sensitivity is cited as higher in patients infected with HIV.

1.7.3.3 Lipoarabinomannan (LAM)

A number of commercial LAM ELISA kits are available for purchase. Until recently these were for urine use only. Immunocompetent patients were shown to be unlikely to have LAM present in their urine.(Lawn & Gupta-Wright 2016) Now, promising results are available from sputum samples. LAM was founds to decline during treatment and be associated with sputum positive and culture status but had no correlation with treatment success (Wood et al. 2012).

1.7.3.4 Soluble urokinase plasminogen activator receptor

Soluble urokinase plasminogen activator receptor has been shown to correlate with death in patients but this was diminished in HIV negative patients (MR 1.14, 95%CI 1.00–1.31), however, it was performed during the war in Guinea-Bissau and thus had a very high drop-out rate (Eugen-Olsen et al. 2002). Another study showed a correlation with two month culture status(Djoba Siawaya et al. 2008).

1.7.3.5 Interleukin-2 Receptor molecules

Soluble Interleukin-2 Receptor molecules are expressed on T-cells in response to mycobacteria. sIL2R has been found to be higher than in health controls in a study of 44 patients and did decline in response to chemotherapy after one month but remain still elevated in comparison to the controls after six months (Chan et al. 1995).

So far no biomarker has a strong enough predictive value to be a surrogate endpoint. Indeed, the vast majority of biomarkers are vastly underpowered with some enrolling less than 20 patients. This leaves the scope for our current work to produce a trial with sufficient patients and samples to detect a difference between patients with good outcomes and those without.

1.7.4 Molecular Markers

Over the last two decades molecular techniques, particularly PCR, have been developed for diagnosis and the monitoring of tuberculosis treatment. Currently, there is one FDA approved platform: GeneXpert MTB/RIF assay (Cepheid, Sunnyvale, CA, USA). This utilises a hemi-nested, DNA, beacon probe for the *rpoB* gene and the insertion sequence *IS6110*. It has a very high sensitivity and specificity in both smear positive and smear negative patients (Sensitivity: Smear positive 99.8%; Smear negative 90.2% and Specificity: 98.1%) (Boehme et al. 2010). This correlates very well before treatment with both smear and culture, however, as treatment progresses it remains positive after culture and smear become negative (Friedrich et al. 2013). In a phase II study of

rifapentine dose escalation involving 105 patients, there was a small but statistically significant difference between quantitative GeneXpert at 8 weeks between culture positive and culture negative patients (Jayakumar et al. 2016).

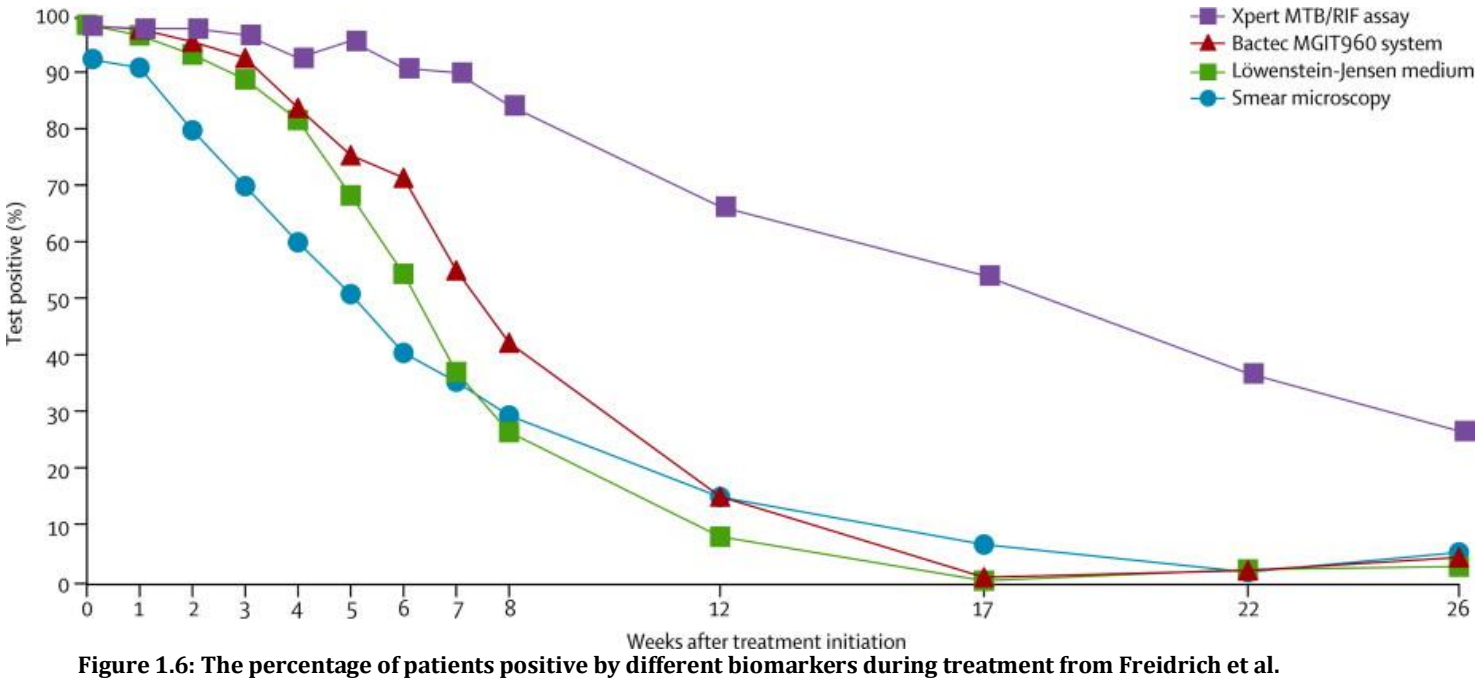

Figure 1.6: The percentage of patients positive by different biomarkers during treatment from Freidrich et al.

It is thought that the DNA measures in both viable and non-viable cells; despite there being a filtration step to select only intact cells before extraction (Banada et al. 2010; Helb et al. 2010).

Two methods of exclusively measuring viable cells have been developed: the first use DNA-intercalating dye and the second use the far less stable RNA species. The dyes that have been used so far are ethidium bromide monoazide and propidium monoazide. They work by infiltrating "dead" cells by passing through the imperforate membrane and then photo-inducing crosslinking rendering the DNA insoluble; and therefore not amenable to PCR(Nocker et al. 2006; Kralik et al. 2010; Josefsen et al. 2010; Pholwat et al. 2012; Rudi et al. 2005; Soejima et al. 2008).

A paper in *Tuberculosis* compared culture and smear with RT-qPCR treated after the addition of propidium monoazide. This displayed a high specificity of 84.6% and sensitivity of 84.6% when compared to *M. tuberculosis* colony-forming units counting. However, this was with a high cut off of 666 viable cells per ml and the methodology failed to accurately quantify by underestimated the CFU counts (de Assunção et al. 2014) .

The instability of RNA means that it is unlikely to remain intact once the bacilli are non-viable. A number of different RNA species have been trialled for this reason. Vliet et al showed in 1994 that *M. smegmatis* 16S rRNA correlates better with CFU than 16S DNA before and after treatment with antibiotics (Van der Vliet et al. 1994). This was applied to monitoring 22 patients' treatment response but yet again the 16S rRNA was remained positive after culture was negative (D. F. Moore et al. 1996). In 1999, five molecular markers: M 85B (alpha antigen), messenger RNA (mRNA), 16S ribosomal RNA (rRNA), and IS6110 DNA; were used to measure the response in 19 patients over the first two weeks treatment (DESJARDIN et al. 2012).

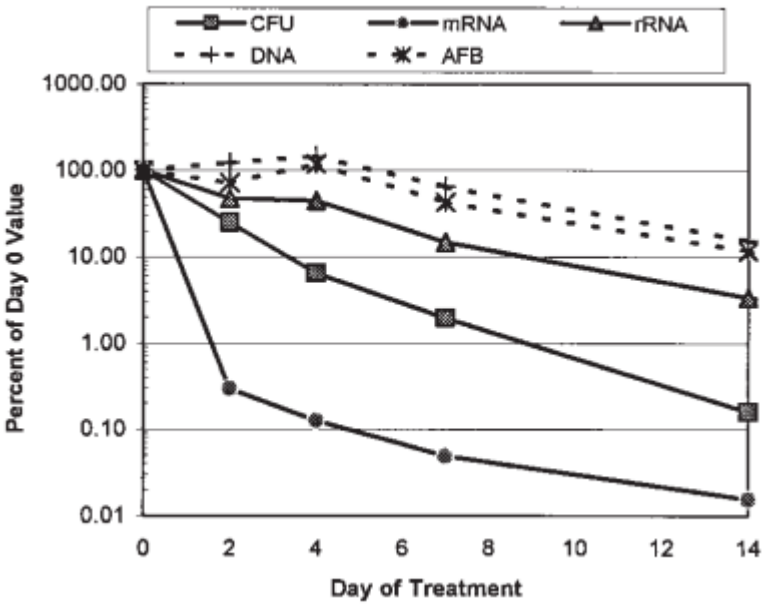

Figure 1.7: The percentage of patients positive by different molecular markers during treatment from Des Jardin et al.

In this study rRNA appeared to correlate far better with solid culture whereas mRNA declined too quickly and DNA the reverse.

1.7.4.1 Mycobacterial Load Assay

It has been proposed that decline in bacterial load may be the most accurate measure of response to therapy. In 2011 the Gillespie group developed a new molecular based assay using 16s rRNA Reverse Transcriptase Quantitative PCR for quantification of viable *M. tuberculosis* bacterial load from sputum during treatment. In this assay, a novel spiked internal control has been included to normalise extraction efficiency between different samples; and this has improved the reproducibility of the assay and allows for very accurate measurement of the CFU count (Honeyborne et al. 2011).

Honeyborne et al described a method of normalising the 16S rRNA Ct based on the inhibition of the internal control. This was compared to use of the widely accepted standard curve for the quantification of bacterial load and showed more accurate

quantification. The 16S rRNA assay is being tested in three high burden countries as part of the PANBIOME project (Sabiiti et al. 2016).

A wide array of disparate tuberculosis biomarkers has been published in the literature. With the exception of two-month culture status there have been limited patient numbers in the trials and no correlation with long-term outcomes. The persisting theme is that the small sample size fails to gain statistical significance.

1.8 Ribosomes

The word ribosome derives from "ribo" in ribonucleic acid and from the Greek "soma" meaning body. Ribosomes were first observed in the mid-1950s by George Emil Palade, who used an electron microscope to see dense particles or granules that were ribosomes. He went on to receive the Nobel Prize in 1974 for this work (CADAR & GABOREANU 2014).

Ribosomes consist of two sub units that coalesce around the mRNA to enable translation of the polypeptide chain during protein synthesis. Crystallography has exposed that ribosomes do not participate directly but are thought to act more as a "scaffold" to facilitate protein synthesis (Agmon et al. 2004).

In prokaryotes, the subunits are designated 30S and 50S, and together make up the 70S ribosome. The 30S is further subdivided into the 16S subunit, 1,542 nucleotides (nt) in length complexed with 21 proteins. The 50S is split into the 23S (2,904nt), 5S (120nt) and 31 proteins.

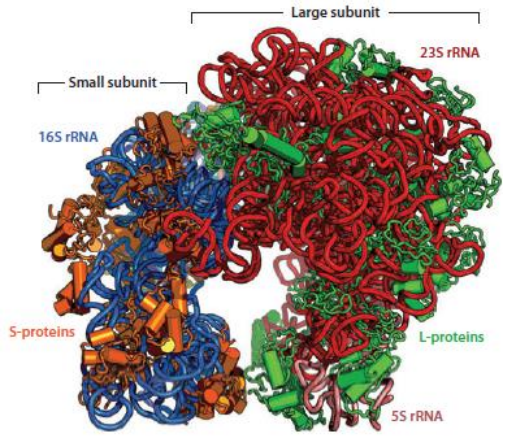

Figure 1.8: Rendering of an *E.coli* 70S Ribosome from Shajani et Al

The ribosome has three binding sites: aminoacyl (A), peptidyl (P) and exit (E). The A site binds an aminoacyl-tRNA; the P site binds a peptidyl-tRNA (a tRNA bound to the peptide being synthesized); and the E site binds a free tRNA before it exits the ribosome. Protein synthesis begins at a start codon AUG near the 5' end of the mRNA. mRNA binds to the P site of the ribosome first. The ribosome is able to identify the start codon by use of the Shine-Dalgarno sequence of the mRNA in prokaryotes and Kozak box in eukaryotes. Peptide bonds continue to form until a stop codon is reached and then the two ribosomal subunits dissociate and protein synthesis halts.

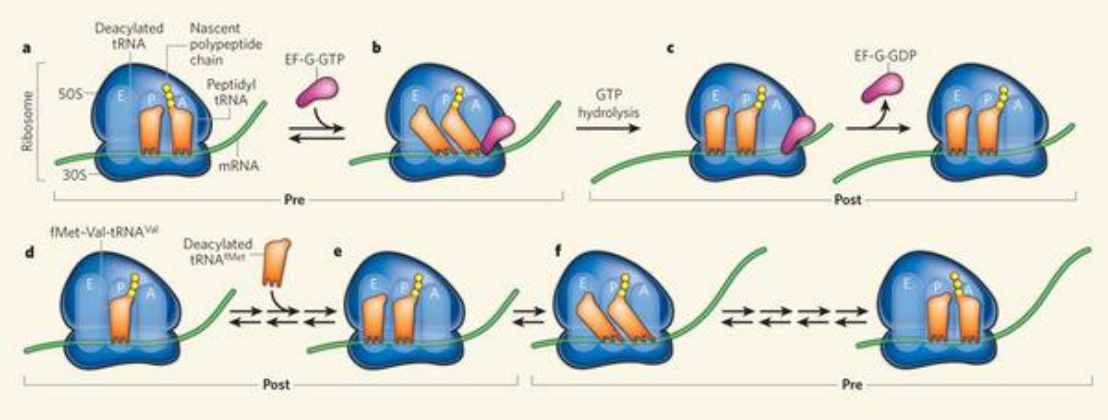

Figure 1.9: Ribosomal Processing from Ehrenberg et al

1.8.1 Ribosomal Synthesis

In the 1950s researchers were coming to the conclusion that the 30S, 50S, 70S and 100S ribosomal subunits that they were studying were the same 70S molecule in different physical states. In 1958, Tissieres and colleagues found that the 70S could be further subdivided into the large and small subunit (Tissieres & Watson 1958). Traub and Nomura then made a major breakthrough in understanding that the 30S could be formed in vitro from free rRNA and ribosomal proteins without any additional components. This established that all the information required for assembly is encoded within the rRNA and proteins themselves (Traub & Nomura 1968). From these experiments Nourma was able to infer that the proteins assemble in a hierarchical fashion and developed Nourma maps that remain relatively unchanged after 40 years(Mizushima & Nomura 1970) (Held et al. 1974; GRONDEK & CULVER 2004).

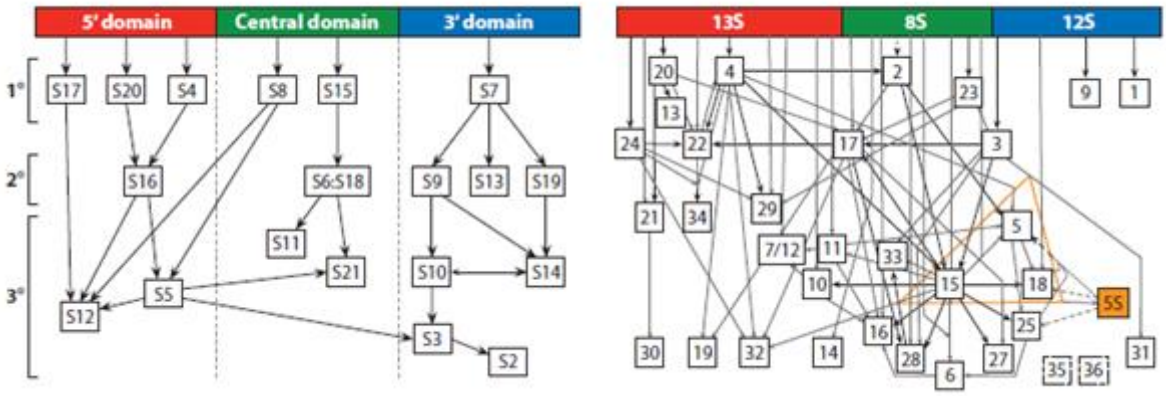

Figure 1.10: Nomura maps from Shajani et al.

The rRNA and proteins undergo many enzymatic-processing steps with multiple co-factors to produce the completed Ribosome. It is during the initial steps that the precursor rRNA is processed. The ribosome is encoded in one operon, *rrn*, that produces polycistronic rRNA. This is the cleaved by RNase III to the produce three precursors.

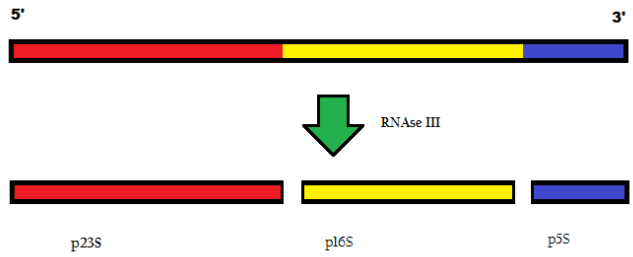

Figure 1.11: Precursor rRNA Synthesis

1.8.1.1 Pre-16S rRNA

The pre-16S has an extra 33nt at the 3' end and 115nt at the 5' end. The cleavage of the 5' end occurs before the 3' end. Then pre-16S rRNA is intially cleaved by RNase E to leave an additional 66nt at the 5' and then this is finally removed by RNase G. The final maturation steps of the 3' end remains unknown (Li, Pandit & Deutscher 1999b; Refaii & Alix 2009; King & Schlessinger 1983).

1.8.1.2 23SS rRNA

The 23S rRNA is more variable having either 7 to 9 extra nt at the 3' end and 3 to 7 at the 5' end. The 3' end is cleaved by RNase T and the final maturation of the 5' end is unknown (Li, Pandit & Deutscher 1999a; King et al. 1986).

1.8.1.3 5S rRNA

The 5S rRNA has an additional 42nt at the 3' end and 84 nt at the 5' end. RNase E cleaves both ends leaving 3 nt at each end. RNase T causes the final maturation of the 3' end and the 5' end final processing remains unknown (RAY & Apirion 1979; Cangelosi & Brabant 1997; Ghora & Apirion 1979).

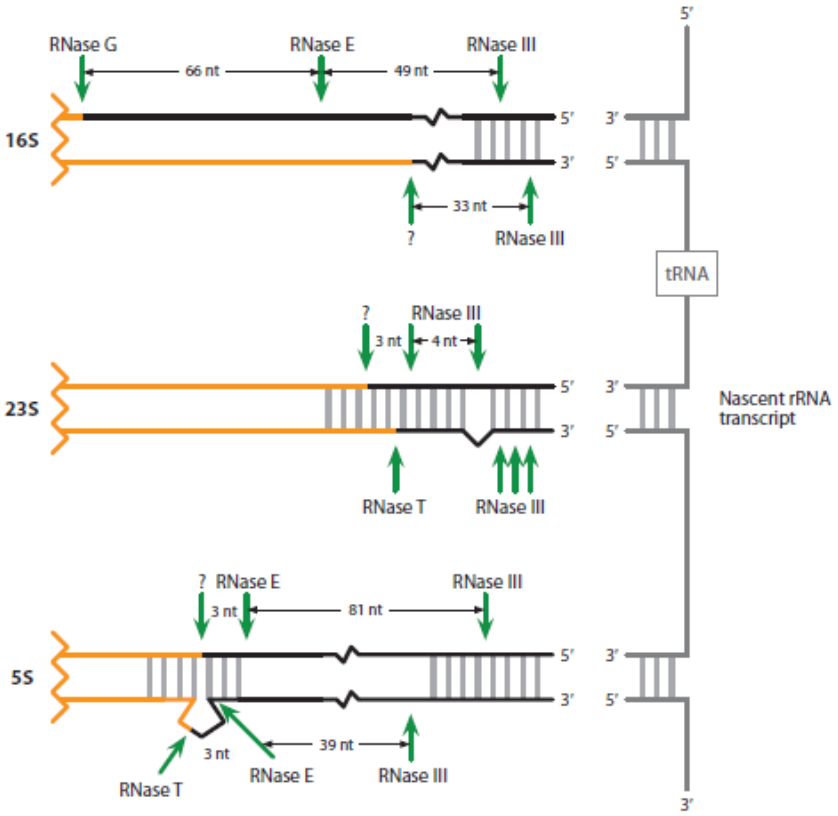

Figure 1.12: Precursor synthesis from Shajani et al.

1.9 Pre-16S rRNA

Three papers were written by Cangelosi in the late 1990s on pre16 rRNA detection to determine bacterial viability (Cangelosi & Brabant 1997; Cangelosi et al. 1996;

Britschgi & Cangelosi 1995). The first two papers looked at detecting phenotypic resistance using precursor rRNA, first in *E. coli* using rifampicin and then in *M. tuberculosis* using rifampicin and Ciprofloxacin. Both papers showed a comparable decline of precursors inversely proportional to the number of resistant clones present in the culture when treated with antibiotics. The third study found that when *E. coli* was deprived of nutrients the pre-RNA was depleted. They also showed that chloramphenicol, that prevents rRNA maturation, halted pre-rRNA depletion under all conditions. This work was not taken any further at the time due to inadequacies in technology at the time; specifically the semi-quantitative methodology employed.

They proposed that precursor ribosomal RNA would be present in actively growing cells. These precursors are relatively abundant accounting for only 2–5% of total rRNA in exponentially growing cells and represents approximately 60% of total transcription in yeast cells. Pre-rRNA sequences are phylogenetically specific, which facilitates their detection in complex samples.

If as proposed, pre-16S rRNA, by measuring actively growing cells could more accurately reflect the viable bacilli than DNA methods such as GeneXpert.

1.10 Trans-translation

Trans-translation is a process mediated by the molecule tm-RNA. Tm-RNA is a unique RNA species. It was initially discovered when David Apirion and colleagues were evaluating RNA half-lives(RAY & Apirion 1979). They discovered a 10S, stable RNA species which was named with the gene small stable RNA (*ssrA*). The molecule was renamed tm-RNA when two papers recognised that tm-RNA could be amino-acetylated by alanine tRNA synthase and that it could tag truncated proteins with a peptide sequence that was postulated to be for degradation (KoMINE et al. 1994).

Bacterial tm-RNA acts as a quality control system; that regulates protein synthesis and recycles stalled ribosomes. It does this by initially binding to the stalled ribosome and then attaching a short ssrA peptide tag (AANDENYALAA) to the C-terminus of the nascent peptide that encodes for proteolysis (Tu et al. 1995).

Tm-RNA is one of the most abundant RNAs in bacteria with *trans*-translation occurring 13,000 times per cell division in exponentially growing *E. coli* (S. D. Moore & Sauer 2005). Tm-RNA has been shown to be up regulated during various models of dormancy and so called viable, non-cultural bacilli (Ignatov et al. 2015).

2 Chapter 2: Developing pre-16S rRNA and tm-RNA assays

2.1 Introduction

The aim of this chapter is to describe the development of two novel assays to improve or complement the existing MBL assay introduced in Chapter 1.

The novel aspect of the MBL assay was to attempt to measure viable bacilli. (Honeyborne et al. 2011; Honeyborne et al. 2014) The assay had already demonstrated the ability to very accurately quantify bacterial load of cultured *Mycobacterium tuberculosis* in media, artificial sputum and pooled sputum. In one hundred and eleven patients the assay successfully monitored treatment response by declining during treatment. There was a significant difference in the bi-exponential model fitted to data of those that achieved cure compared to patients that relapsed. Following this success, the assay was taken forward to assess its ability to act a surrogate end point in clinical trials.

However, unpublished data from the Gillespie group suggests that 16S rRNA remains present when *Mycobacterial* cells are no longer viable. It was postulated that 16S rRNA remained stable within the non-viable cells due to the complex secondary structure of the rRNA previously described.

In an attempt to more accurately detect only the viable bacilli two less stable RNA molecules were selected: tm-RNA and pre-16S rRNA. Both of these RNA species have secondary structures making them more stable than mRNA but are less stable than 16S rRNA. It was hoped that by being more stable than mRNA that these molecules would remain detectable within sputum but undetectable in non-viable bacilli.

2.2 Aim

The purpose of this chapter was to design and develop novel assays building on the mycobacterial load methodology. Two novel genes were selected based on their similar properties to 16S rRNA: tm-RNA and pre-16S rRNA. The assays were designed *in silico* to be highly specific. Then the assay conditions and reactant concentrations were optimised to improve sensitivity. Finally, the assays were required to be duplexed with *phyB* internal control used by the MBL assay ensuring there was no competition between PCR reactions.

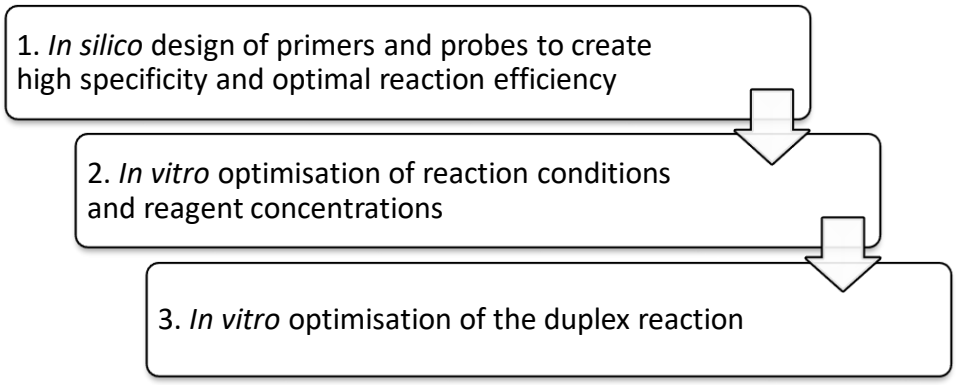

Figure 2.1: Flow chart of the three steps of assay design for the pre-16S rRNA and tm-RNA assays

2.2.1 RNA Extraction

RNA was extracted using the Ambion RNA pure link kit (Ambion, UK). 0.65g of 0.1mm glass beads (PEQlab, Germany) were weighed and added to Lysing Matrix B tubes (MPBio, USA). The *Mycobacterium bovis BCG* pellets were thawed from the -80°C freezer and then re-suspended in 950µl of lysis buffer supplemented with1% β-mercaptoethanol and 50ng of *phyB* internal control. The lysis buffer and pellet were then transferred to the lysing tubes and homogenised using the Precellys ® (CNIM, France) for 40 seconds at 6000rpm. Lysing matrix tubes were then centrifuged at 12000g for 5 minutes. 800µl supernatant was removed and the RNA precipitated using an equal volume 70% ice-cold ethanol. 600µl of the mixture was passed through the spin cartridge at 12000g for 15 seconds and repeated until there was no mixture

remaining. The spin cartridge membrane was washed first with 700µl of wash buffer I and the twice with 500µl of wash buffer II by centrifuging at 12000g for 15 seconds. Drying of the membrane was achieved by centrifuging for further minute. 50µl of RNase-free water was added to the spin cartridge and incubated at room temperature for one minute to elute the RNA. The solution was then passed through the membrane by centrifuging for 15 seconds at 12000g.

DNase treatment was performed using the TURBO DNA-free™ Kit (Ambion, UK) to remove genomic DNA. 10µl of 10x turbo DNase buffer and 1µl of Turbo DNase enzyme was added to each sample and incubated at 37°C for 30 minutes. After half an hour a further 1µl of Turbo DNase enzyme was added and the sample was incubated for another 30 minutes. The reaction was then ceased by 10µl of homogenized DNase inactivation reagent and incubated at room temperature for five minutes. The inactivation reagent was viscous and to maintain homogeneity the sample was vortex repeatedly. After incubation the inactivation reagent was removed by centrifugation at 10000g for two minutes and then removal of the supernatant.

2.2.2 Preparation of PhyB Internal Control

A 1957bp region of the potato *phyB* gene was used as the internal control according to the Honeyborne et al protocol.(Honeyborne et al. 2011) The purpose of the internal control is to control for variability of RNA extraction and any potential PCR inhibition. The original template was generated by freeze drying potato tuber and then reducing it to powder in a pestle and mortar. Genomic DNA (gDNA) was then extracted. Modified PCR primers were used to amplify the region of interest (phyB 1957bp gene fragment) using the HotStartTaq DNA (Qiagen, Germany) polymerase kit (Table 3.1). The forward primer has the 1957bp sequence for *phy B* and a T7 promoter designed into the primer to allow reverse transcriptase to transcribe the sequence into mRNA *in vitro*.

Component	DNA Template	F+R Primer (10µM)	10x Buffer	Mg^{2+}	dNTP	Taq	H_2O	Total Volume
Volume (µl)	2.5	1	2.5	1.5	0.625	0.4	15.475	25

Table 2.1: Master Mix Components

2.2.2.1 Thermal profile

The Taq polymerase was activated at a temperature of 95°C for 15 minutes. Cycling started with denaturing of the double stranded DNA at 94°C for 30 seconds. This was followed by annealing of the primers at 70°C for 45 seconds and extension of the product at 72°C for 2 minutes. The process was repeated for forty cycles to ensure adequate generation of final product. After the final cycle a further extension phase of 10 minutes at 72°C was utilised to promote completion of the partially extended products. A final hold temperature of 4°C prevented degradation of the cDNA.

	Primer	Sequence
F	**Sol *phy B***	5'-TAATACTCACTATAGGGACCACCATGGGTTCACTCACAATCAAAGCATTCA-3'
R	**Sol *phy B***	5'-TCATGGAATTTCGACCGCCACCCACAGCTTCC-3'

Table 2.2: Sol *phyB* Primer Sequences

The resulting PCR product was checked using a 1% electrophoresis gel at 60V for 40min to confirm the fragment was correct length according to the DNA ladder. The fragments were then extracted out of the gel using Gel extraction kit (Qiagen, Germany). The quantity of the purified product was measured using Nanodrop. The internal control RNA was then generated by *in vitro* transcription of the gel purified phyB 1957bp PCR product at 37°C for 16h using the Megascript T7 kit (Ambion, UK). Each reaction mixture was made of 20µl of nuclease water, 2µl of ATP, 2µl of CTP, 2µl of GTP; 2µl of UTP, 2µl of 10X reaction buffer, 0.1-1µg of linear DNA template and 2µl of enzyme mix was added. This was incubated at 37°C for 16 hours. The RNA concentration was measured using the Nanodrop to assess quality and Qubit for accurate quantification.

Then IC RNA was then stored at 50ng/µl in 20µl aliquots to reduce freeze-thawing cycles and thus RNA decay.

2.2.3 Reverse Transcriptase-quantitative Polymerase Chain Reaction (RT-qPCR)

Duplex RT-qPCRs for the two targets: pre-16S rRNA and tm-RNA; were performed based on Honeyborne et al published protocol using the Quantitect PCR kit (Qiagen, UK) and primers - dual labelled probes (MWG Eorofins, Germany). Each reaction mixture was consisted of 5µL 2x Quantitect Multiplex RT-PCR No ROX Master mix, 200nM (final) each of forward primer, reverse primer and dual labelled probe, 0.1µL Quantitect Multiplex RT Mix and volume adjusted to 10µL with RNase free water plus 2µL of sample RNA extract. A no RT mix was made in parallel and used as a negative control to ensure that only RNA transcripts and not bacterial genomic DNA were being detected. The RT containing reaction mixtures were run in duplicate for each sample whilst the no RT reaction were run in singles using Rotor-Gene Q 5-plex HRM platform (Qiagen, UK) with the following parameters: single steps of 50°C for 30 minutes and 95°C for 15 minutes followed by 40 cycles of 94°C for 45 seconds and 60°C for 75 seconds. Background threshold was set the same for both genes in a run.

Component	**Sample**	**Mastermix**	**RT mix**	**Target Forward and Reverse Primer (10µM)**	**Target Probe (20µM)**	***PhyB* Forward and Reverse Primer (10µM)**	***PhyB* Probe (20µM)**	**RNAse free Water**	**Total Volume**
Volume (µl)	2	5	0.1	0.2	0.1	0.2	0.1	2.3	10

Table 2.3: Constituents of RT-qPCR reaction

2.2.4 RT-qPCR Analysis

Analysis of the RT-qPCR results was performed using the Rotorgene software (Qiagen, Germany). All raw amplification curves were visually inspected to determine if

exponential amplification had occurred. If this was not the case, the reaction was deemed negative.

The "Dynamic Tube" function was utilised so that the average background of each well was ascertained just before amplification commenced. The "Slope Correction" function was used for samples where the baseline fluorescence was variable. Threshold was set at 0.01 ensuring that the amplification plots were in the exponential phase.

2.2.5 Primer and Probe Selection

The *PhyB* Internal Control primers and probes synthesised as described previously in Honeyborne at al. (Honeyborne et al. 2011). The sequences are detailed in table 2.4.

PRIMER/PROBE	SEQUENCE
IC-Forward	5'-GCACAGGGTTGATGTTGGTATTGTC-3'
IC-Reverse	5'-CAAATGAGAAATAGCCCTCACTGCAAG-3'
IC-Probe	5'JOE-GCAGGGTCCTCAGTTCTAGCAGGCTCCA-3'BHQ1

Table 2.4: Honeyborne et al. published *PhyB* IC Primers and Probes.(Honeyborne et al. 2011)

To determine appropriate primers and probe for pre-16S rRNA and tm-RNA, first, the sequence for pre-16S rRNA and tm-RNA were located on PubMed® gene database. Then a blast search was conducted to find the specific DNA sequence. Then using beacon designer® (PREMIER Biosoft, USA), the exact sequence and length primers and probes were selected with the best characteristics to produce optimum PCR efficiency. A range of 1 to 8 $\log_{10}$ CFU/ml of diluted RNA was used to assess each assay, as would be expected range in patient sputum samples.

2.2.6 Optimisation of PCR conditions and reagent concentrations

To be able to run the two new assays in tandem with the MBL assay the PCR conditions were kept the same and detailed below in table 3.5. The Taq polymerase was activated at a temperature of 95°C for 15 minutes. Cycling started with denaturing of the double stranded DNA at 94°C for 25 seconds. This was followed by annealing of the primers and extension of the product at 60°C for 60 seconds.

Step	Temperature and duration
Reverse Transcriptase	50°C/30min
Taq Polymerase	95°C/15min
Denaturing	94°C/45s
Extension	60°C/60s
Cycles	40

Table 2.5: RT-qPCR cycling conditions for MBL and set up of novel assays.

The next step was to vary the concentrations of the reagents of the mastermix and the concentrations of the oligonucleotides. The Qiagen Quantitech mastermix is specifically designed to be optimised for multiplexing reactions. Therefore in the first instance the primer and probe concentrations were optimised to achieve ideal PCR efficiency.

2.2.7 Optimising primer and probe concentrations

Primers and probe concentrations were optimised by calculating reaction efficiencies for concentrations ranging from 50-400nM. Target RNA serially diluted in eight tenfold dilutions was amplified and standard curves generated and the resultant Ct values were used to calculate reaction efficiency. This was done by first deriving a linear model to fit the data with the formal efficiency=mx+c. Then using the value of m the efficient was determined using the formula: efficiency = $10^{(-1/m)}$ -1. Threshold values were set at 0.01. The optimum primer concentration was deemed to be that which gave efficiency between 0.9 to 1.1 and a wide quantification range. First the primers were adjusted and then using the concentration derived the probe concentration was optimised.

2.2.8 Duplexing

The next step was to duplexing the novel tm-RNA and pre-16S rRNA assay with their own with the *phyB* internal control assay. There are a number of concerns with duplexing two PCR reactions listed below:

1. The reagents could interact i.e. the oligonucleotides could form crosslinks if there is inter-primer/probe homology.
2. The substrates of the one PCR reaction could react with the oligonucleotides of the other reaction
3. When both reactions are occurring there could be competitive inhibition. For example, if one reaction occurs earlier than the other then it could deplete all the dNTPs before the second reaction begins.

The first two issues can be checked *a priori* by *in silico* BLAST search of the primers and probes designed for each reaction against the new substrate now present within the reaction. The third concern can be assessed by comparing the efficiency of the reaction when both reactions are occurring to the singleplex reaction efficiency. This was done by adding 50ng of *phyB* RNA internal control to the *M. bovis BCG* culture as would be performed in the MBL assay protocol. Then duplex reaction was run on samples containing both *phyB* and *M. bovis BCG* and the efficiencies recorded.

2.3 Results

2.3.1 Optimisation of Primers and Probes

The primer and probes of each reaction were developed separately.

2.3.1.1 M. bovis BCG pre-16S rRNA RT-qPCR reaction optimisation

The pre-16S rRNA primer concentrations were varied between 50-400nM. The resulting reaction efficiencies and quantification ranges are detailed in table 2.6.

Primer Concentration	Efficiency	Range of neat RNA extract quantified (log_{10} eCFU/ml)
50nM	0.93	6-7
100nM	1.18	5-8
200nM	1.09	4-8
400nM	1.01	5-8

Table 2.6: Pre-16S rRNA primer concentrations and resulting efficiencies and range of quantification

The 50nM efficiency was acceptable but only when the quantification range was between 6 and 7. The quantification range was better at 100nM but the efficiency was too far from 1. The 200nM concentration gave the widest quantification range and acceptable reaction efficiency. The 400nM gave the best reaction efficiency with a slightly lower quantification range than the 200nM concentration. The optimum primer concentration would be between 200nM and 400nM from the concentrations tested. The 200nM concentration gave the largest range of quantification with an acceptable efficiency and therefore this concentration was carried forward into the next set up stage. Table 2.7 details the results of varying probe concentrations using 200nM of primers.

Probe Concentration	Efficiency	Range of neat RNA extract quantified (log_{10} eCFU/ml)
50nM	0.91	4-8
100nM	0.90	4-8
200nM	0.91	4-8
400nM	0.94	4-8

Table 2.7: Pre-16S rRNA primer concentrations and resulting efficiencies and range of quantification

All of the probe concentrations gave acceptable efficiencies and quantification ranges. For ease of use 200nM was selected for both the *M. bovis BCG* primers and probe.

2.3.1.2 M. bovis BCG tm-RNA

The same set of experiments was repeated for *M. bovis BCG* tm-RNA. The concentrations of primers were varied first and the results tabulated in table 2.8.

Primer Concentration	Efficiency	Range of neat RNA extract quantified (log_{10} eCFU/ml)
50nM	0.87	6-8
100nM	0.97	2-8
200nM	1.03	2-8
400nM	1.09	2-8

Table 2.8: Tm-RNA probe concentrations and resulting efficiencies and range of quantification

Quantification and efficiency was acceptable between the range of 100nM to 400nM. Once again 200nM was selected.

Then using a primer concentration of 200nM the probe concentration was varied from 50 to 100nM.

Probe Concentration	Efficiency	Range of neat RNA extract quantified (log_{10} eCFU/ml)
50nM	0.92	3-8
100nM	0.97	2-8
200nM	0.94	2-8
400nM	0.90	3-8

Table 2.9: *M.bovis BCG* tm-RNA probe concentrations and quantification range

All the concentrations tested of tm-RNA probe gave acceptable efficiencies. The quantification range was widest with 100 and 200nM. The optimum concentration would therefore lie between these two concentrations, 200nM was again selected.

2.3.1.3 Duplexing

The set up assays were performed in singleplex to ensure that there was completion between the *M. bovis BCG* reactions and the *phyB* internal control reaction the efficiencies were rechecked when a duplex reaction was being run.

Target	Efficiency	Range of neat RNA extract quantified (log_{10} eCFU/ml)
Pre-16S rRNA	1.04	4-8
Tm-RNA	0.98	2-8

Table 2.10: Efficiencies and quantification ranges for the pre-16S rRNA and tm-RNA assays when duplexed with *phyB* assay.

The reaction efficiencies and quantification ranges did not change when the reactions were run in duplex.

2.4 Discussion

The purpose of these series of experiments was to create two assays that could work in tandem with the 16S rRNA (MBL) assay to quantify *M. tuberculosis*. The first aim was to create assays that could be run on the same sample and at the same time as MBL. Therefore, the methods in terms of RNA extraction and RT-qPCR should be the same as those for MBL. The second aim was to use the successful *phyB* internal control that improved accuracy and reliability of quantification of *M. tuberculosis*. To achieve all of these goals the following steps were undertaken detailed in figure 2.1.

2.4.1 M. bovis BCG

M. bovis BCG was an ideal surrogate for *M. tuberculosis* in assay development as the target sequences were conserved between both *M. tuberculosis* and *M. bovis BCG*. The lack of virulence of *M. tuberculosis BCG* meant it could be used in a CL2 laboratory and reduced any potential health risks.

2.4.2 In vitro optimisation

The duplex *M. bovis BCG* 16S rRNA and tm-RNA assays produced good reaction efficiencies on extracted culture. In singleplex reactions there is a potential that the reaction can be inhibited or fail. Duplexing the reaction with the internal control prevents the false negative results. The difficulty with duplex reactions is that they often

interact and compete for the same reagents. This reduces the efficiency of the reaction and alters the accuracy and reliability of quantification.

Optimisation of the assays produced acceptable results without extensive checkerboard experiments to achieve adequate reaction efficiencies. This could be in part due to the particular Qiagen mastermix used. The Qiagen mastermix used has three unique properties separating from conventional mastermixes that improve specificity and efficiency. The first is that NH_4 will destabilize mismatched primers. Synthetic Factor MP, an innovative PCR additive, increases the local concentration of primers at the template. Together with K+ and other cations, synthetic Factor MP stabilizes specifically bound primers, allowing efficient primer extension by HotStarTaq DNA Polymerase. Finally, the addition of random primers to the mix increases local concentrations of primers through macromolecular crowding.

The primers were specific to *Mycobacterium tuberculosis* target gene. The reaction is very efficient through an expected range of bacillary loads.

2.5 Conculsion

Two novel assays had been successfully developed first *in silico* and then *in vitro*. It was now time to test them *in vivo*.

3 Chapter 3: Comparison 16S rRNA, pre-16S rRNA and tm-RNA

3.1 Introduction

The mycobacterial load assay had been successfully developed by the Gillespie group and was published in two papers.(Honeyborne et al. 2011; Honeyborne et al. 2014) The assay had demonstrated the ability to very accurately quantify bacterial load of cultured *Mycobacterium tuberculosis* in media, artificial sputum and pooled sputum. In one hundred and eleven patients the assay successfully monitored treatment response by declining during treatment. There was a significant difference in the bi-exponential model fitted to data of those that achieved cure compared to patients that relapsed. Following this success, the assay was taken forward to assess its ability to act as a surrogate end point in clinical trials. Unpublished data from the Gillespie group suggests that 16S rRNA remains present when *Mycobacterial* cells are no longer viable. In an attempt to more accurately detect viable *Mycobacterial* cells two less stable RNA molecules were selected: tm-RNA and pre-16S rRNA. Both of these RNA species have secondary structures making them more stable than mRNA but are less stable than 16S rRNA. The assays were designed using the beacon designer® (PREMIER Biosoft, USA) by Dr Katarina Oravcova.

3.1.1 Pan-African Consortium for the Evaluation of Anti-tuberculosis Antibiotics Biomarker Extension (PANBIOME) Project

PANBIOME are part of the Pan-African Consortium for the Evaluation of Anti-tuberculosis Antibiotics (PanACEA) funded by European & Developing Countries Clinical Trials Partnership (EDCTP). The remit of PANBIOME is to develop molecular tools to assess treatment response as part of the PanACEA clinical trials programme and in

doing so establish molecular diagnostics; develop capacity and participate in training. A large-scale biomarker trial investigating the MBL assay was to be undertaken at four sites: Kilimanjaro Christian Research Institute Biotechnology Laboratory, Moshi, Tanzania; Mbeya Medical Research Centre, Mbeya, Tanzania; College of Medicine, University of Malawi, Blantyre, Malawi; Mozambique National Institute of Health, Maputo, Mozambique. The samples collected at the Tanzanian sites in Moshi and Mbeya were as part of the MAMS-TB-01 clinical trial whereas; in Maputo and Blantyre patients were recruited independently for PANBIOME.

The original intent was to take the novel pre-16S rRNA and tm-RNA assays to the field and assess their ability to monitor response and compare with the MBL assay.

3.1.2 MAMS-TB-01 Clinical Trial

Phase III clinical trials in tuberculosis have been expensive. A more cost effective and rapid drug development programme is required for tuberculosis as there is a large number of lead compounds being developed and an exponentially greater number of combinations to be investigated. (Ma et al. 2010; Zumla et al. 2014) The complete title of MAMS-TB-01 is "A multiple arm, multiple stage (MAMS), phase 2, open label, randomized, controlled clinical trial to evaluate four treatment regimens including SQ109, two increased doses of rifampicin, and moxifloxacin in adult subjects with newly diagnosed, smear positive pulmonary tuberculosis".(Boeree & Heinrich n.d.) MAMS-TB-01 utilises a unique design adapted from cancer trials: multiple arm and multiple stage. The design allows for the assessment of numerous treatments using small patient numbers and enables drug development to move seamlessly from phase II to III. The MAMS methodology starts with a phase II trial of a number of treatment regimens. Then, the number of arms is dynamically reduced until only the regimens that are not ineffective remain in a final phase III trial. The reduction of arms is achieved by performing interim analyses after fixed periods of time and dropping those treatments

that are not achieving a particular hazard ratio for a surrogate endpoint. For the MAMS method to be effective the analysis of the surrogate endpoint must be available rapidly and must correlate with the definitive outcome.

In MAMS-TB-01 the endpoint is culture conversion at three months. The time for a negative result in MGIT culture is 42 days making any interim analyses slow. A molecular biomarker could achieve the rapidity required. Assessment of any potential biomarker would have to occur within phase III trials to demonstrate correlation with primary outcomes. To achieve the aim of improving the interim analyses and discovering if molecular methods correlate with long-term clinical endpoints the MAMS-TB-01 trial has assessment of molecular bacterial load as a secondary outcome.

	Secondary Efficacy Outcomes
1	Time to stable culture conversion to negative on solid media (defined as two negative cultures without an intervening positive culture)
2	Time to first negative culture in liquid media
3	Time to first negative culture on solid media
4	Proportion of patients converting to negative sputum culture in liquid media (defined as two negative cultures without an intervening positive culture) at each time point during treatment
5	Proportion of patients converting to negative sputum culture on solid media (defined as two negative cultures without an intervening positive culture) at each time point during treatment
6	Rate of change in time to positivity in BD MGIT 960® liquid culture during treatment
7	**Rate of change in molecular bacterial load (MBL) assay during treatment**
8	Rate of change in GeneXpert MTB/RIF (Xpert) quantitative PCR result during treatment
9	Proportion of treatment failures and patients developing drug resistance

Table 3.1: The secondary efficacy outcomes from MAMS-TB-01 clinical trial

MAMS-TB-01 methodology has a number of limitations and difficulties with implementation, type I and type II error that has been previously discussed (Sydes et al. 2009).

MAMS-TB-01 is being conducted in three sites in Tanzania and four sites in South Africa. There are fours treatment arms plus the control arm. The treatment arms varied the intensive phase of treatment. Arm 1 used high dose rifampicin at 35mg/kg. Arm 2 replaced ethambutol with SQ109 (300mg). Arm 3 again replaced ethambutol with SQ109 (300mg) and used higher dose rifampicin at 20mg/kg. Arm 4 substituted moxifloxacin (400mg) for ethambutol and used high dose rifampicin at 20mg/kg. The control followed the dose regimen as recommended by the WHO. Figure 4.1 details the four initial treatment arms that began the phase II trial.

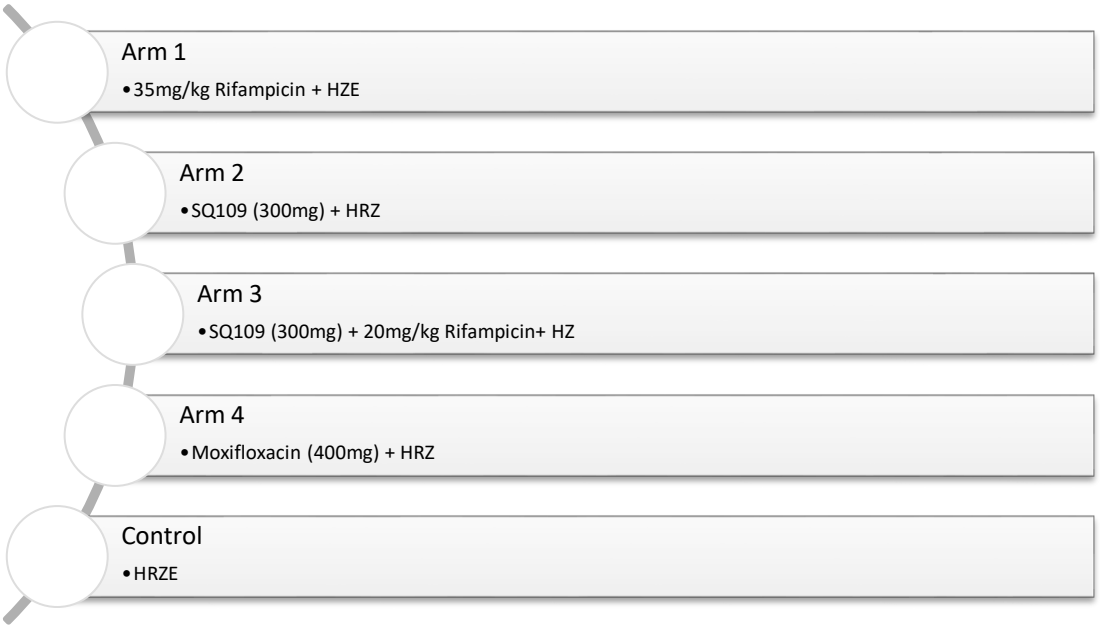

Figure 3.1: Diagram of the four arms of treatment for MAMS with the control arm. Doses are as per the WHO guidelines unless otherwise stated. H - Isoniazid, R - Rifampicin, Z - Pyrazinamide, E - Ethambutol.

3.1.3 Background to Sputum Processing

Prior to the application of any assay sputum processing is performed for two reasons: first to liquefy the sputum to allow for easy manipulation and second to decontaminate, thus removing any other organisms other than *Mycobacteria*.

Liquefaction can be either mechanical by bead beating or chemical. The majority of mycobacterial specimens are contaminated with faster growing bacteria.

Petroff's method, using NaOH, is the most common decontaminant and also serves as a mucolytic agent. Care must be taken to get the correct concentration, as it is only slightly less harmful to mycobacteria than the common contaminating bacteria. Killing of mycobacteria increases with the temperature of the acid and concentration. Harsh killing can kill up to 20-90% of mycobacteria reducing quantification by 1 $\log_{10}$ CFU/ml. DTT and several other enzymes effectively liquefy sputum and when used in combination with NaOH they reduce the concentration of NaOH required. Thus, improving mycobacterial recovery. Respiratory secretions likely contaminated with pseudomonas can be decontaminated first with NaOH-NALC and then 5% oxalic acid solution. NALC quickly loses it's activity in solution and therefore must be prepared fresh each day. After decontamination PBS (pH 6.8) is used to neutralise and homogenise the solution prior to centrifugation.

All manipulation of suspected *Mycobacterium tuberculosis* samples must be performed in a category three laboratory and result in not insignificant risk to the operator therefore any reduction in this processing is preferable. Below is the typical pathway of sputum processing in a clinical laboratory.

The MBL assay can be performed without allowing any sputum processing to occur. However, there are number of reasons why this is not preferable. The first reason is the ease of incorporation of the assay within the clinical laboratory where all samples are already being processed and then subdivided for individual tests. The added benefit using an aliquot of the same sample is that the new assay can be directly compared to the classical microbiology techniques.

3.2 Aim

The aim was to evaluate and compare two novel markers for the detection and enumeration of *Mycobacterium tuberculosis* in the field comparing with both current measures and clinical outcome using samples from MAMS-TB-01 at KCRI.

3.2.1 MAMS-TB-01

The sputum collection was processed following the MAMS-TB-01 trial protocol. Both 'early morning specimens' and 'spot specimens' were collected. To be defined as an early morning sputum the sample was collected after waking where the patient inhales three times then expectorates. The same method was used for spot samples but they were taken at clinic. The information on where samples were EMS or SS was not available. Pooled sputum specimens where the cumulative sputum is collected over a 16-hour period between 4pm and 8am, was not selected, as although greater yield was achieved there was also a higher rate of contamination and were not used in this study. Sputum samples were collected in sterile, single use, screw capped containers in clinic at Kibong'oto Hospital in Tanzania. Transport was in cool box containing cool packs aiming to get the temperature between 2 to 8°C. Temperatures of the cool boxes were measured on arrival to KCRI and documented. Samples were not deemed to be of high enough if they were less than 2ml or consisted primarily of blood or salvia. Any samples not processed that were not processed with 30 mins of arrival of at the lab were kept refrigerated and was then processed within 48 hours. Reproducibility of sputum processing was improved by only allowing 7 patient samples and one negative control to be handled at one time.

To 500ml of 4% NaOH, 10g of NALC was added and gently agitated to dissolve. Following this 500ml of 2.9% sodium citrate was added to the mixture. This generated the decontamination mixture of 2% NaOH; 1% NALC; 1.45% sodium citrate. All sputum samples were transferred to individual sterile 50ml falcon centrifuge tubes. An equal volume of decontamination mixture was then added to the 50ml falcon tube. To enable

liquefaction the tube was vortex for 15 to 20 seconds. The tubes were left to stand for 20 mins and then volume of the tube was brought up to 50ml using PBS (pH 6.8). The tube was again vortexed prior centrifugation at 3000g for 15min at 4C. The supernatant was then discarded and the pellet suspended in 2ml of PBS (pH 6.8). Aliquots of the 2ml of suspended pellet were then used for smear microscopy; inoculation of MGIT tubes, LJ slopes and blood agar plates. MPT64 AG test was used for the confirmation of *M. tuberculosis.*

3.2.2 RNA preservation

Two patient sputum samples were collected in the clinic at each time point, one early morning and one spot sample. The entirety of the early morning sample was used for routine bacteriology detailed above and the spot sputum was transferred into 5 M GTC, 0.1 M Tris-HCl (pH 7.5), and 1% β-mercaptoethanol, within four hours after expectoration in order to preserve the *M. tuberculosis* RNA. Samples were transferred to the laboratory within 2 h and then frozen at −80°C until RNA extraction.

Patient sputum samples were stored at -80°C after the addition 4 ml of 5 M GTC (Promega, USA) 17 mM N-lauroylsarcosine sodium salt, 25 mM trisodium citrate (pH 7.0 with 1 M HCl), 1% Tween 80, and 0.7% β-mercaptoethanol for each 1ml sputum.

3.2.3 Preparation of Standards

BCG was sub-cultured for 19 days to prepare stock of ~10^7 CFU/ml. Exact CFUs were calculated using the modified Miles-Misra method. The 100ul of stock was added to 900ul of artificial sputum and then 4ml of GTC + 1% beta-mecaptoethanol. This was then stored at -80°C with the patient samples until RNA extraction. For the low standard 100ul of a 1 in 1000 dilution was used. The standards were generated firstly at University College London by Dr Honeyborne then later on site at KCRI. Standards were quality assured by sacrificing and extracting two high and two low standards and ensuring the predicted bacterial load by 16S rRNA was within 1 estimated $\log_{10}$ CFU/ml of the value derived from modified Miles-Misra method.

3.2.4 Generating the Internal Control

Multiple 50µl aliquots of 50ng/µl *phyB* internal control were generated as detailed in chapter 2.

3.2.5 RNA Extraction

The extraction protocol was based on the acidified phenol method from Honeyborne et al (Honeyborne et al. 2011). Patient sputum was extracted in sets of 13, 1 baseline sample plus a further 12 sputa taken each week during treatment. For each extraction, 2 high standards (log_{10} 7) and 2 low standards (log_{10} 5) were extracted along with the patient set as positive controls. Prior to extraction, samples and standards were thawed at room temperature and then spiked with 50ng of Internal control *phyB* RNA.

Extraction was conducted in two stages. In first stage *M. tuberculosis* bacilli were lysed using Precellys 24 homogeniser (pEQlab) by bead beating for 40s at 6000rpm to release nucleic acids in the category three laboratory (CL3). Hood, pipettes and racks were cleaned with RNase away. Each 10ml sample of 1 part sputum to 4 parts GTC was homogenised by repeated pipetting. The homogenate was then divided into separate 15ml Falcon tubes. 50ng of IC RNA was the added to each of the samples and standards and then centrifuged at 3,000g for 30min. After centrifugation, the supernatant was decanted off into a disinfectant bottle containing 2% tristel. Then 950µl of RNApro solution was added and then mixed until the pellet was dislodged. This was then transferred to the blue lysis matrix B tubes (MP Biomedical, USA). The pellet was the lysed in the Fastprep bead beater at 6000rpm for 40s. After this stage the lysate has been determined non-viable and as such the rest of the extraction was completed in the CL2. Lysising matrix B tubes were then centrifuged at 13,000g for 10mins and then left to stand at room temperature (RT) for 5min. The liquid part of the lysising matrix B tubes was transferred to the eppendorf containing 300µl of chloroform, ensuring not to take any of the matrix or debris (approx. 700µl taken per sample). The eppendorf was then vortexed for 10s and left to stand at RT for 5min and then centrifuged for 5min at 13,000g to separate out the aqueous phase. The aqueous phase (approx. 350µl) was then pipetted into new eppendorf tubes and to this 500µl of 100% ice-cold ethanol was added. DNA was left to precipitate overnight at -20°C. Using a microfuge chilled to 4°C

the tubes were then centrifuged at 13,000g for 30min. The supernant was removed and discarded and then the pellet was washed using 70% ice-cold ethanol and dried on the heat block at 50°C for 30min. RNA was then re-suspended in 100µl of RNase free water and DNAse treatment was then performed as detailed in 3.6. After the DNAse treatment the RNA was then stored at -80°C to await quantification by RT-qPCR.

3.2.6 DNase Treatment

As DNA from the primary sample could alter the quantitative RNA result, a DNase treatment step was performed using the Turbo DNase kit (Ambion, UK). 5µl of 10x Turbo DNase and 1µl Turbo DNase was added to each RNA sample and mixed gently then incubated at 37°C for 30 min shaking at 1000rpm. A further 1µl of DNase enzyme was then added and the sample was incubated for another 30 min. The reaction was stopped by adding 5µl homogenized DNase inactivation reagent and incubation at RT for 5 min with X3 vortexing to mix the contents. The mixture was centrifuged at 10,000g for 1.5min and the supernatant (pure RNA) was transferred to a new tube and stored at -80°C.

3.2.7 Reverse Transcriptase-quantitative Polymerase Chain Reaction (RT-qPCR)

Duplex RT qPCRs for the three targets including 16S rRNA were performed based on Honeyborne et al published protocol using the Quantitect PCR kit (Qiagen, UK) and primers - dual labelled probes (MWG Eorofins, Germany). Each reaction mixture was made of 12.5µL 2x Quantitect Multiplex RT-PCR No ROX Master mix, 200nM (final) each of forward primer, reverse primer and dual labelled probe, 0.25µL Quantitect Multiplex RT Mix and volume adjusted to 20µL with RNase free water plus 5µL of sample RNA extract. A no RT mix was made in parallel and used as a negative control to ensure that only RNA transcripts and not bacterial genomic DNA were being detected. The RT containing reaction mixtures were run in duplicate for each sample whilst the no RT

reaction were run in singles using Rotor-Gene Q 5-plex HRM platform (Qiagen, UK) with the following parameters: single steps of 50°C for 30 minutes and 95°C for 15 minutes followed by 40 cycles of 94°C for 45 seconds and 60°C for 75 seconds. Background threshold was set the same for both genes in a run. The extracts were run for the three targets 16S-rRNA, tm-RNA and pre-16s rRNA.

3.2.8 Comparing dilute versus neat extracted RNA

Diluting the extracted RNA 1 in 10 can reduce the inhibition seen from sputum samples and thus improve accuracy of quantification. The limit of detection of both pre-16S rRNA and tm-RNA are both high in-vitro and therefore the method of diluting the extracted RNA 1 in 10 potentially lose a significant amount of Boolean data. To determine if this hypothesis was accurate: four patient sets, 52 samples, were run both neat and dilute. The number of Boolean data points generated was compared using a two-tailed t-test.

3.3 Statistical and Analytical Methods

All statistical analyses were performed in Ri386 3.1.0 (The R Foundation for Statistical Computing, Austria). A Shapiro-Wilk's test and a visual inspection of their histograms, normal Q-Q plots and box plots were used to check for normality. Paired, two tailed students t-tests were used to compare results from the *phyB* internal control.

3.4 Results

A total of ninety-one patient samples from seven patients were processed for 16S rRNA, pre16S rRNA and tm-RNA. The corresponding mycobacteriological data was collated, including MGIT and LJ.

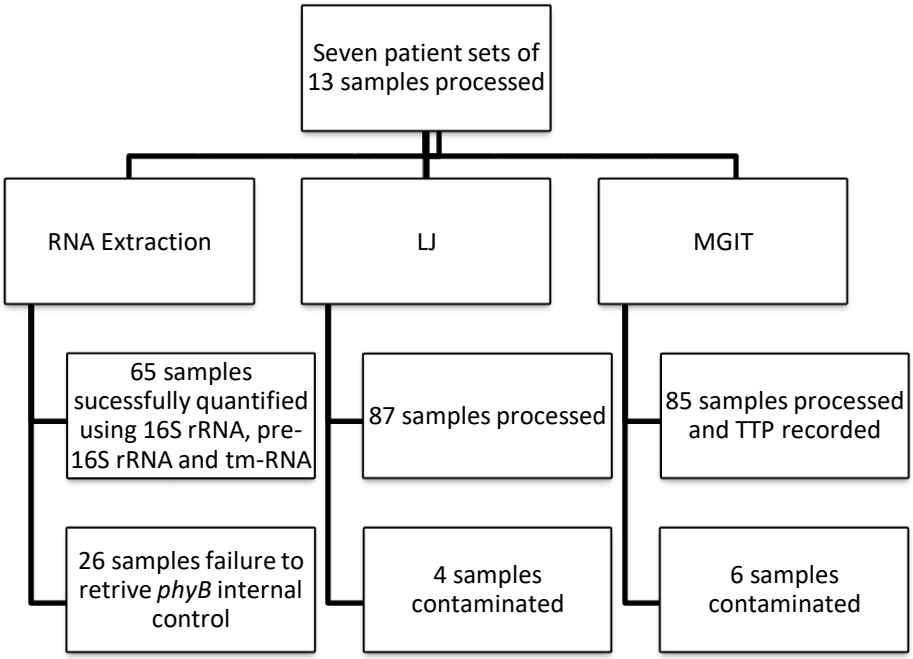

Figure 3.2: Flow chart of sputum processing summarising molecular and culture results

3.4.1 Comparing dilute versus neat extracted RNA

Four patient sets of 13 samples each were quantified from either 1in 10 diluted or neat extracts. The total number of positive results was tabulated in Table 3.2.

	p16	**tm**
Total	52	52
Positive results in the diluted extracts	7	11
Positive results in the undiluted extracts	5	9
Positive results from running both dilute and undiluted	7	11

Table 3.2: The number of positive results returned from 1 in 10 diluted and neat extracted RNA

Although there was more data generated using the dilute extracts there were no more positive results gained from running both 1 in 10 dilutions and neat extracted RNA.

3.4.2 The Internal Control

Towards the end of the experimental series a change in the *phyB* internal control was noted. The absolute values for *phyB* control were reviewed and plotted in the figure 3.4.

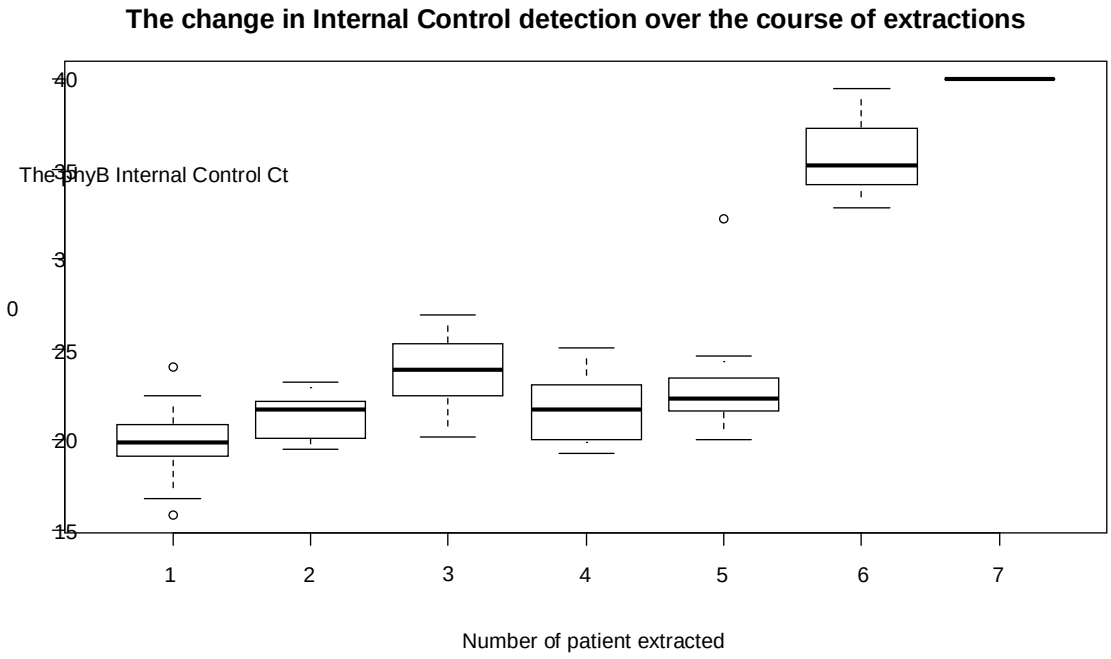

Figure 3.3: Boxplots of the *phyB* internal control Ct for all samples extracted within each patient set. Patient sets are numbered in order that they were extracted

The figure is a boxplot of the internal control Ct's of each successive patient extraction. The first five patient extractions achieved an acceptable range of Ct's: 15-25. The mean *phyB* internal control Ct increased after the 6th patient set extraction and then was not retrieved in the final patient. This should suggest a failure of extraction or the presence of PCR inhibitors if the internal control was functioning as expected. The high and low standards for patient 6 and 7 were not significantly different than the first five patients. Student's t test p value equals 0.23 and 0.16 for the low and high standard respectively.

If the reaction was inhibited or the extraction failed the target cycle thresholds would be expected to be similar to the internal control. The Ct's for *M. tuberculosis* 16S rRNA and *phyB* internal control for patient 6 are plotted below in figure 3.5.

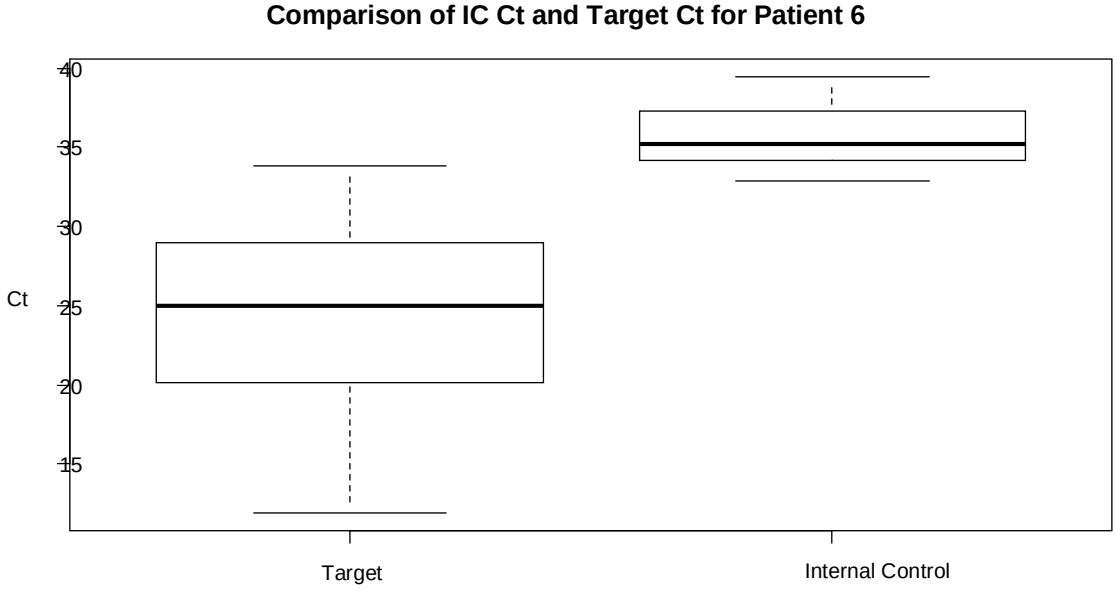

Figure 3.4: The range of Ct's for patient samples comparing the target *M. tuberculosis* 16S rRNA with the *phyB* internal control from the same sample

The Ct's measured for 16S rRNA were within the expected range but the *phyB* internal control Ct's where significantly higher (unpaired two tailed student t-test $p=2.84x10^{-12}$). One in 10 dilutions did not improve internal control Ct's. This would suggest that extraction of the patient samples had been successful and the samples did not contain any inhibitors.

To further investigate the reason for failure of internal control retrieval; high and low standards with known concentrations of *M. bovis BCG* were extracted and amplified. Two high and low standards (L/H 3 and 4) were extracted using a newly generated *phyB* internal control and two more using the original batch (L/H 5 and 6) of internal control. The results were compared to previous low (L1 and L2) and high (H1 and H2) standards that were extracted before processing patient sets began.

Old Standards	PhyB Ct	16S rRNA Ct
L1	21.1	21.3
L2	20.5	21.6
H1	20.5	8.7
H2	21.9	8.9

Table 3.3: Results of the *phyB* Ct and 16S rRNA from the standards extracted prior to patient extractions

New Standards	PhyB Ct	16S rRNA Ct
L3 – Old phyB	33.0	22.5
L4 – Old phyB	33.4	23.4
L5 – New phyB	26.91	19.14
L6 – New phyB	28.07	18.83
H3 – Old phyB	34.8	9.5
H4 – Old phyB	36.1	8.8
H5 – New phyB	30.82	7.07
H6 – New phyB	29.75	7.63

Table 3.4: Results of the *phyB* Ct and 16S rRNA from the standards extracted after to patient extractions

The standards produced similar Ct's for 16S rRNA (t-test p=0.9) showing good extraction and limited inhibition of the extract. However, the *phyB* internal controls Ct's were significantly higher (t-test $p=1.96x10^{-5}$) and more variable.

To ascertain the reason behind this; the RNA concentrations were rechecked using the Nanodrop 2000 (Thermo scientific, USA) but they remained unchanged at 50ng/µl with the same 260/280 and 230/260 ratios. Integrity of the fragments was check by running series dilutions of the neat *phyB* internal control. This produced substantially lower Ct's than previously.

3.4.3 Normality

The results of the Sharipo-Wilk's test are summarised in Table 3.5.

Marker	Sharipo-Wilk's W	Sharipo-Wilk's p value	n
TTP	0.97	0.32	49
Log_{24}TTP	0.94	0.01	49
16S rRNA	0.97	0.66	29
Pre-16S rRNA	0.89	0.01	23
Tm-RNA	0.95	0.05	48

Table 3.5: Results of Sharipo-Wilk's test for the quantitative markers to assess normality

The data set is small with less the fifty results for each marker. None of the results of the Sharipo-Wilk's test are significant (<0.01) to reject the null hypothesis that the data is normally distributed. The histogram, Q-Q plots and boxplots appeared normally distributed.

3.4.4 Data Summary

Two patients were excluded from analysis due to technical issues with the RNA quantification. The remaining five patients were positive for MGIT, 16S rRNA, pre-16S rRNA and tm-RNA at baseline, where the test was performed.

	LJ	MGIT TTP (hours)	16S rRNA (log_{10} eCFU/ml)	p16S rRNA (log_{10} eCFU/ml)	tm-RNA (log_{10} eCFU/ml)
Min	NA	95	0.4	1.5	0.04
Max.	NA	927	6.2	6.3	5.2
No Detection	18	49	29	23	48
n	65	65	65	65	65
Missing Data	4 (6%)	5 (8%)	0	0	0

Table 3.6: Summary of Quantitative data for the six patients with successful RNA extraction

The MGIT time to positivity had a range from 95 to 927 hours. Mean time to positivity was around 17 days. The estimated CFU/ml ranged from around 0 to 6 log_{10} for each of the markers. The majority of tm-RNA and MGIT results were positive whereas the majority of 16S rRNA, pre-16S rRNA and LJ results were negative. In the 65 samples where the internal control was successfully retrieved RNA markers gave a result, however, in both culture techniques 5-10% samples were contaminated. The changing pattern of positivity for all of the markers is illustrated in figure 3.6.

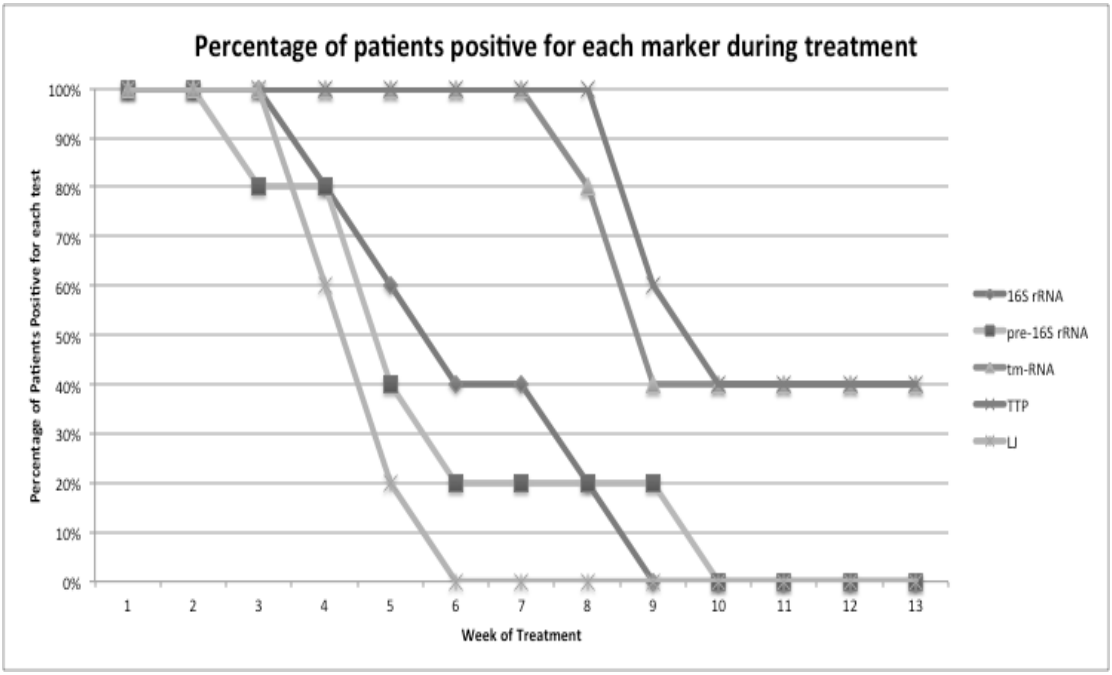

Figure 3.5: The percentage of the cohort of five patients that were positive for 16s rRNA, pre-16S rRNA, tm-RNA, MGIT and LJ for each week during the first twelve weeks of treatment

All five of the markers demonstrate a fall in response to treatment as evidenced by the proportion of sputum samples becoming negative. LJ has the steepest gradient of decline and the five patients have become negative by week six. All of the sputum samples are negative for 16S rRNA and pre-16S rRNA by week 9 and 10 and decline at a similar rate. The slowest markers to turn negative are MGIT and tm-RNA and two patients were still MGIT and tm-RNA positive at the end of twelve weeks. Both of these patients failed to convert and were MGIT positive at the end of treatment and are therefore defined as treatment failures.

To explore this relationship in more detail the bacterial loads of at each week for the individual patients were plotted to determine how the quantitative data is changing over the course of treatment.

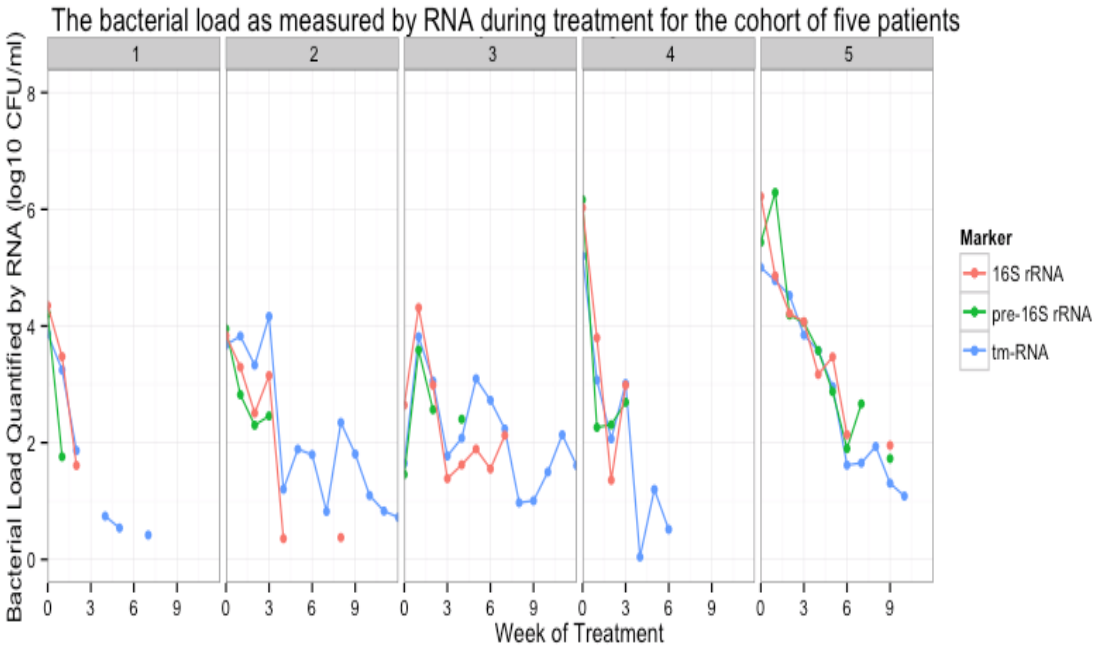

Figure 3.6: Combined plots of the five patient's $\log_{10}$ bacterial load as estimated by 16S rRNA, pre-16S rRNA and tm-RNA over the first twelve weeks of treatment including baseline

The estimated bacterial loads are similar at each time point and follow the same trend of decline in response to treatment. Patient 2 and 3 are the patients that were subsequently defined as treatment failures. In these patients the starting estimated bacterial loads were lower and the gradient of decline is less steep.

3.5 Discussion

The first requisite of a biomarker for monitoring treatment response is to change during treatment. For all three markers this was true as the Boolean and quantitative measures declined in response to treatment. The estimated bacterial loads were all within a range that might be expected during treatment. Most promisingly, there appeared to be differences between the decline of the RNA markers in those patients who were deemed to be treatment failures and those who were not.

3.5.1 Dilution of samples

There were more tm-RNA positive results than 16S rRNA. This is despite the higher limit of detection *in vitro* of tm-RNA, 3 $\log_{10}$ CFU/ml versus 1-2 $\log_{10}$ CFU/ml respectively. The two technical explanations are that: the tm-RNA is non-specifically amplifying or that the 16S rRNA is failing to amplify. The evidence against non-specific amplification of the tm-RNA reaction is that the negative template controls did not amplify. Therefore a template must be being amplified. This could be weak amplification of similar sequence of RNA. However, the trend of decline might not be expected to continue through all the samples if this was the case and it does. The tm-RNA is present when MGIT is positive implying that template is likely to be present. It could be that the 16S rRNA reaction is being selectively inhibited more than the tm-RNA reaction. If this is the case then potentially diluting the samples could give more positive 16S rRNA results. It must be noted that this is a small data set and interpretation is only preliminary.

3.5.2 The Internal Control

It is noticeable that after the fifth extraction the *phyB* internal control failed to amplify as efficiently and became more variable. Clearly extraction was good and there was no inhibition of the samples this was confirmed by extraction of the new high and low standards. The Nanodrop confirmed that stock *phyB* RNA was still present and not contaminated, however, RT-qPCR of the neat RNA showed a decline in the quantity of *phyB* product. This would suggest that the integrity of the RNA had been lost.

It is possible that the Nanodrop readings were incorrect but this seems unlikely as it was working to produce the correct dilutions of the *phyB* internal control initially. The $A_{260/280}$ ratio can be reduced by low pH, thus, reducing sensitivity of detection of protein contamination. The measurements were taken from the RNA dissolved in water. If a buffered solution had been used there may have contamination detected.

The *phyB* RNA was stored in over 20 aliquots making contamination unlikely. The most probable explanation is that the -80°C freezer lost power, as was frequent, and defrosted thus allowing degradation of the RNA. The initial batch was stored in GTC and therefore would explain why there was minor *phyB* RNA detectable whereas the second batch that was eluted in RNA free water and was completely undetectable. Further *phyB* RNA was transcribed and gave good Nanodrop readings and Ct's from a neat standard curves. However, when it came time to preform patient sample extraction the -80°C freezer had again lost power and was reading +2°C. The RNA had again been degraded and lost. It was decided to cease further patient extraction until the internal control was working reliably.

Running a gel electrophoresis could have checked RNA integrity, however, the reagents were not shipped for performing this. It was felt there was substantial collateral evidence not to pay for shipping of reagents.

The *phyB* internal control was 'free' mRNA and therefore susceptible to degradation. In Africa this can be a problem where room temperature is high and power supply unreliable. The internal control worked very well in the carefully regulated, resource heavy environment of the laboratory in St Andrews but when taken to the field its labile nature was exposed. A more robust internal control was required that would remain stable at room temperature. It was postulated that RNA within a cell would provide the robustness and portability required. The second aspect that made a cellular control appealing was that it would reflect the process that is occurring to the target. The crucial step in RNA extraction of *M. tuberculosis* is cell lysis because of the thick mycolic cell wall.(Yuan et al. 2012) Lysing efficiency can also be reduced if sputum is highly mucoid. It was postulated that another *Mycobacteria* with a similar mycolic cell wall would better replicate the processes occurring to the target than mRNA.

3.6 Conclusions

The pilot evaluation of the two novel biomarkers was very promising. However, technical problems with the internal control meant no further extractions took place. Before any meaningful discussion of the results can occur further data needs to be accrued and in order do this the internal control needed to be functioning optimally.

4 Chapter 4: Assay Development and Optimisation

4.1 Introduction

The lack of an appropriate control curtailed work in KCRI and made it clear that further assay development was required. The labile nature of the *phyB* meant that the assay was not reliable and reproducible. Accurate control quantification is required to ensure that simultaneous target gene amplification is not being inhibited. The lack of robustness of the internal control was the primary issue after patient 5 the internal control was close to undetectable, see figure 3.4. The integrity of the *phyB* mRNA had been lost. It was clear for the assay to function in the field a more robust assay was required. The purpose of this chapter is to develop a more robust and improved internal control.

4.1.1 Controls

A control develops the robustness of any assay. It can improve the validity of the result by reducing both false positives and negatives. Secondarily it can enhance the reproducibility of the quantification of the assay between runs by having comparable standards of known magnitude.

In the context of RT-qPCR, the purpose of a control is to verify that sufficient extraction and amplification has occurred and that during these steps there has not been any loss or contamination of the sample that would affect detection or quantification. In order to reflect what is occurring to the target, ideally the standard would be very similar in nature to the target. This would mean that if the internal control were exposed to parallel deleterious conditions the reduction of the control would be the same as the reduction of the target.

There are a number of different types of molecular assay controls. The appropriateness and specification of the controls depends upon whether the test is qualitative or quantitative. In broad terms molecular controls can be broken down into three categories: Amplification controls, extraction controls and internal controls.

4.1.2 Amplification Controls

For every run both a positive and negative control are required. For quantitative assays a minimum of two positive controls is required. The greater number of positive controls of quantity allows for the adjustment of the standard curve. Ideally one would run a complete standard curve to allow for variation in the quantification of each concentration of target RNA. For example due to dNTP exhaustion.

The positive control can be synthesised in many ways: extracted nucleic acid, specimens known to contain target nucleic acid or produced by spiking the target organism into specimens known not to contain the specific nucleic acid.

Preferably any control mirrors the sample being analysed. The reason for matching the control is to reflect any interactions that may be occurring. The control should obviously not be any risk to health. The high control should be at a level to give consistent results and the low control should be close enough to the limit of detection such as to challenge the assay. Having the positive control near the limit of detection maximises the chances of detecting any issues with the assay.

4.1.3 Extraction Controls

Extraction of the target from the sample is an independent step from the amplification of the target gene and therefore a separate control can be developed for this step. Indeed in some assays only an extraction control is included.

The crucial step in RNA extraction of *M. tuberculosis* is cell lysis. This is because of the thick mycolic cell wall present in all mycobacterial cells. Furthermore, lysing

efficiency can also be reduced if sputum is highly mucoid. Thus, an extraction control utilised must reflect the difficulty and variability in lysing efficiency. As this was the critical step., it was postulated that a mycobacterial species may best reflect this.

4.1.4 Internal Controls

An internal control is a control that is present within the sample being analysed. For example in the detection of blood borne viruses one could use primers for a conserved human gene when detecting the viral DNA. Or in the instance of isolating a resistance gene such as *rpoB* a *M. tuberculosis* housekeeping gene could be used. Sputum samples contain variable quantities of human nucleic acids, which may not be sufficient to give reliable detection. Therefore, human DNA was not selected as the internal control.

4.1.5 The Novel Extraction Control

It was postulated that another *Mycobacteria* with a similar mycolic cell wall would better replicate the processes occurring to the target RNA rather than *phyB* mRNA. *Mycobacterium marinum* was suggested because it was in ready supply within the lab and also unlikely to present in clinical isolates. By multiplexing the detection of *M. marinum* and *M. tuberculosis,* the new *M. marinum* extraction control could act as an amplification control in the same way as the *phyB* mRNA had previously.

4.2 Aim

i. To design a more robust, reproducible assay with an internal control that reflects the processes involved in quantifying the target RNA.

ii. To create a portable reproducible and stable internal control

4.3 Assay optimisation

In vitro work was being undertaken in the Gillespie lab on drug development with *M. marinum* in zebra fish models. The same putative targets: 16S rRNA, pre-16S rRNA and tm-RNA were being used to assess anti-mycobacterial lead compounds. The existence of

an already working assay biased the choice of gene target. However, theoretically it could be beneficial to be targeting similar species of RNA to the target.

4.3.1 Primer Design

First inter-primer homology was compared for *M. tuberculosis* and *M. marinum* genes of interest. These are detailed in table 4.1 and 4.2.

Gene	Primer/Probe	Sequence (5' to 3')
pre-16s rRNA	Forward Primer	TGT GTT TGG TGT TAT GTT TTG TTG
	Reverse Primer	GAT ACC TGA CAA GAC GCC AAT
	Probe	FAM-TTT TTT GAC TAC ACC TTA TCA CCC CCG T-BHQ1
tm-RNA	Forward Primer	CGTCATCCTGGCTAGTTC
	Reverse Primer	CTACGGCATTCCCTCAAG
	Probe	FAM- AGT CCG CTA TGT CTC TGC TCG-BHQ1
16S rRNA	Forward Primer	CTGGGAAACTGGGTCTAA
	Reverse Primer	CACCAACAAGCTGATAGG
	Probe	FAM-ACATGAATCCCGTGGTCCTATCCG-BHQ1

Figure 4.1: Mycobacterium marinum primer and probe sequences for 16S rRNA, pre-16S rRNA and tm-RNA

Gene	Primer/Probe	Sequence (5' to 3')
pre-16S rRNA	Forward Primer	TTT TGG CCA TGC TCT TGA T
	Reverse Primer	AAA GGG AGC CAA AGG TAT TT
	Probe	FAM-CGT TGT CGG GGG CGT GGC-BHQ1
tm-RNA	Forward Primer	CGTCATCTCGGCTAGTTC
	Reverse Primer	CTACGGCATTCCCTCAAG
	Probe	FAM-AGT TCG CTA TGC CTC TGC TCG-BHQ1
16S rRNA	Forward Primer	GTGATCTGCCCTGCACTTC
	Reverse Primer	ATCCCACACCGCTAAAGCG
	Probe	AGGACCACGGATGCATGTCTTGT

Figure 4.2: Mycobacterium tuberculosis primer and probe sequences for 16S rRNA, pre-16S rRNA and tm-RNA

4.3.2 Optimisation of the MM tm-RNA and BCG 16S-rRNA assay conditions

The *Mycobacterium tuberculosis* assay conditions had been optimised as described previously in Chapter 2. The *Mycobacterium marinum* being used in the zebra fish models at the time were using the same FAM probe as the *M. tuberculosis* probes. In order to collect the amplification data in a separate channel a new dye was required. A yellow probe, Hex, was selected as suspected to multiplex well with the FAM probe. Cycling conditions were not varied. Initially the primer concentrations were varied to assess improvement in PCR efficiency.

4.3.3 The effect of primer concentration on Mycobacterium marinum tm-RNA PCR efficiency

First, 3.5 x10^9 CFUs of MM RNA was extracted using the Ambion® (Thermo Fisher Scientific, USA) protocol previously described in 1.1.1. This was used to create a standard curve of ten, 1 in 10 dilutions and this was run in duplicate with 4 master mixes consisting of differing final primer concentrations (50nM, 100nM, 200nM, 400nM). Linear regression of the standard curve was performed and the efficiency was calculated using the formula: Efficiency = 10^ (-1/slope). The following efficiencies and R^2 were generated.

Primer Concentration	Efficiency	R^2	Range in log_{10} CFU/ml
50nM	1.00	0.998	2-9
100nM	1.00	0.999	2-9
200nM	1.00	0.997	2-9
400nM	1.04	0.998	2-9

Table 4.1: The efficiencies and ranges of the differing primer concentrations from 50-400nM for M. marinum tm-RNA

All concentrations gave acceptable efficiencies, between 0.90 and 1.10, and an acceptable range. The 200nM concentration was selected and then used for the rest of the optimisation process.

4.3.4 The effect of probe concentration on MM tm-RNA PCR efficiency

The same experiment was performed as above but with changing the probe concentration instead of the primer concentration.

Probe Concentration	Efficiency	R^2	Range in log_{10} CFU/ml
50nM	1.05	0.999	2-9
100nM	1.08	0.997	2-9
200nM	1.05	0.999	2-9
400nM	0.91	0.998	3-9

Table 4.2: The efficiencies and ranges of the differing probe concentrations from 50-400nM for *M. marinum* tm-RNA

Again all concentrations gave acceptable efficiencies, between 0.90 and 1.10, and an acceptable range. The 200nM concentration was selected and then used for the rest of the optimisation process.

4.3.5 Assay Conditions

The singleplex assays described in chapter 2 are as follows:

Assay	BCG 16S-rRNA	MM tm-RNA
Primer Concentration	200nM	200nM
Probe Concentration	200nM	200nM
Reverse Transcriptase	x1	x1
Master Mix	x1	x1
Reverse Transcriptase	50°C/30min	50°C/30min
Taq Polymerase	95°C	95°C
Denaturing	94°C/45s	94°C/45s
Extension	60°C/60s	60°C/60s
Cycles	40	40

Table 4.3: Summary of the singleplex assay conditions for *M. bovis BCG* 16S rRNA and *M. marinum* tm-RNA

4.3.6 Duplexing

Standard curves from $1.8x10^9$ CFU/ml of *M. marinum* and $1.3x10^7$ CFU/ml *M. bovis BCG* were run for the duplex reactions and the efficiency was reassessed.

The first multiplex reaction was to combine *M. bovis BCG* 16SrRNA with new *M. marinum* tm-RNA and run with the mixture of both *M. bovis BCG* and *M. marinum*. The results are outlined in the table 4.4 below.

Reaction	**Efficiency**	**R^2**	**Quantification range log_{10} CFU/ml**
***M. bovis BCG* 16SrRNA**	0.98	0.998	1-7
***M. marinum* tm-RNA**	1.00	0.997	2-9

Table 4.4: The efficiencies and ranges for the duplexed *M. tuberculosis* 16S rRNA and *M. marinum* tm-RNA assays

Then *M. bovis BCG* pre-16SrRNA was multiplexed with the new control. The results are detailed in table 4.5.

Reaction	**Efficiency**	**R^2**	**Quantification range log_{10} CFU/ml**
***M. bovis BCG* pre-16SrRNA**	1.01	0.989	4-7
***M. marinum* tm-RNA**	0.95	0.979	2-9

Table 4.5: The efficiencies and ranges for the duplexed *M. tuberculosis* pre-16S rRNA and *M. marinum* tm-RNA assays

Finally, *M. bovis BCG* tm-RNA was multiplexed with the new control. Again the results are detailed in table 4.6.

Reaction	**Efficiency**	**R^2**	**Quantification range log_{10} CFU/ml**
***M. bovis BCG* tm-RNA**	1.05	0.945	2-7
***M. marinum* tm-RNA**	0.98	0.999	2-9

Table 4.6: The efficiencies and ranges for the duplexed *M. tuberculosis* tm-RNA and *M. marinum* tm-RNA assays

There was no significant change in the efficiencies or range of quantification on duplexing the three assays.

4.3.7 Cross detection between M. marinum tm-RNA and M. bovis BCG 16S rRNA assays

The next step was to ensure that there was no cross detection between the target and the control. To evaluate this a standard curve of seven 1 in 10 dilutions of 3.5 $x10^9$ CFU/ml extracted *M. marinum* RNA was run for *M. bovis BCG* 16S rRNA, pre-16S rRNA and tm-RNA detection. This was repeated for *M. bovis BCG* at a concentration of 1.3 $x10^7$; run for *M. marinum* tm-RNA.

***M. Marinum* Concentration (log_{10} CFU/ml)**	***M. bovis BCG* pre-16S rRNA Ct**
3.5 $x10^9$	Negative
3.5 $x10^8$	Negative
3.5 $x10^7$	Negative
3.5 $x10^6$	Negative
3.5 $x10^5$	Negative
3.5 $x10^4$	Negative
3.5 $x10^3$	Negative

Table 4.7: Different concentrations of *M. marinum* run for *M. bovis BCG* pre-16S rRNA

There was no detection of *M. marinum* by *M. bovis BCG* pre-16S rRNA.

***M. Marinum* Concentration (log_{10} CFU/ml)**	***M. bovis BCG* tm-RNA Ct**
3.5 $x10^9$	Negative
3.5 $x10^8$	Negative
3.5 $x10^7$	Negative
3.5 $x10^6$	Negative
3.5 $x10^5$	Negative
3.5 $x10^4$	Negative
3.5 $x10^3$	Negative

Table 4.8: Different concentrations of *M. marinum* run for *M. bovis BCG* tm-RNA

There was no detection of *M. marinum* by *M. bovis BCG* tm-RNA.

M. bovis BCG Concentration (log_{10} CFU/ml)	*M. marinum* tm-RNA Ct
1.3 x10^7	Negative
1.3 x10^6	Negative
1.3 x10^5	Negative
1.3 x10^4	Negative
1.3 x10^3	Negative
1.3 x10^2	Negative
1.3 x10^1	Negative

Table 4.9: Different concentrations of *M. bovis BCG* run for *M. marinum BCG* tm-RNA

There was no detection of *M. bovis BCG* by the *M. marinum* tm-RNA reaction.

M. Marinum Concentration (log_{10} CFU/ml)	*M.bovis BCG* 16S-rRNA Ct (Std Dev)
3.5 x10^9	25.49 (0.38)
3.5 x10^8	25.645 (0.83)
3.5 x10^7	28.22(0.41)
3.5 x10^6	30.75 (0.44)
3.5 x10^5	32.615 (0.46)
3.5 x10^4	32.87
3.5 x10^3	Negative

Table 4.10: Different concentrations of *M. marinum* run for *M. bovis BCG* 16S rRNA

M. marinum was detected by the *M. bovis BCG* 16S rRNA for concentrations greater than 3.5x10^4. The amplification plots for the concentrations below 6 log_{10} *Mycobacterium marinum* were not exponetial and would normally be deemed negative.

The *M. bovis BCG* tm-RNA, pre-16S rRNA and the *M. marinum* tm-RNA were specific and showed no evidence of cross detection. However, *M. bovis BCG* 16S-rRNA primer and probes were non-specifically amplifying *M. marinum* RNA.

4.3.8 Selecting the optimal M. marinum concentration

At higher concentrations of *M. marinum* the *M. bovis BCG* 16S rRNA was non-specifically amplifying. Therefore, to prevent cross detection of the target but maintain reliable detection of control the optimal concentration of *M. marinum* internal control had to be determined. Extraction of the same sample will produce a variation in the final concentration of *M. marinum* total RNA. To ascertain the extent of this variation a range

of *M. marinum* cultures were grown into the log phase and extracted in artificial sputum to mimic patient sample conditions. The *M. tuberculosis* 16S rRNA PCR was then run on the extracts of *M. marinum* RNA.

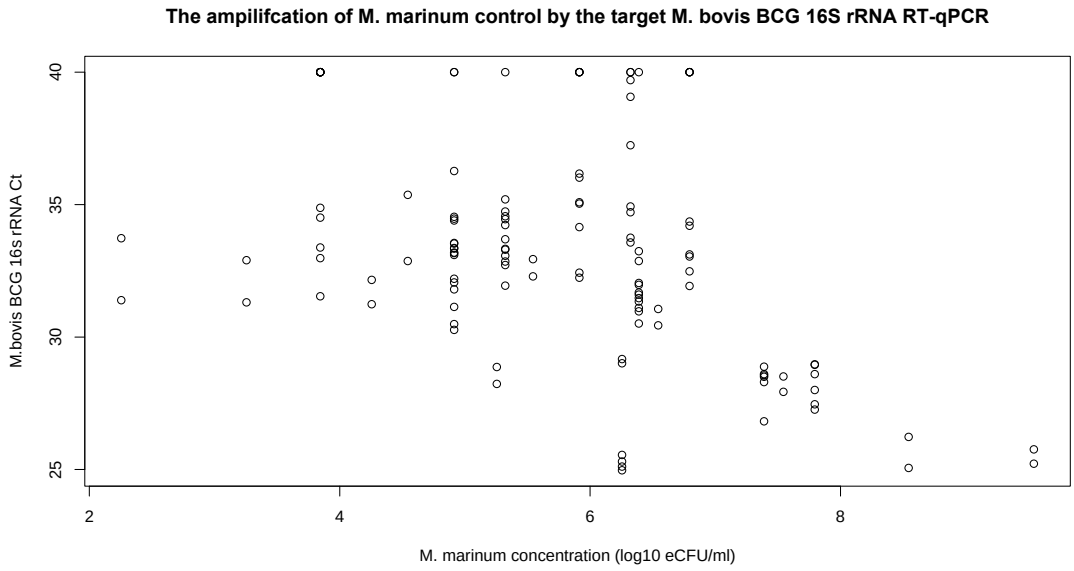

Figure 4.3: Scatterplot of the different concentrations of *M. marinum* in CFU/ml extracted and run for *M. bovis BCG* 16S rRNA

A total of 124 extracts of *M. marinum* RNA were run for *M. bovis BCG* 16S rRNA RT-qPCR. Figure 4.3 shows the variation in *M. bovis BCG* 16S rRNA Ct of different CFU/ml concentrations of *M. marinum*. There is substantial variation in Ct for each known concentration of *Mycobacterium marinum*. Only concentrations above $1x10^5$ gave Ct's below 30.

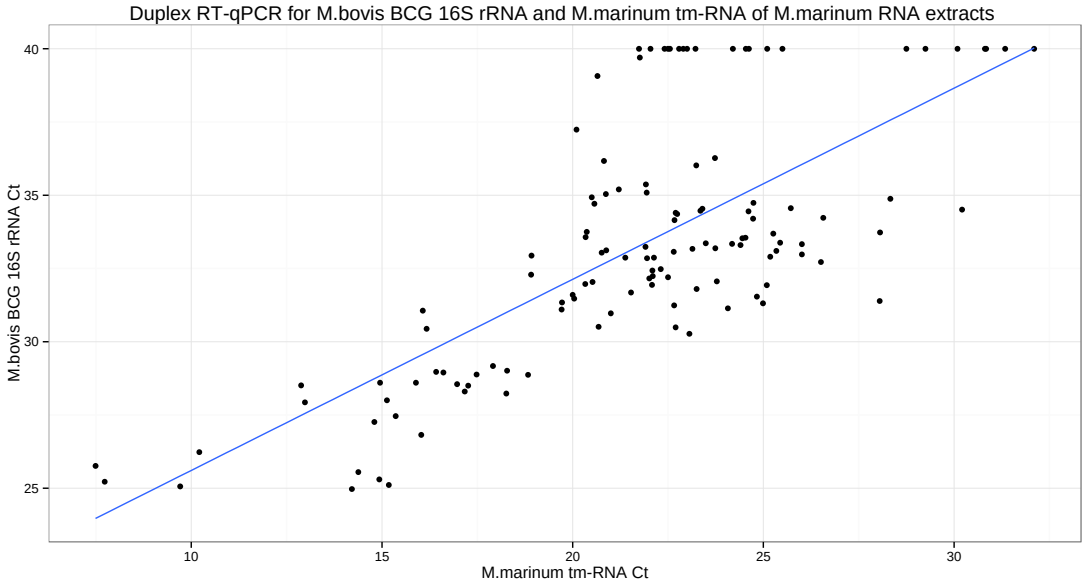

Figure 4.4: Scatterplot and linear regression of M.marinum tm-RNA Ct against M.bovis BCG 16S rRNA for M. marinum RNA extracts

Figure 4.4 shows the variation in *M. bovis BCG* 16S rRNA Ct across different Cts of *M. marinum* tm-RNA detected within the same duplex PCR reaction. There is a stronger correlation of *M. marinum* tm-RNA Ct than CFU for *M. bovis BCG* 16SrRNA Ct. Here it can be seen that above a *M. marinum* tm-RNA Ct of 20 there was no detection in the BCG channel below at Ct of 30.

4.4 Results

4.4.1 Internal Control

4.4.1.1 Lysing Efficiency

To compare correlation of lysing efficiency of the *phyB* and *M. marinum* tm-RNA controls, 10^6 CFU/ml of BCG was spiked with both 5µg of phyB mRNA and 10^5 CFU/ml of Mm and homogenized (Precellys 24, pEQLab, Germany) in triplicates under varying quantities of cell lysing beads (0mg, 10mg, 30mg, 70mg and no bead beating). RNA was subsequently isolated from the lysates and RT-qPCR run to evaluate response of the two

controls to poor lysing conditions. First the response of the target, *M. bovis BCG* 16S rRNA Ct, was plotted for the different lysing conditions.

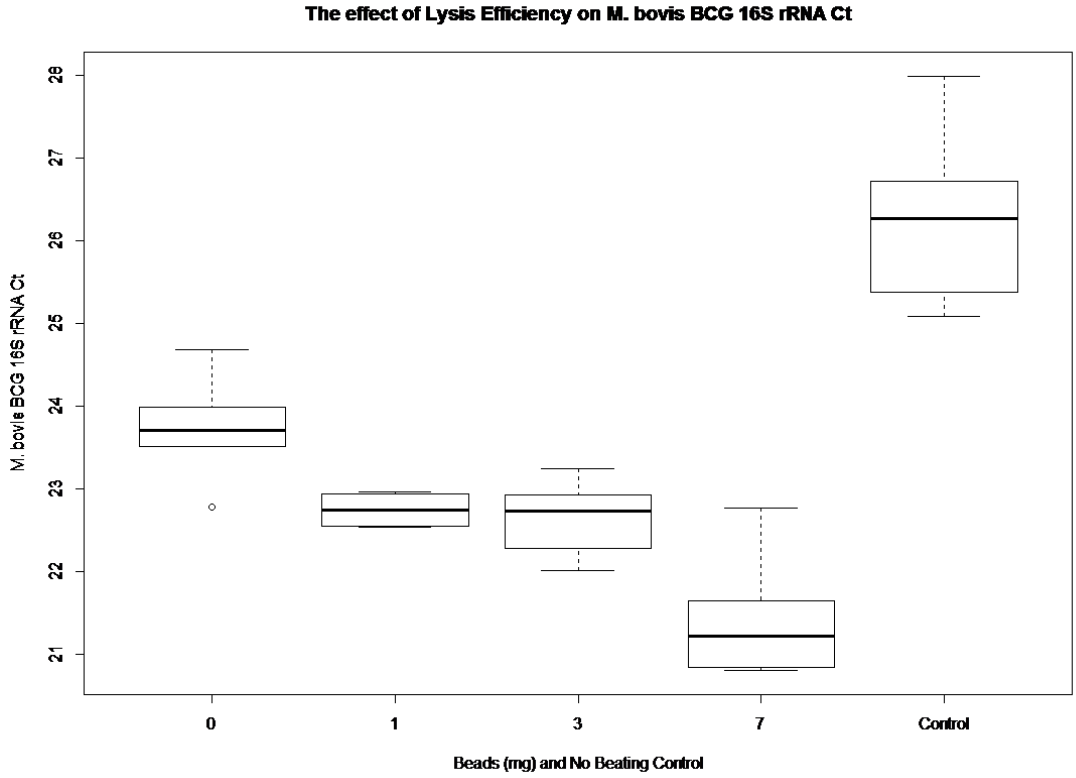

Figure 4.5: The effect on M.bovis BCG 16S rRNA Ct by reducing lysing efficiency through changing the amount of beads added to the lysing matrix B tubes and a no beating control.

A reduction in lysis efficiency by reducing the quantity of beads or through the absence of beating increased *M. bovis BCG* 16S rRNA Ct. Students t-test p equals 0.0001.

Any control should follow the same trend as the target; the *phyB* Ct for the same samples was plotted in figure 4.6.

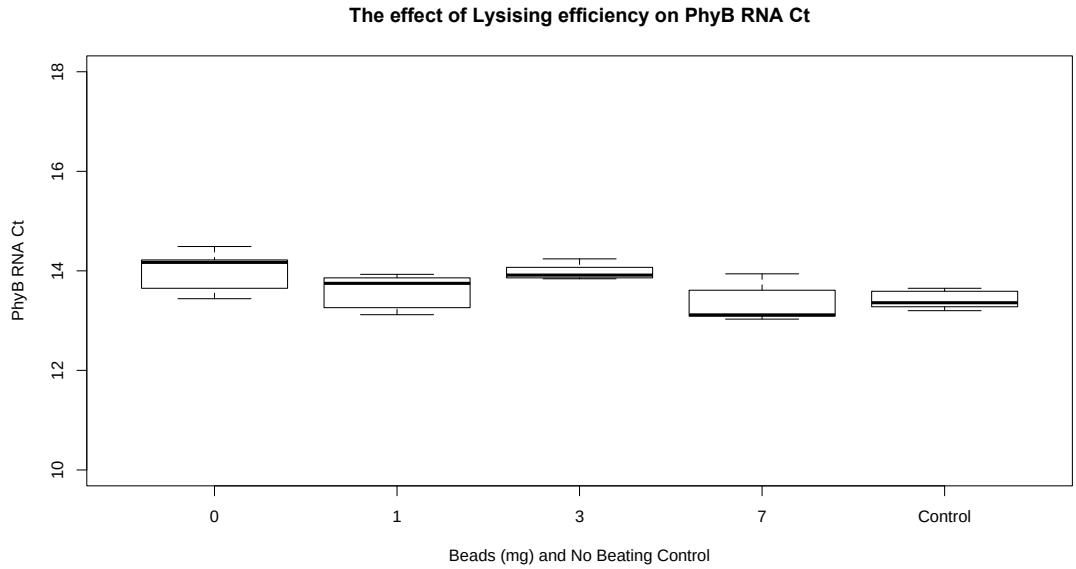

Figure 4.6: The effect on *phyB* Ct by reducing lysing efficiency through changing the amount of beads added to the lysing matrix B tubes and a no beating control.

A reduction in lysis efficiency by reducing the quantity of beads or through the absence of beating did not reduce *PhyB* Ct; student's t-test p equals 0.02.

Finally, the *M. marinum* tm-RNA Cts were plotted in figure 4.7.

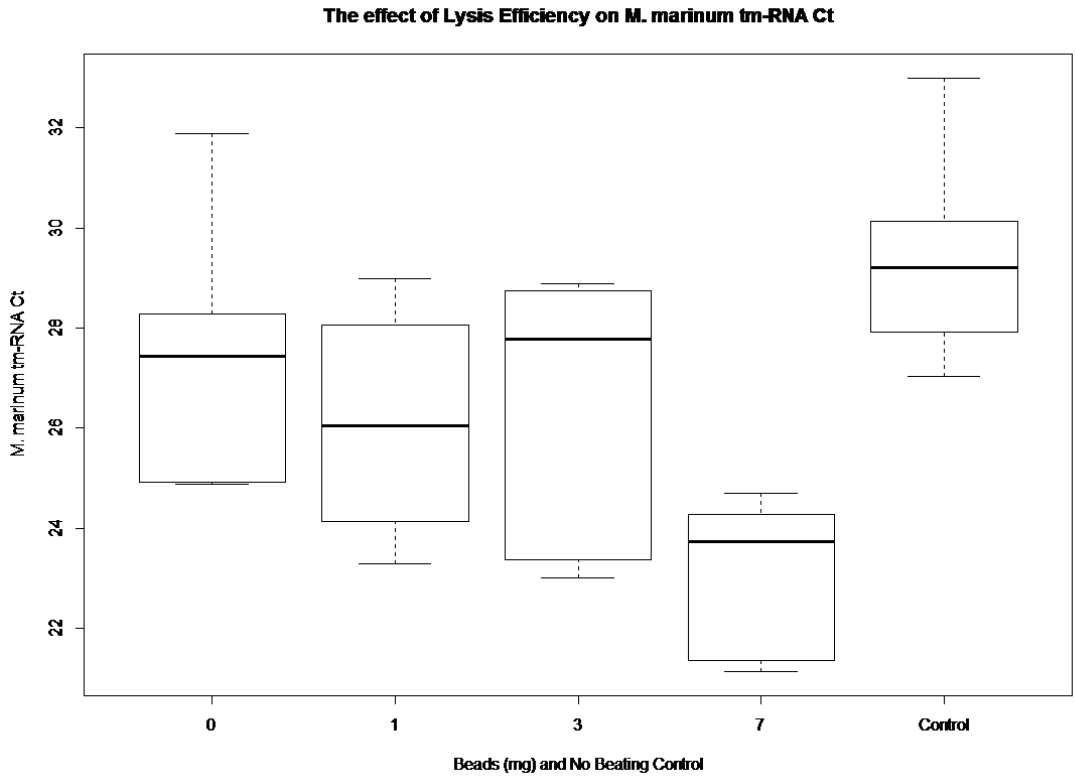

Figure 4.7: The effect on *M. marinum* tm-RNA Ct by reducing lysing efficiency through changing the amount of beads added to the lysing matrix B tubes and a no beating control.

A reduction in lysis efficiency by reducing the quantity of beads or through the absence of beating increased *M. marinum* tm-RNA Ct by 6. The difference was statistically significant; student's t-test p equals 0.0004.

4.4.2 Correlation of Lysis Efficiency

The increase in *M. bovis BCG* 16S rRNA Ct should be reflected in the control. To further investigate the relationship between controls and target the Ct for each control was plotted against *M. bovis BCG* 16S rRNA Ct.

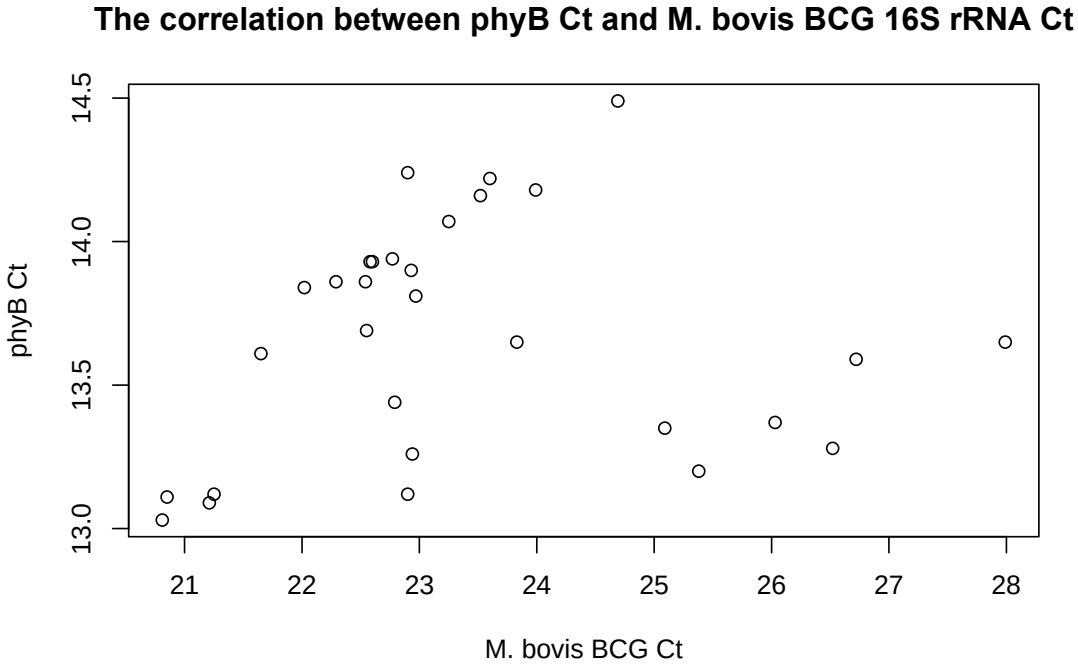

Figure 4.8: Scatterplot of *phyB* Ct against *M. bovis BCG* 16S rRNA Ct

Linear regression showed no correlation between the change in *M. bovis BCG* 16S rRNA caused by reduction in lysing efficiency and *PhyB* Ct.

(Multiple R-squared: 0.01102, Adjusted R-squared: -0.0243 F-statistic: 0.312 on 1 and 28 DF, p-value: 0.5809)

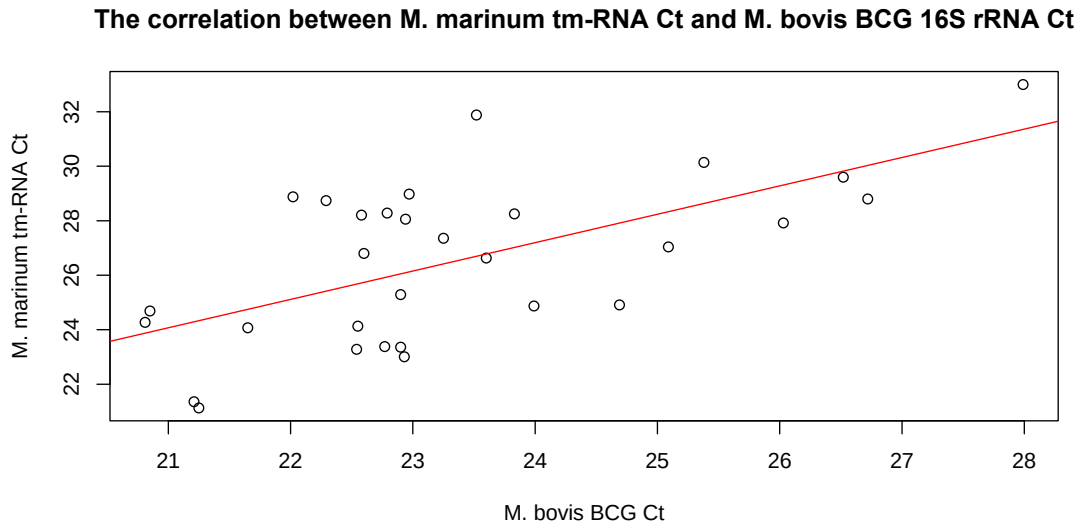

Figure 4.9: Scatterplot and linear regression of *M. marinum* tm-RNA Ct against *M. bovis BCG* 16S rRNA Ct

Linear regression displayed a correlation between *M. marinum* tm-RNA and *M. bovis BCG* 16S rRNA.

(Multiple R-squared: 0.3887, Adjusted R-squared: 0.3668; F-statistic: 17.8 on 1 and 28 DF, p-value: 0.0002)

4.4.3 Controls and Standards Stability

Control stability is important in shipping and storing reagents. To assess the stability of each control and standard, each was left at room temperature for one week. It was suggested that if temperature control was an issue then RNA could be stored in GTC to prevent degradation by nucleases.

First *phyB* internal control was prepared as specified in chapter 2. Six 100µl of the 500ng/µl *phyB* stock, *M. marinum*, *M. bovis BCG* was added to 900µl of GTC. Three of each control were extracted and three were left at room temperature for one week and then extracted. The RNA extracts were then run for *M. bovis BCG* 16S rRNA, tm-RNA, pre-16S rRNA; *M. marinum* tm-RNA and *phyB.*

Target	Initial Ct (mean)	Final Ct (mean)	Difference Ct	Paired t test p value
***M. bovis BCG* 16S rRNA**	18.9	20.2	+1.36	0.12
***M. bovis BCG* pre-16S rRNA**	24.6	25.7	+1.01	0.02
***M. bovis BCG* tm-RNA**	21.6	22.8	+0.84	0.23
***M. marinum* tm-RNA**	17.5	18.4	+0.92	0.015
PhyB	9.7	11.5	+1.79	0.008

Table 4.11: Stability of internal and positive controls after one week at room temperature

All of the controls did decline in quantity after one week at room temperature. The difference was less than one $\log_{10}$.

4.4.4 Sputum Processing

Three of the common methods for sputum were compared to evaluate robustness of the assay. A 100µl of 10^5 CFU/ml *M. bovis BCG* was spiked into 900µl of artificial sputum and liquefied using Sputasol, 2% NALC-NaOH or 5% Oxalic Acid decontamination step mimicking the clinical TB laboratory sputum treatment procedures. 1ml of artificial sputum spiked with BCG was transferred to a 50ml falcon. To this an equal volume of Sputasol, NALC-NaOH or Oxalic acid was added. For the control 1ml of PBS was added. The tubes were then vortexed for 20s to ensure liquefaction. The mixture was left to stand for 30 minutes. Then PBS (pH 6.8) was added to bring the total volume to 50ml. This was then centrifuged at 3,000 G for 30mins in a bucket centrifuge. After centrifugation the supernatant was gently tipped off and discarded. The pellet was then re-suspended in lysis buffer containing β-Mercaptoethanol and extracted using the Ambion® kit. RT-qPCR was run in technical duplicate for 16S-rRNA, p16-rRNA and tm-RNA and plotted below.

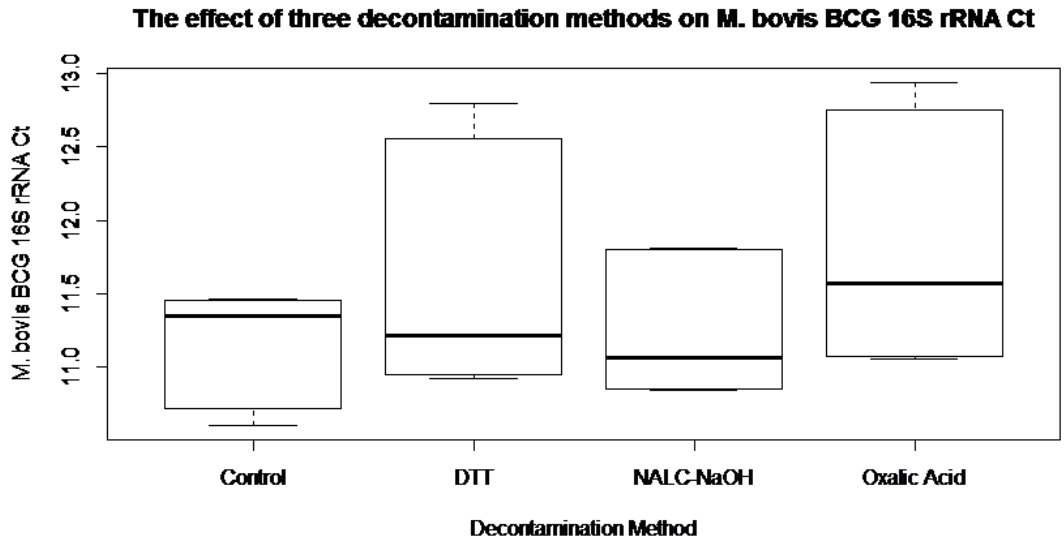

Figure 4.10: The effect of three decontamination methods on *M. bovis BCG* 16S rRNA Ct: DTT, NALC-NaOH and Oxalic Acid.

One-way ANOVA and Tukey multiple comparisons of means showed no significant differences in the different decontamination methods on *M. bovis BCG* 16S rRNA quantification (p=0.285).

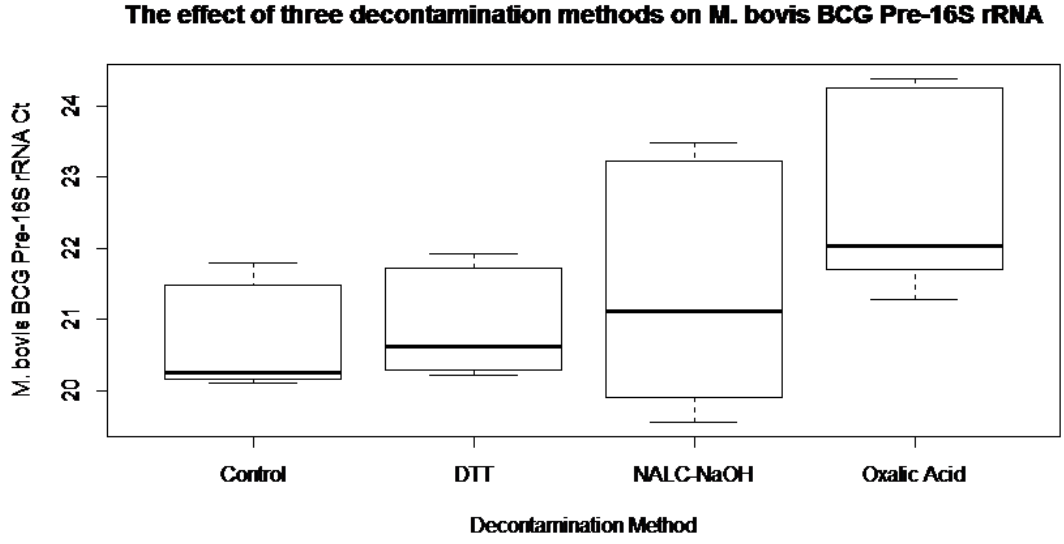

Figure 4.11: The effect of three decontamination methods on *M. bovis BCG* pre-16S rRNA Ct: DTT, NALC-NaOH and Oxalic Acid.

One-way ANOVA showed a statistically significant difference between the methodologies (p=0.0458) for *M. bovis BCG* pre-16S rRNA. Tukey multiple comparisons of means showed that the Oxalic Acid-Control was the only significant difference (p=0.047). However, this was less than 1 log difference (1.94 Ct; 95% CI 0.02-3.85 Ct).

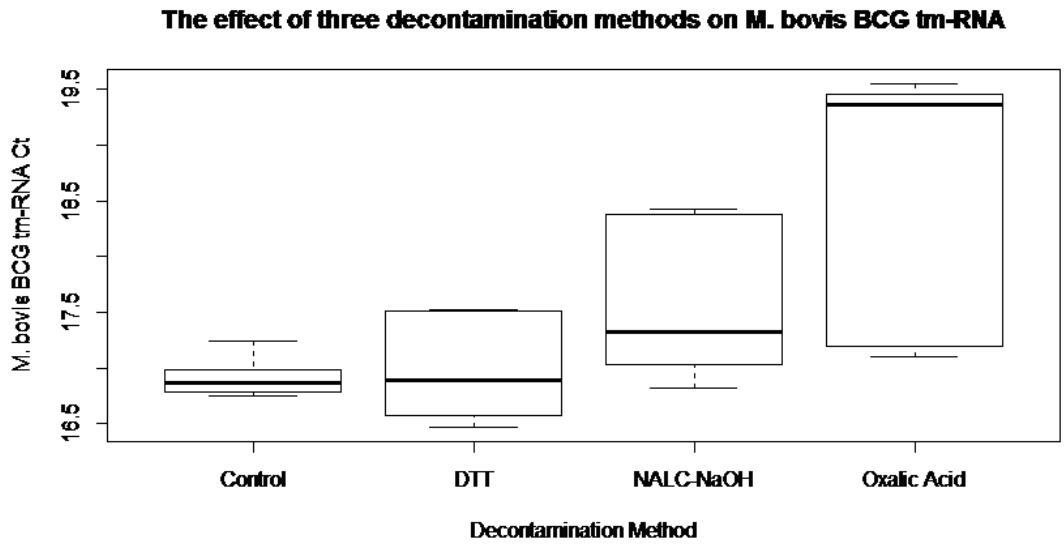

Figure 4.12: The effect of three decontamination methods on *M. bovis BCG* tm-RNA Ct: DTT, NALC-NaOH and Oxalic Acid.

One-way ANOVA showed a statistically significant difference between the methodologies (p= 0.00153). Tukey multiple comparisons of means again showed that the Oxalic Acid-Control was the only significant difference (p=0.0025). However, this was less than 1 log difference (1.75 Ct; 95% CI 0.58-2.93 Ct).

Three different decontamination methods do not affect the quantification of the different targets by more than one log.

4.4.5 Specificity

To assess specificity the *M. bovis BCG* 16S rRNA, pre16S rRNA, tm-RNA and *M. marinum* tm-RNA assays were run against a number of pathogens that had been extracted using the Ambion kit.

Bacteria	*M. bovis BCG* 16S rRNA	*M. bovis BCG* pre-16S rRNA	*M. bovis BCG* tm-RNA	*M. marinum* tm-RNA
Haemophilus influenzae	No	No	No	No
Streptococcus pneumoniae	No	No	No	No
Methicillin-resistant Staphylococcus aureus ATCC 29213	No	No	No	No
Klebsiella pneumoniae AT BAA1706 Sus	No	No	No	No
Staphylococcus aureus subsp. aureus Rosenbach ATCC 25923	No	No	No	No
Burkholerdia sp				
Stenotrophomonas maltophilia	No	No	No	No
Enterobacter cloacae	No	No	No	No
Citrobacter koseri	No	No	No	No
Proteus mirabilis ATCC 35659	No	No	No	No
Stenotrophomonas maltophilia	No	No	No	No
Enterococcus faecium	No	No	No	No
Candida albicans	No	No	No	No
Enterobacter aerogenes	No	No	No	No
Enterococcus faecalis	No	No	No	No
Streptococcus agalactiae ATCC12386	No	No	No	No
Acinetobacter baumannii	No	No	No	No
Streptococcus pyogenes ATCC 19615	No	No	No	No
Serratia marcescens	No	No	No	No

Table 4.12: Common Pathogens/Commensals extracted and run for *M. tuberculosis* 16S rRNA, pre-16S rRNA, tm-RNA and *M. marinum* tm-RNA

The four assays were specific and did not detect any other microorganisms potentially present in the clinical samples.

Bacteria	*M. bovis BCG* 16S rRNA	*M. bovis BCG* pre-16S rRNA	*M. bovis BCG* tm-RNA	*M. marinum* tm-RNA
Mycobacterium tuberculosis complex	Yes	Yes	Yes	No
M. marinum	No	No	No	Yes
M smegmatis	No	No	No	No
M. Avium complex	No	No	No	No
M. fortuitum	No	No	No	No

Table 4.13: Specificity of the four assays for a selection of different *Mycobacteria*

4.4.6 Assay reproducibility

To be applicable in different settings the assay results should be reproducible irrespective of the environment it is performed. To this end, well-characterized panels of BCG at concentration 10^7 and 10^4 cells/ml GTC were supplied by University of St. Andrews to four African laboratories participating in the PanACEA Biomarker Expansion programme (PANBIOME) study. The laboratories independently processed the samples including RNA extraction and qPCR to determine bacterial load and variance of results between the sites was explored.

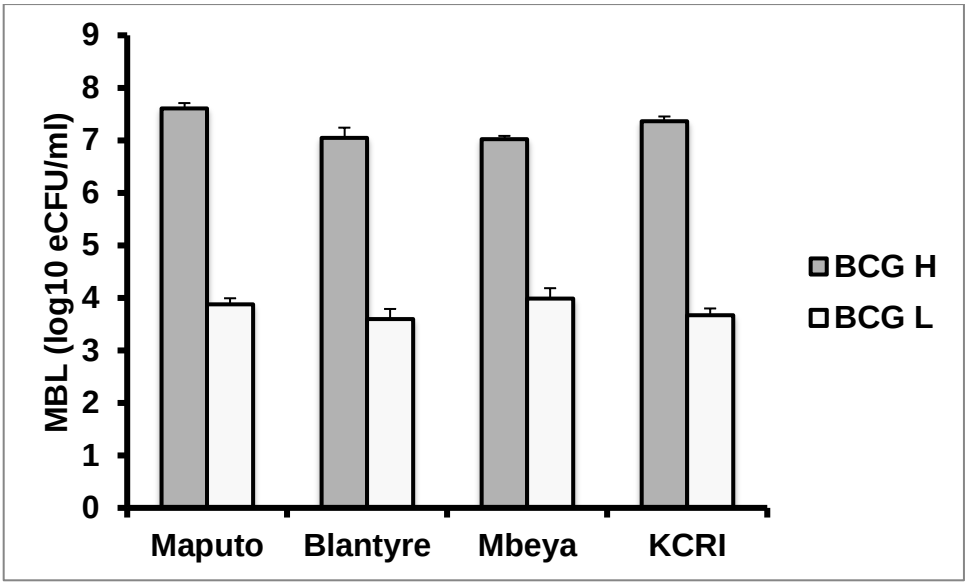

Figure 4.13: Quantifications of standards at four African sites: Maputo, Mozambique; Blantyre, Malawi; Mbeya, Tanzania and Kilimajaro Christian Research Institute, Moshi, Tanzania.

The high and low standards were quantified within one $\log_{10}$. ANOVA showed this was not statistically significant.

4.5 Discussion

4.5.1 Robustness and reproducibility

For an assay to be successful in the field it must be both robust and reproducible. The new *M. marinum* proved to be both. There are a number of advantages of the *M. marinum* control over the *phyB* control. First, the *M. marinum* control better reflects the extraction process over the *phyB*. The removal of beads during the extraction process created a wide variation in mechanical lysing efficiency. The *phyB* internal control retrieval did not alter with reduction of beads. This is unsurprising as structural integrity 'free' mRNA is unlikely to be altered by the shear forces generated. *M. marinum* undergoes the same process as the target *M. bovis BCG* gene and a correlation was shown between the tm-RNA Ct and the 16S rRNA Ct, figure 4.9.

PCR is known for it's high specificity and this was shown across a panel of respiratory pathogen and common pathogens/commensals, table 4.13 and 4.12.

Generation of *phyB* is not only time consuming but also technically demanding. The reagents are very expensive costing hundreds of pounds to produce the amount of mRNA required. *M. marinum* is very inexpensive and easily produced. The critical step is to get the quantity correct to not interfere with quantification of the target RNA.

4.5.2 Selecting the optimal M. marinum concentration

The issue with adding a predetermined number of CFUs of *M. marinum* is that there is substantial variation in the extraction efficiency, PCR inhibition and relative expression of RNA. Therefore, a set number of CFUs will give a different quantity of *M. marinum* 16S rRNA that will give a variation of Ct's of *M. bovis BCG* 16S rRNA. The variation of Ct's can be clearly seen in figure 4.4. It was postulated that *M. marinum* tm-RNA extraction and PCR inhibition would be the similar to the cross detection reaction of *M. bovis BCG* 16S rRNA. This would mean that the *M. bovis BCG* 16S rRNA Ct would be more likely to correlate with *M. marinum* tm-RNA Ct rather than *M. marinum* CFU count. The better fit of the linear model to the tm-RNA Ct data over the CFU data confirmed this to be the case. It was concluded that a concentration of around $1x10^5$ CFU/ml of *M. marinum* was unlikely to be cross detected by the *M. bovis BCG* 16S rRNA. Ensuring that the *M. marinum tm-RNA* Ct was not less than 20 and discarding any *M. bovis BCG* 16S rRNA Ct value above 30 could further reduce potential false positives. The reason that the *M. bovis BCG* 16S rRNA cross detected whereas the other targets did not because the 16S rRNA gene is highly conserved across Mycobacteria.

4.6 Conclusion

At the determined concentrations of *M. marinum* the novel control was both robust and reproducible. The assay was deemed ready for further field-testing.

5 Chapter 5: Field testing the M. marinum control

5.1 Introduction

After the failure of the *phyB* internal control the assay had been successfully redeveloped to make it more robust and reproducible for implementation into the clinical laboratory. The pre-16S rRNA and tm-RNA assays combined with the *phyB* internal control had only managed to retrieve data for 5 patients. The internal control had to be entirely redesigned to make it robust and reproducible. The 'correct' concentration of *M. marinum* had been selected. The next step was to validate the pre-16S rRNA and tm-RNA in the field and assess the efficacy of the different biomarkers in clinical samples taken from high burden country in the MAMS-TB-01 trial.

5.2 Aim

The aims were to:

i. To demonstrate the assays are robust and reproducible in the clinical setting

ii. To explore the relationships between the RNA markers

iii. To determine the ability of the assays to monitor treatment response

5.3 Methods

Following the RNA extraction protocol detailed in Chapter 2, a further 40 sets of patient samples from the same patient cohort were extracted. These were then run for 16S rRNA, pre-16S rRNA and tm-RNA following the updated RT-qPCR protocol that included the novel *M. marinum* described in the methods of Chapter 4.

5.4 Statistics

All statistical analyses were performed in Ri386 3.1.0 (The R Foundation for Statistical Computing, Austria). Normality was assessed by visual inspection of histogram, boxplot, Q-Q plot and then a Sharipo-Wilk's test. Phi coefficient was used to calculate the correlation between positive and negative results for LJ, MGIT, 16S rRNA, pre-16S rRNA and tm-RNA. Linear regression was performed for each of the quantitative markers first by week and then against each other. These were assessed using the F-statistic and R^2. Normality and heteroscedasticity were assessed by: plotting the residuals against fitted values; Q-Q plot; plotting of square root of residuals against fitted values and plotting standardised residuals against leverage

5.5 Results

5.5.1 Patient Demographics

There were forty patient serial samples sets analysed. Demographic data was collated from the MAMS trial database. The following parameters were available: sex, age, HIV status, anti-tuberculosis regimen prescribed and susceptibility testing. These are detailed below in table 34.

Variable					
Sex	Male 34		Female 6		
Age	Range 20 to 56		Median 37	Mean 36.5	
HIV	Negative 40		Positive 0		
Regimen	HRZE 12	HR35ZE 6	HRZQ 6	HR20ZQ 7	HR20ZM 9
Resistant	Sensitive 40		Resistant 0		

Table 5.1: Patient Demographics

In the cohort of forty patients the majority were male, 85%. The median and mean age was 37 with a range of 20 to 56 years. All patients were HIV negative and had fully susceptible *Mycobacterium tuberculosis* isolates. There was an even spread of the five possible treatment regimens.

5.5.2 Summary Data

A total of 40 patient sets of 13 samples were quantified using 16S rRNA, pre-16S rRNA and tm-RNA. Giving a total of 520 samples processed. The distribution of the estimated bacterial loads was tabulated with the number of missing data.

Marker	Min. log10 eCFU/ ml	Max. log10 eCFU /ml	Total	Missing Samples
tm-RNA	0.5	6.6	520	0
pre-16S rRNA	1.5	6.7	520	0
16S rRNA	0.8	7.6	520	0

Table 5.2: Summary data for the three RNA markers

There were no missing samples out of the 520 processed. The range of estimated values for all three methodologies of estimating bacterial loads were different.

5.5.3 Histogram of RNA markers

To further examine the variation in estimation of bacterial load; the distribution of the estimated bacterial load as measured by the individual RNA markers was plotted as a histogram.

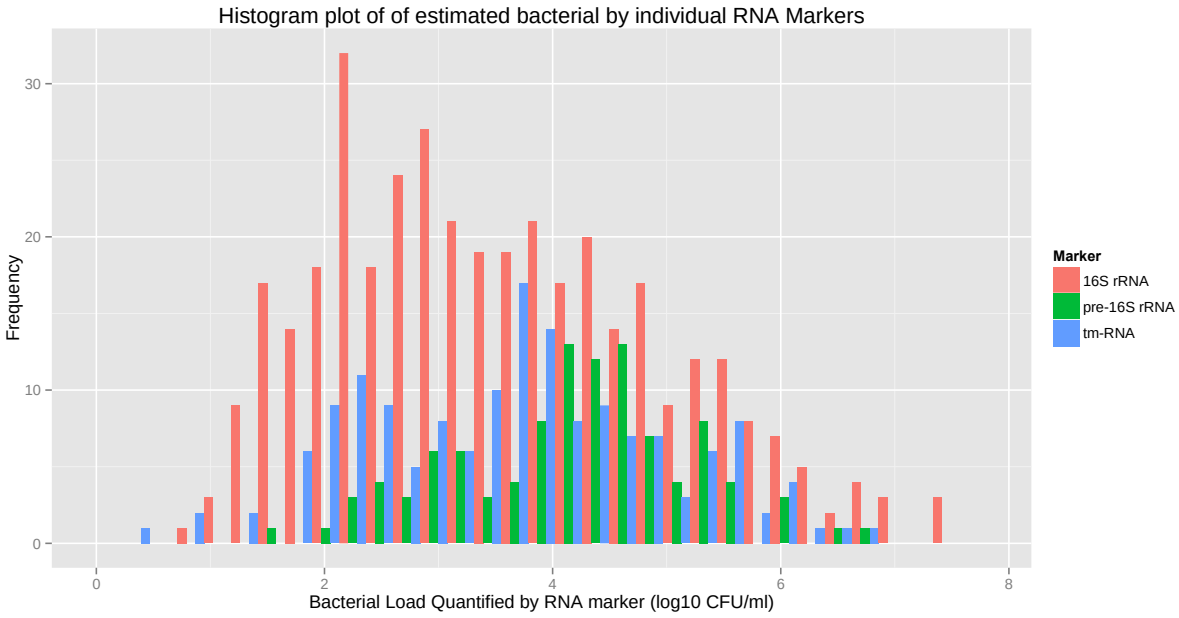

Figure 5.1: Histogram of estimated bacterial loads by individual RNA markers

The histograms of the estimated bacterial loads by three RNA markers have been plotted. None of the three markers showed a normal distribution but potentially more a bimodal distribution with a positive skew. The data was not normally distributed was confirmed with a Sharipo-Wilks test, Q-Q plots and boxplots.

The distribution of MGIT TTD and LJ was tabulated.

Marker	Min. (days)	Max. (days)	Total	Missing Samples	Contamination
Time to detection	0.1	43.2	520	56	46
LJ	-	-	520	35	26

Table 5.3: Summary data for MGIT TTD and LJ

There was no quantitative data for LJ. The missing samples arise from contamination of the media used. Contamination rate in MGIT was 9% and 5% in LJ The difference between missing samples is due to the dataset being incomplete.

Next a histogram was plotted for the quantitative values derived from MGIT time to detection in days.

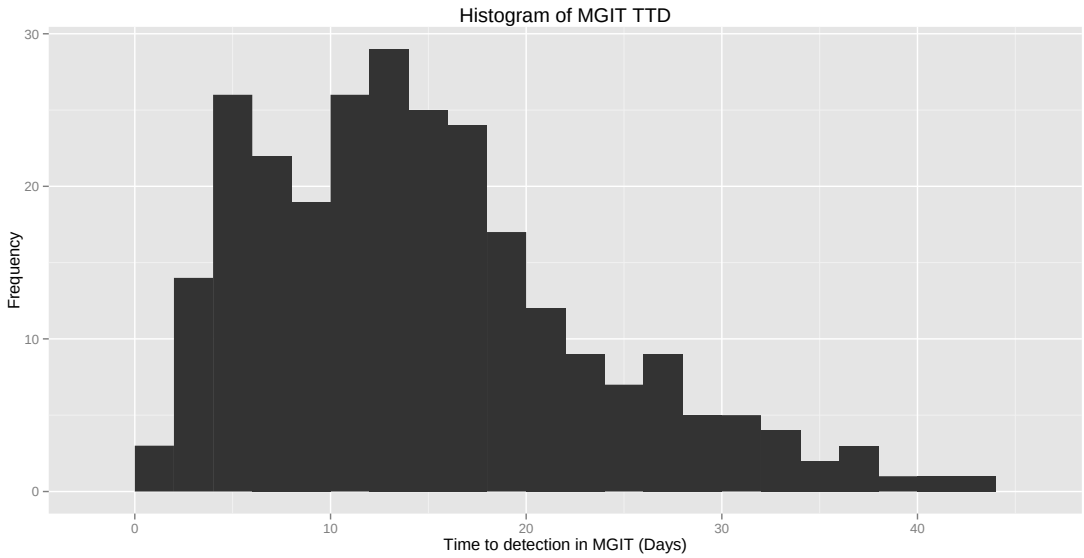

Figure 5.2: Histogram of MGIT time to detection (TTD)

Again there is evidence of a possible bimodal distribution with a positive skew; the mean, 14.3, is higher than the median, 13.1.

5.5.4 Decline of bacterial loads

The bacterial loads estimated by each marker and plotted over each week first as a scatterplot and then as a box plot with whiskers.

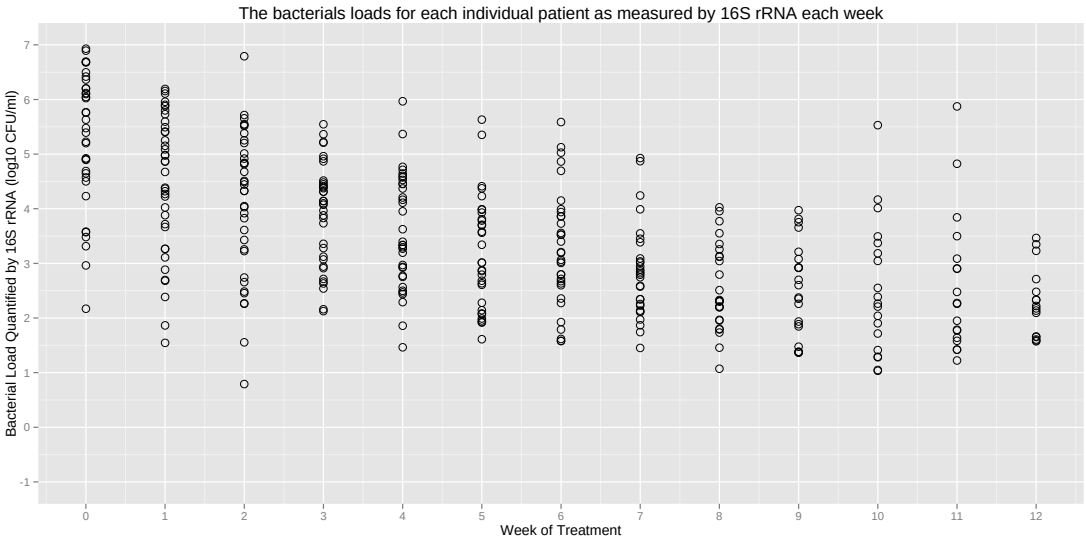

Figure 5.3: **Scatterplot of the bacterial loads for each patient estimated by 16S rRNA for each week**

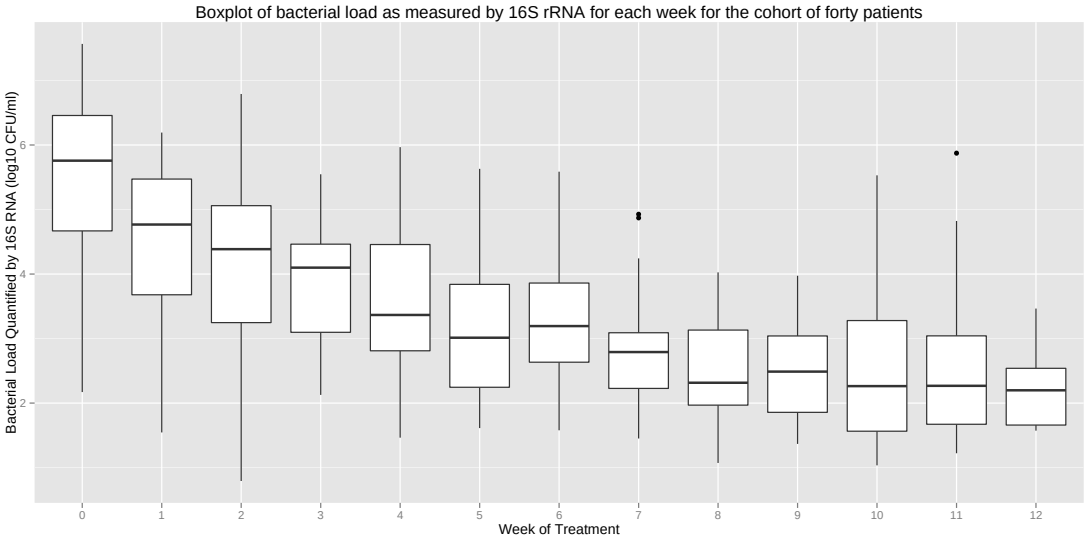

Figure 5.4: Boxplot estimated bacterial loads as measure by 16S rRNA for each week for the cohort of forty patients

There are more samples quantified earlier in treatment. The mean estimated bacterial load declines each week. The range in values is higher earlier in treatment where the higher bacterial loads present and more data points are available. The median bacterial loads are estimated to be higher pre-treatment and decline thereafter.

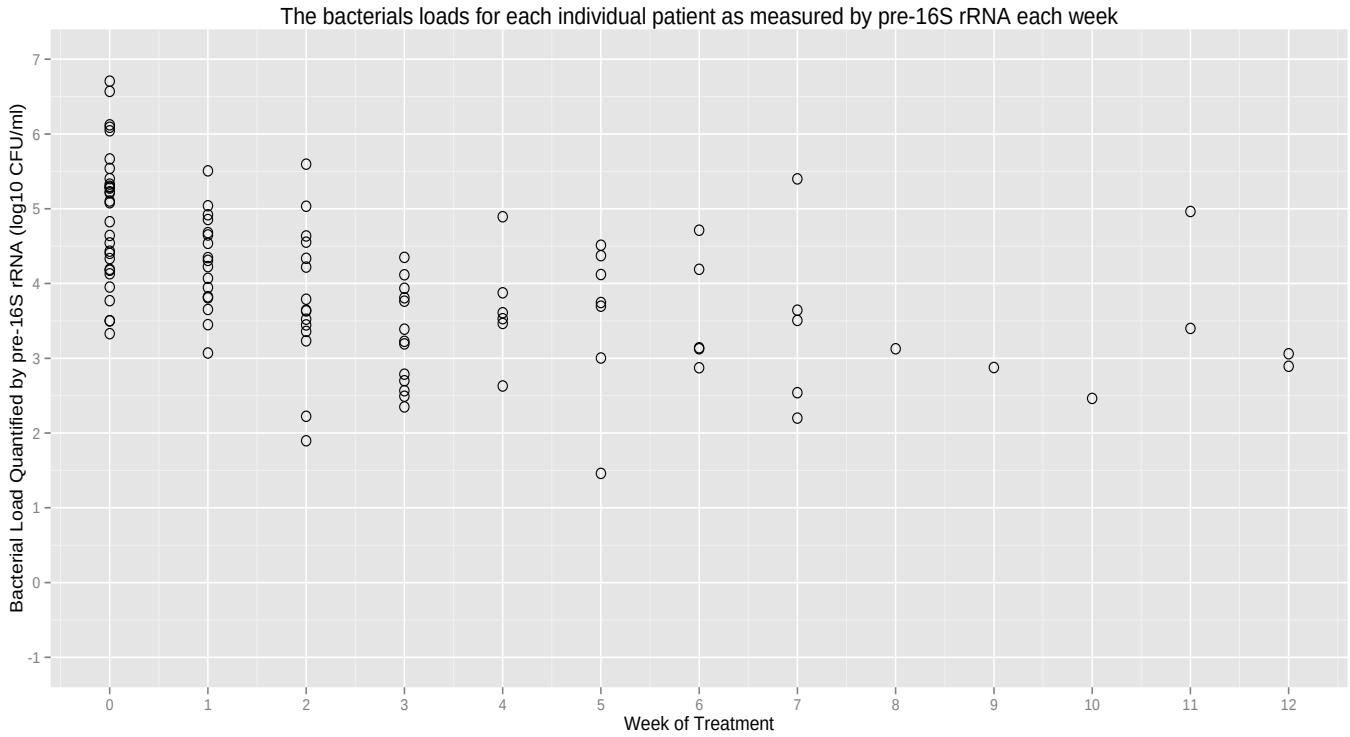

Figure 5.5: Scatterplot of the bacterial loads for each patient estimated by pre-16S rRNA for each week

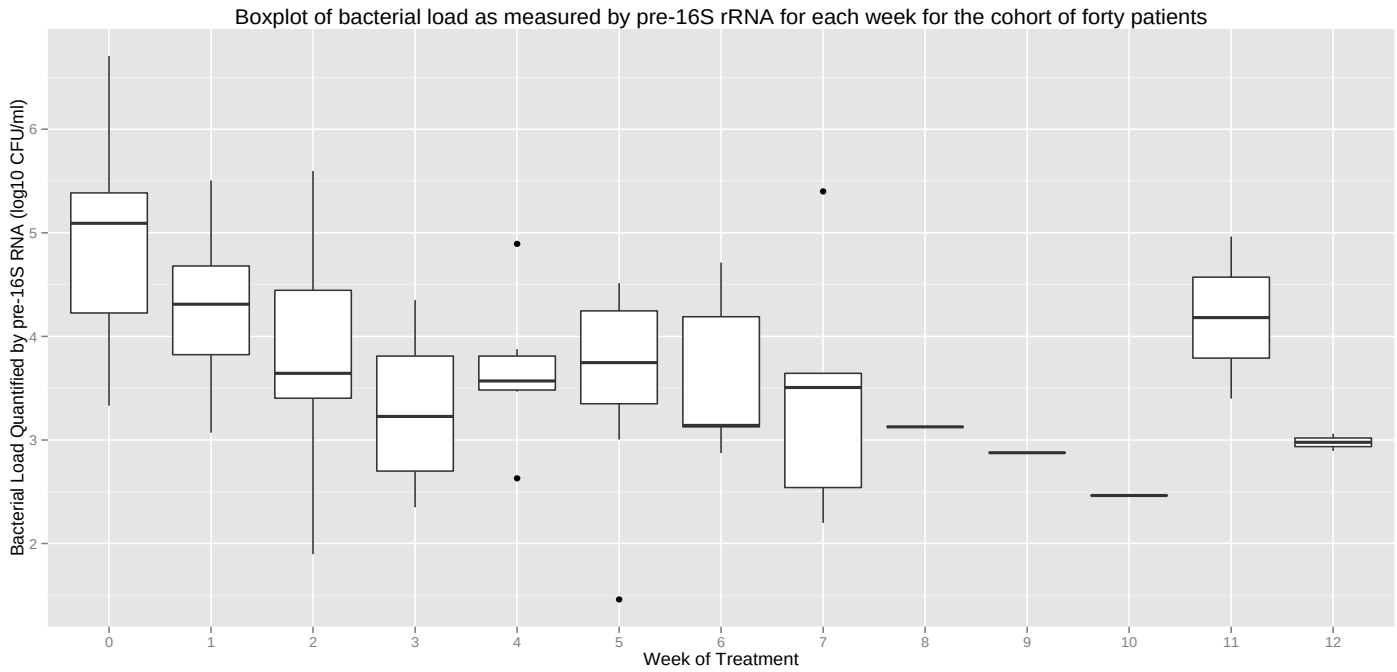

Figure 5.6:Boxplot pre-16S rRNA

The estimated bacterial load as measured pre-16S rRNA is higher than the other markers. There are only two samples estimated below 2 $\log_{10}$ eCFU/ml. There is decline after the initiation of treatment. After the third week the bacterial loads measure remain constant but the majority of samples are negative. The fewer number of positive samples in later weeks and subsequently the range becomes much smaller. After week 3 there were very few patients positive for pre-16S rRNA.

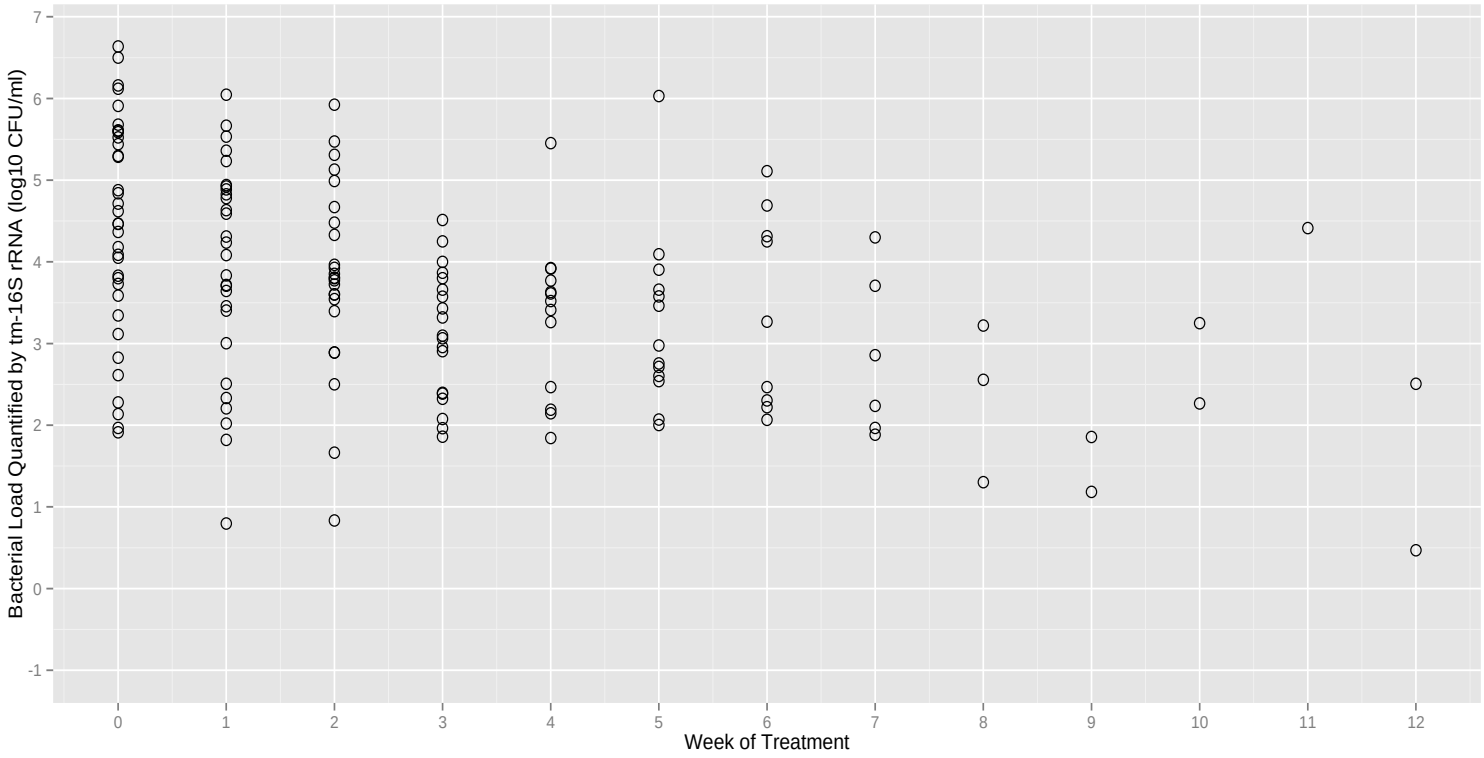

Figure 5.7: Scatterplot he bacterial loads for each patient estimated by pre-16S rRNA for each week

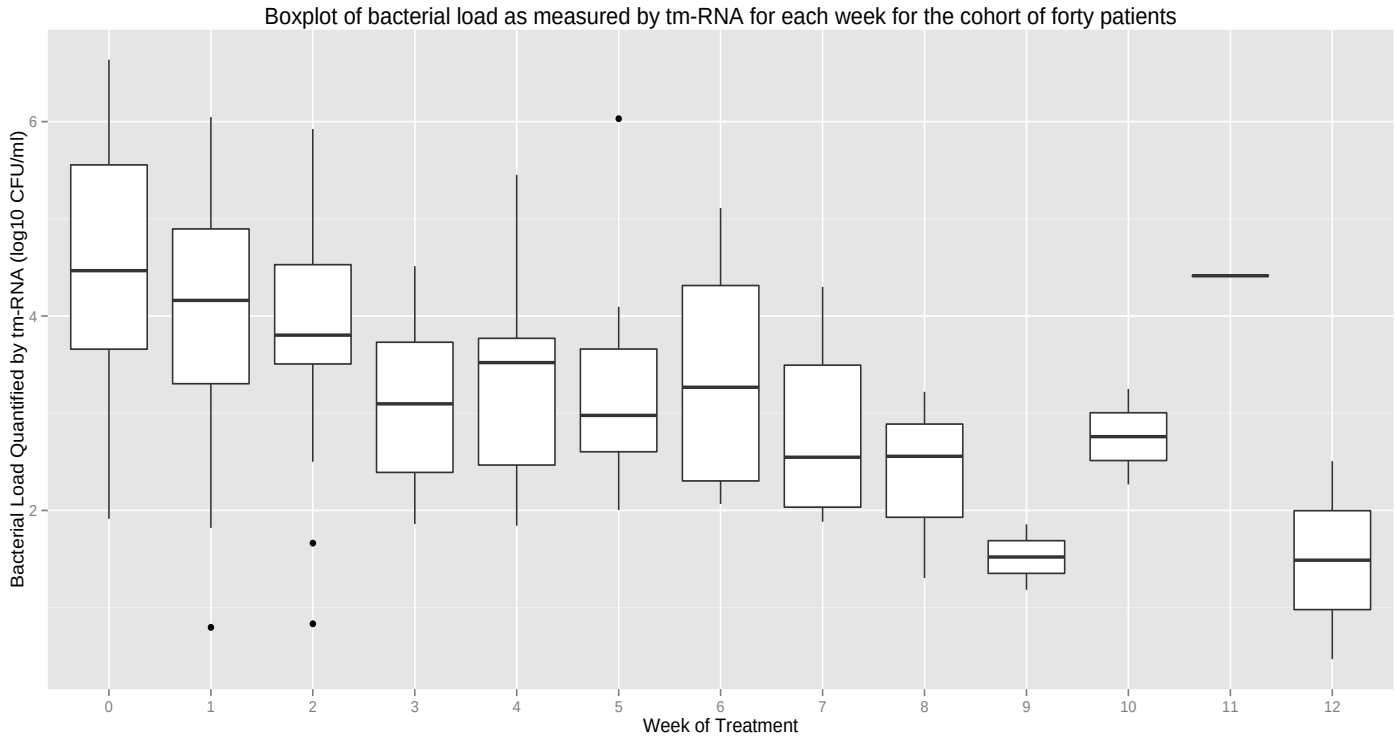

Figure 5.8: Boxplot tm-RNA

The estimated bacterial loads as measured by tm-RNA show the same decline after treatment has begun. There are more samples that are positive in later weeks than that of pre-16S rRNA but fewer than 16S rRNA.

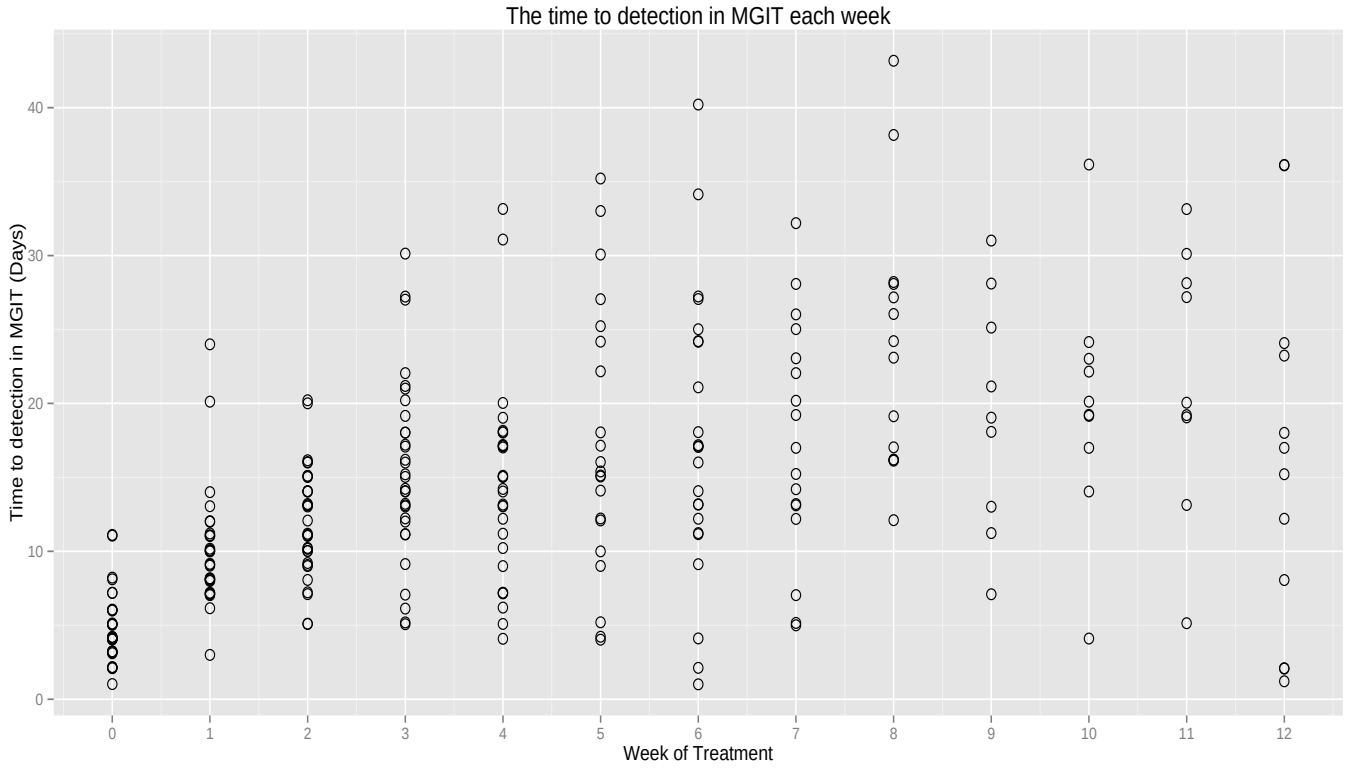

Figure 5.9: Scatterplot of MGIT TTD for each week

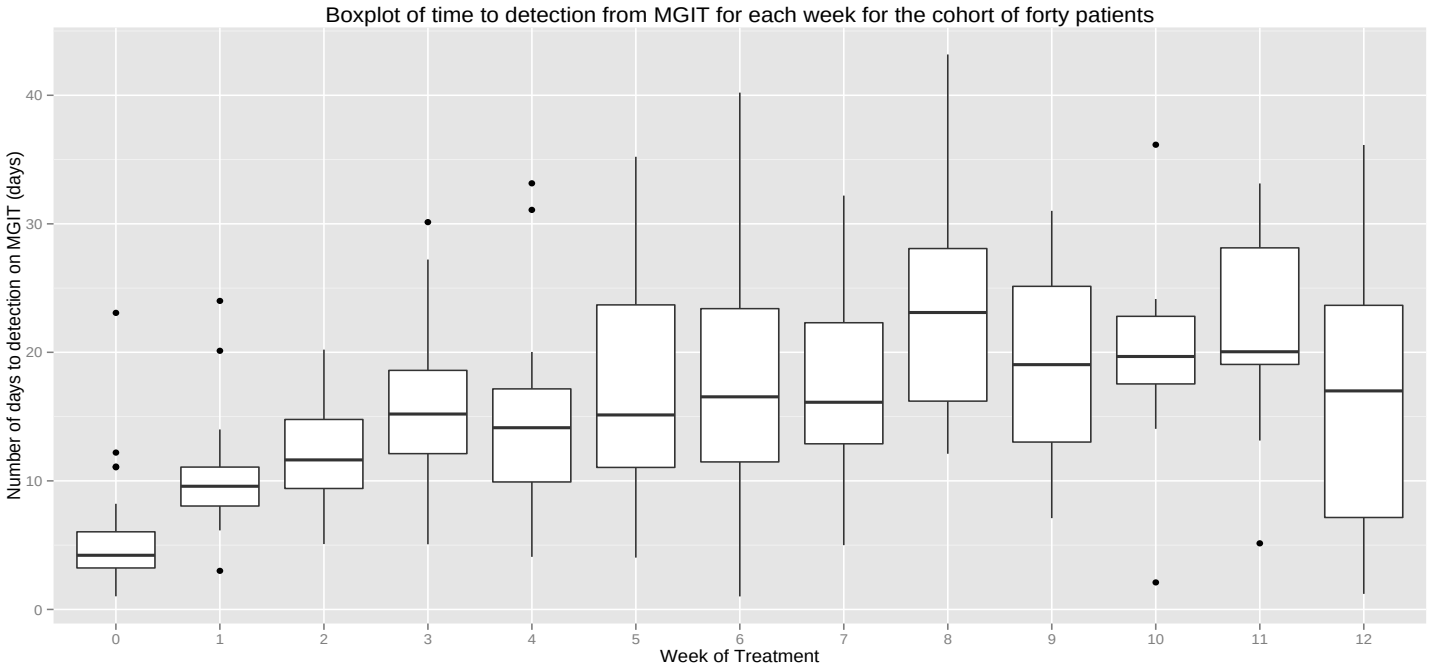

Figure 5.10: Boxplot of MGIT TTD for each week

The lowest values of time are present at the beginning and pre-treatment. Contrary to the molecular data the spread of values for time to detection increases during the course of treatment. Again there are more results available at the start of treatment.

A lattice plot was formed for the three RNA markers. A grey heading titled with the ID number used at KCRI separated each individual patient. Coloured dots were used for each individual marker and if two consecutive points were present a line was drawn between to show the trend.

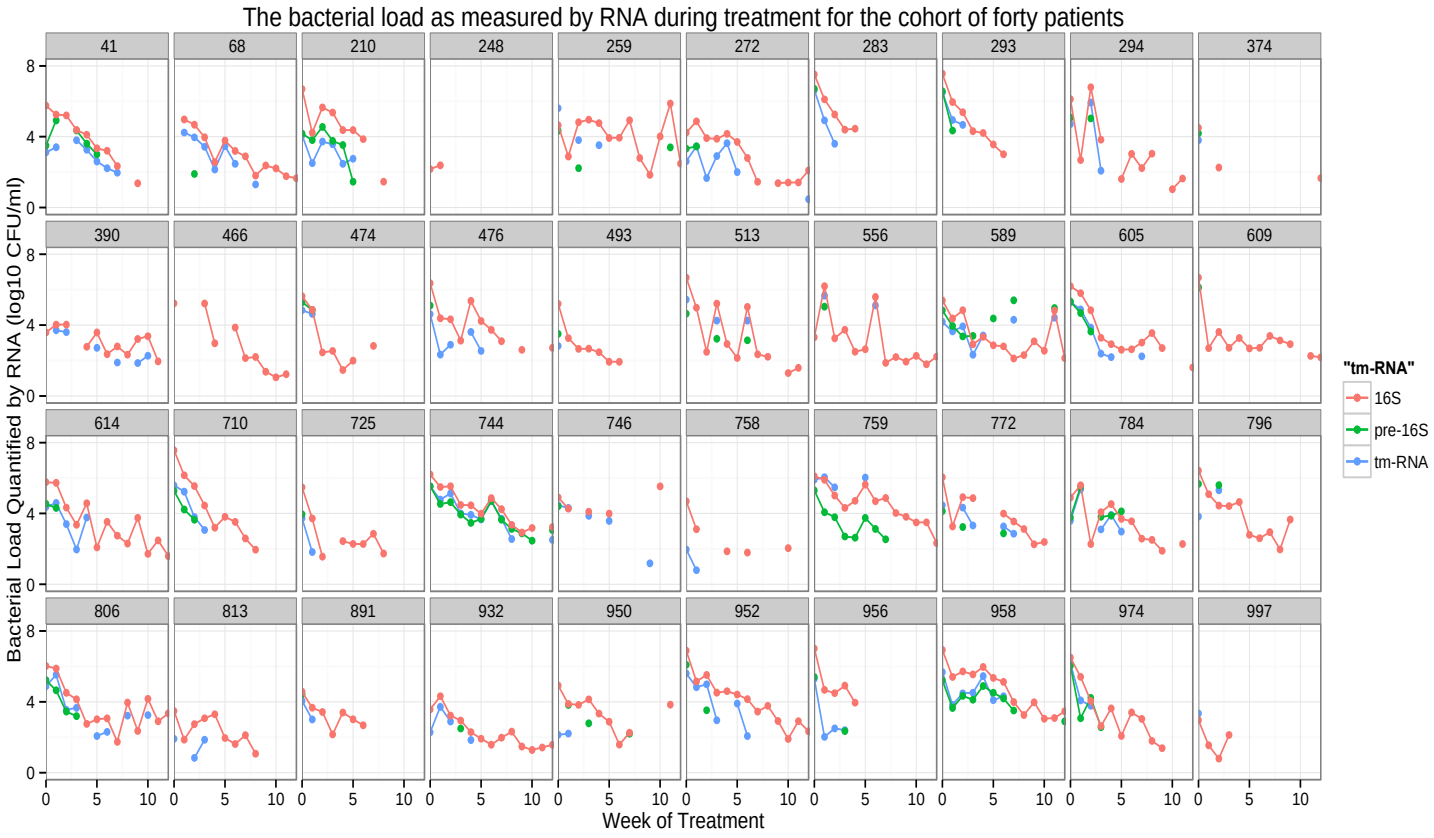

Figure 5.11: Lattice plot RNA markers. Estimated bacterial load against week of treatment with each method represented with a differing colour and subdivided by patient in to boxes headed with the patient ID number.

Although, the trends of for the majority of patient for each marker show a decline over time; they are not the same and estimated CFU values differ for each marker. The 16S rRNA remains positive for longer than the two other RNA markers. Pre-16S rRNA is estimating a higher bacterial load than the other markers.

The same process of drawing a lattice plot for MGIT TTD was performed to allow comparison.

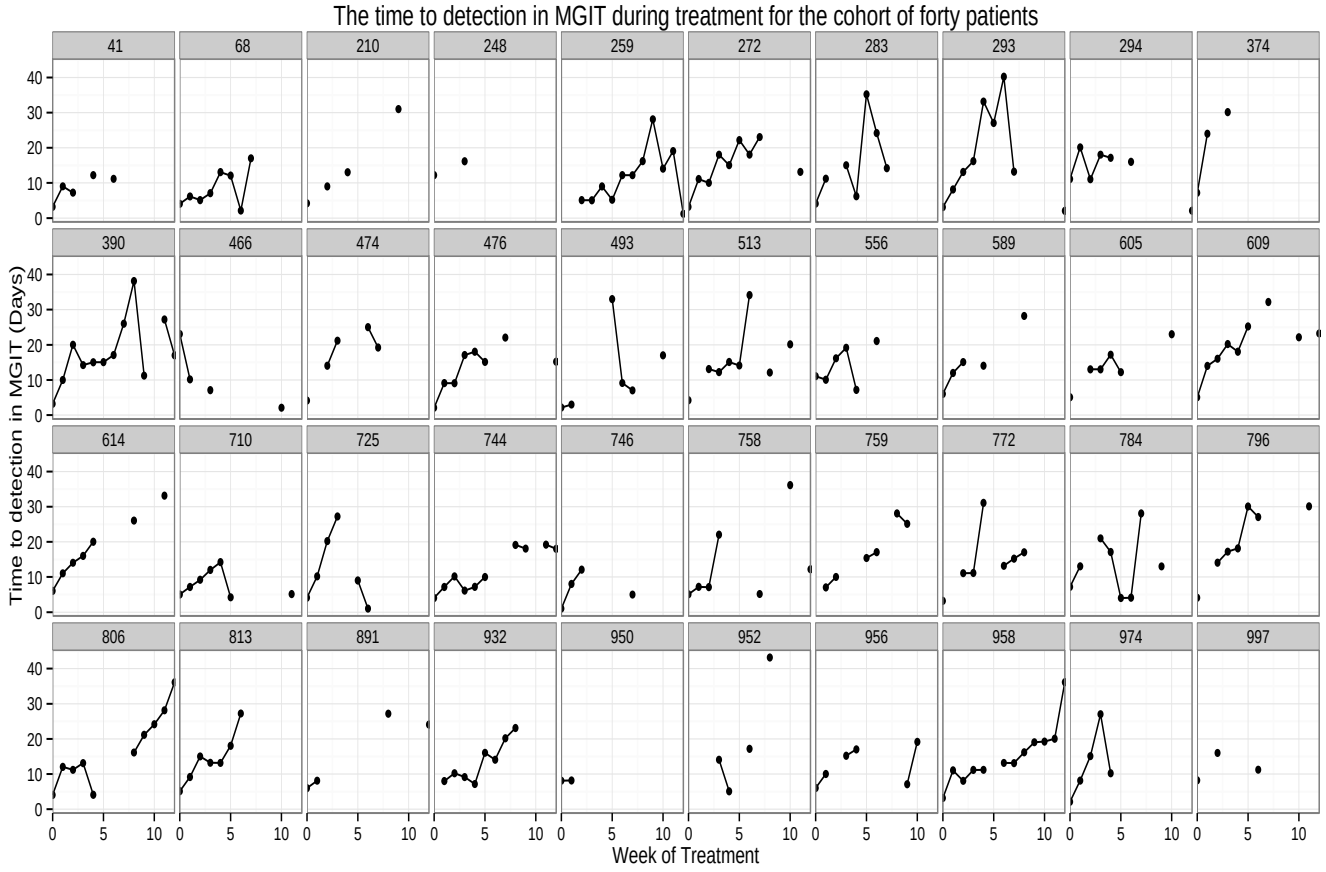

Figure 5.12:Lattice plot MGIT TTD

A general increase in the time to detection can be seen as treatment progresses. However, there is significant variability between individual points. MGIT gives the most data points and remains positive much later in treatment than the two novel molecular methods.

The decline of independent probability testing positive

The independent probability of testing positive each week was plotted in figure 1.

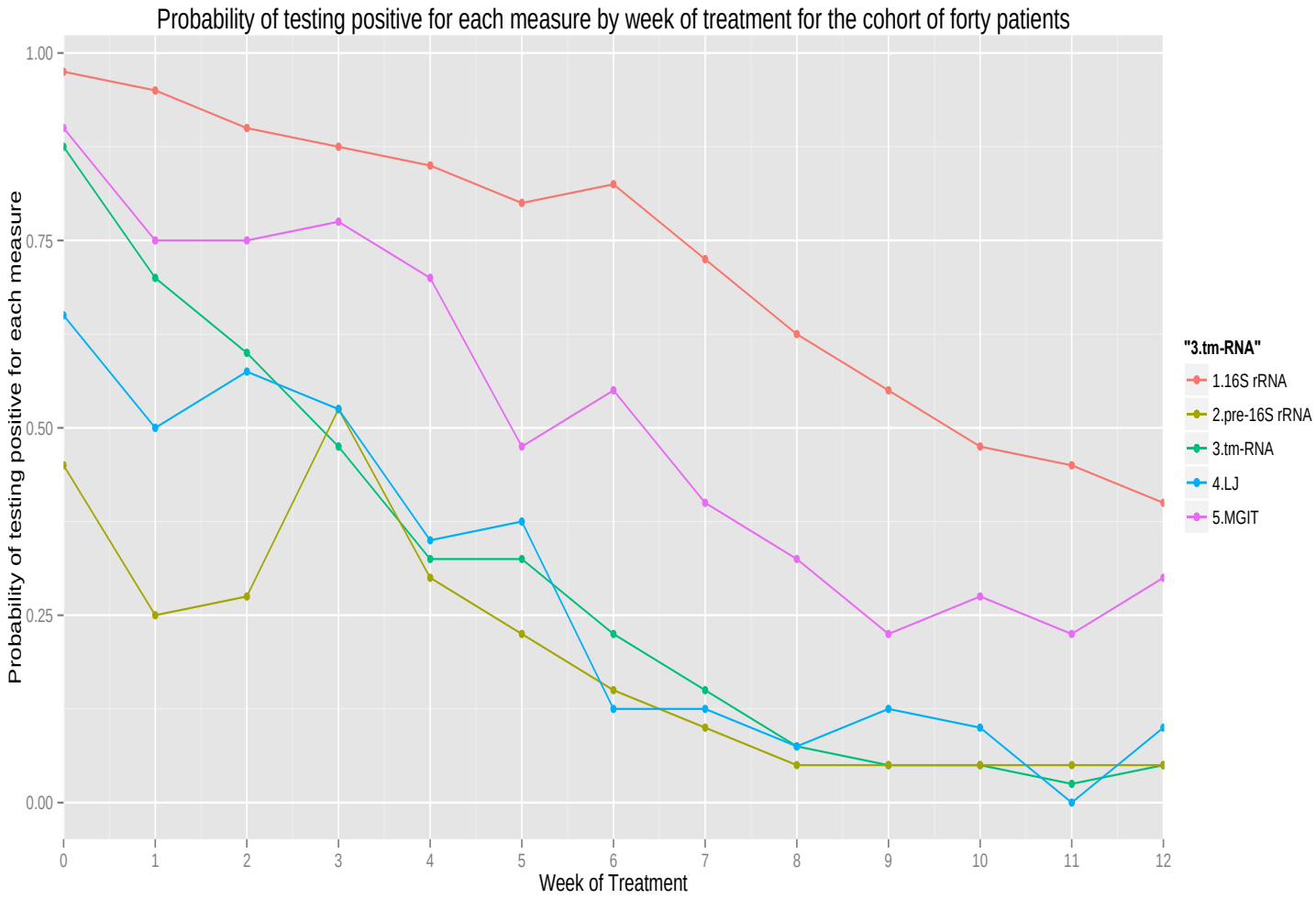

Figure 5.13: Decline in probability of testing positive for each measure by week of treatment for the cohort of forty patients.

The probability of testing positive for all five markers declines over time. No marker is 100% positive at week 0. 16S rRNA has the most positive samples at baseline and at the end of treatment. Under half of patients were positive for pre-16S rRNA prior to treatment. By week 12 over 90% of patients were negative for LJ, tm-RNA and pre-16S rRNA. Half of the patients remained positive for 16S rRNA at week 12.

5.5.5 Linear regressions of quantitative markers over the course of treatment

Linear regressions for each the quantitative data generated from 16S rRNA for each individual patient data set were created. These were then plotted for comparison.

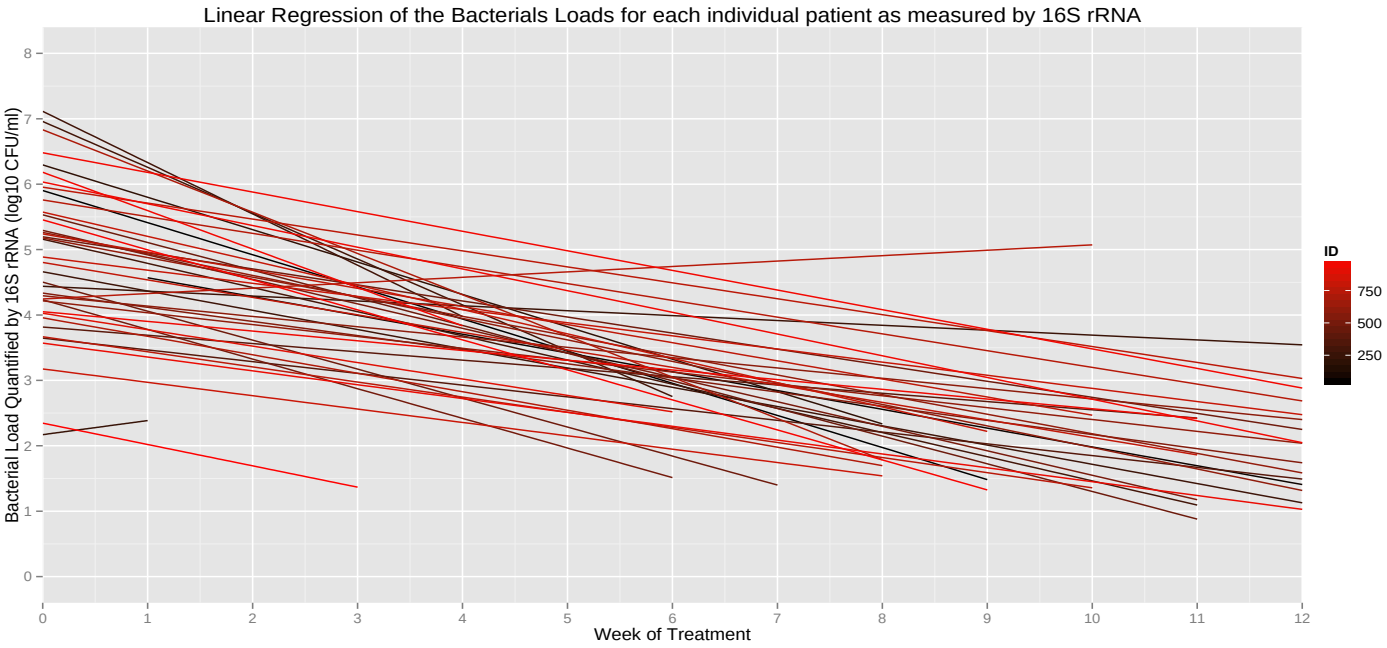

Figure 5.14: Linear regression of the estimated bacterial loads using 16S rRNA for each individual patient denoted by a red grey scale.

The majority of patients show a decline over treatment. The gradients of decline are similar. The patients with highest bacterial loads show the steepest decline. There are few patients with a linear regression suggesting a trend in increasing bacterial load.

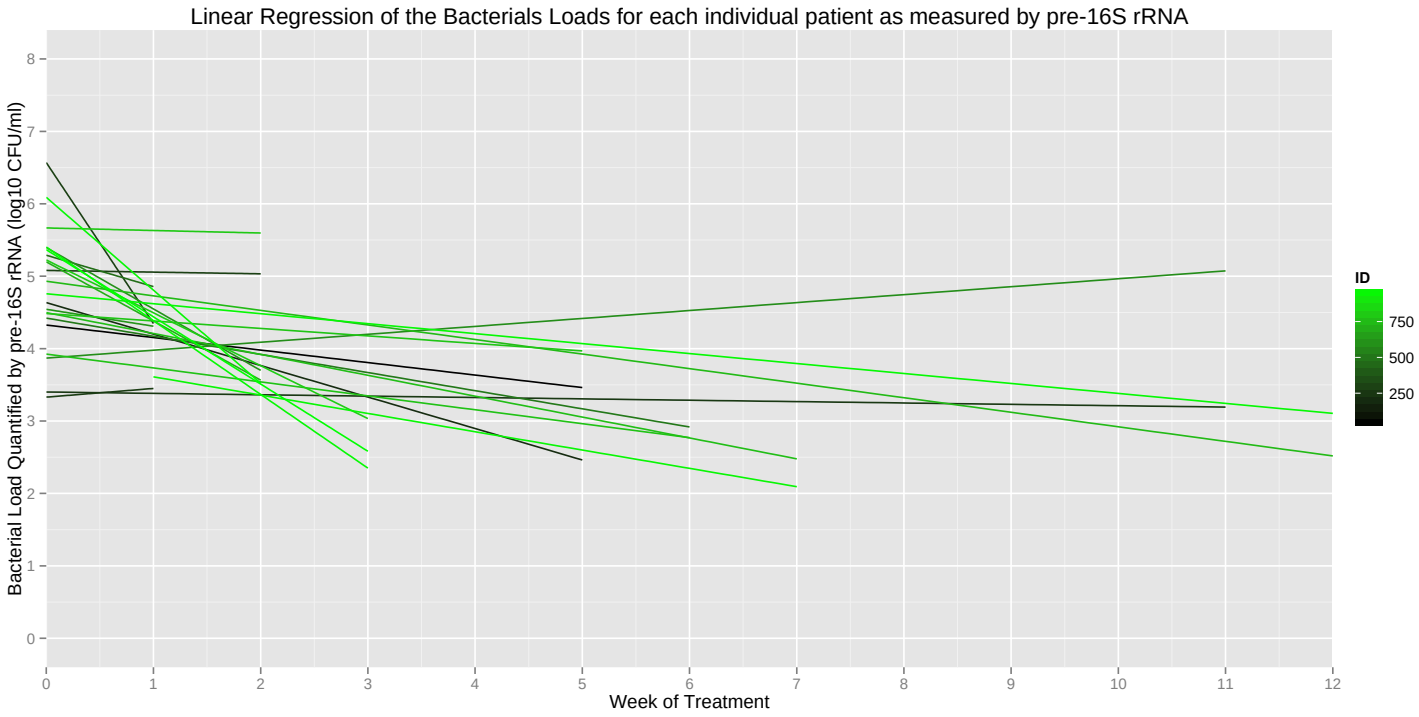

Figure 5.15: Linear regression of the estimated bacterial loads using pre-16S rRNA for each individual patient denoted by a green-grey scale.

There are fewer data available for pre-16S rRNA as there are less bacterial loads quantified to regress. There is more variation in the gradients of regression for pre-16S rRNA.

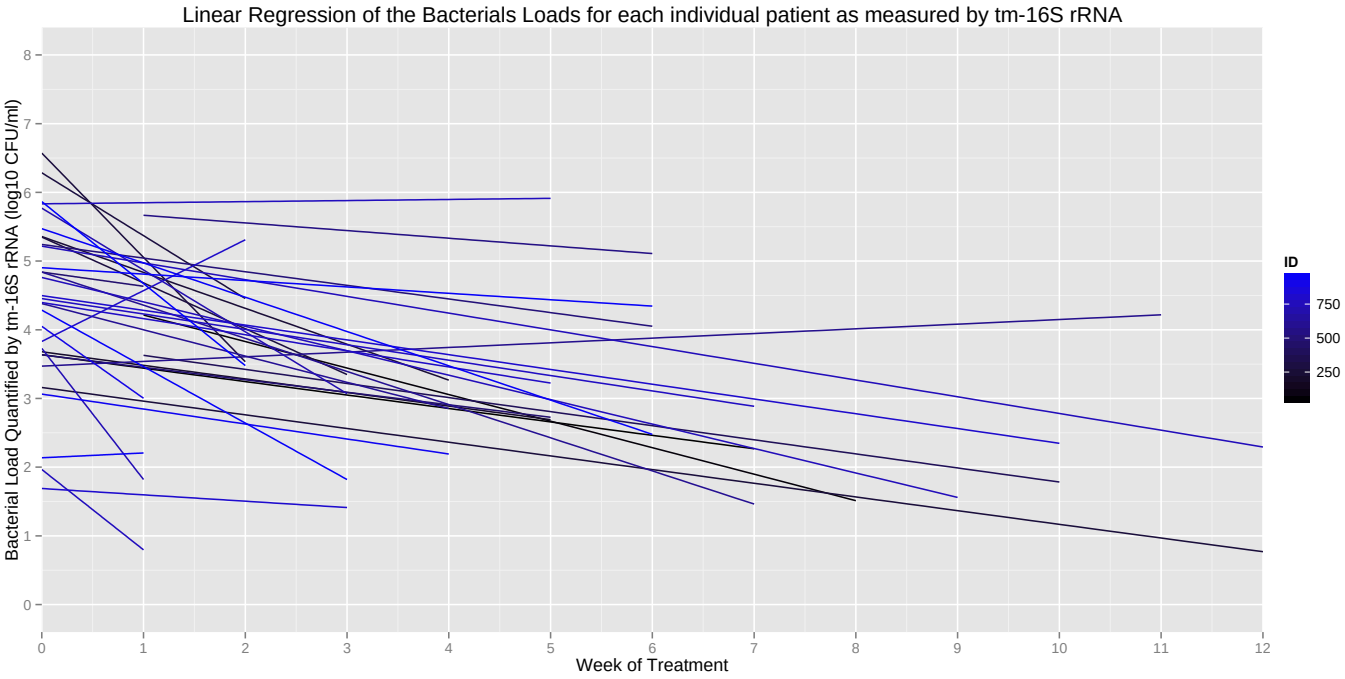

Figure 5.16: Linear regression of the estimated bacterial loads using tm-RNA for each individual patient denoted by a red grey scale.

The gradients of the linear regression of bacterial load estimated by tm-RNA are variable.

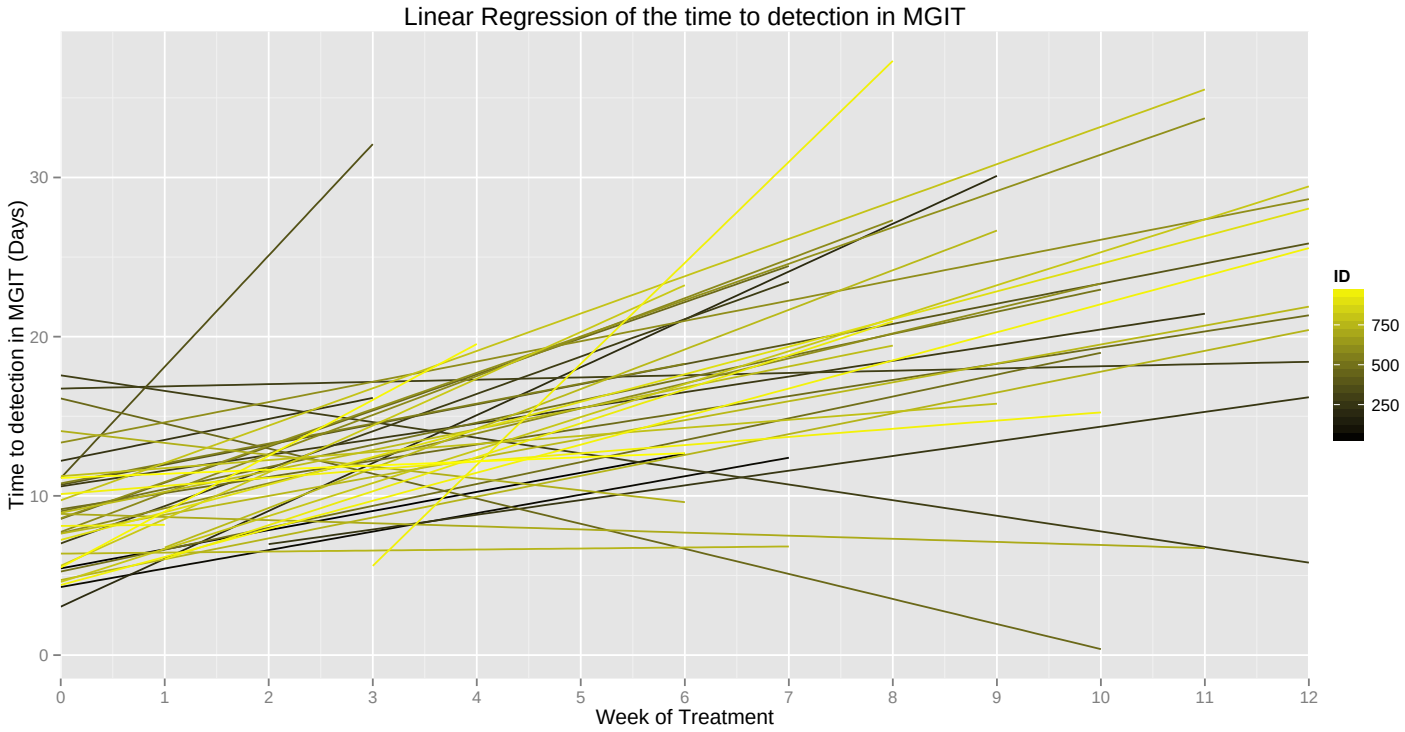

Figure 5.17: Linear regression of the time to detection in MGIT for each individual patient denoted by a yellow grey scale.

There are five patients that show a decrease in time to positivity over the course of treatment but the overall trend is an increase in time to positivity during treatment. There is again substantial variation in the rate of this increase.

Correlation of the quantitative markers

The estimated bacterial load quantified by 16S rRNA was plotted against MGIT TTD and linear regression of the data was performed.

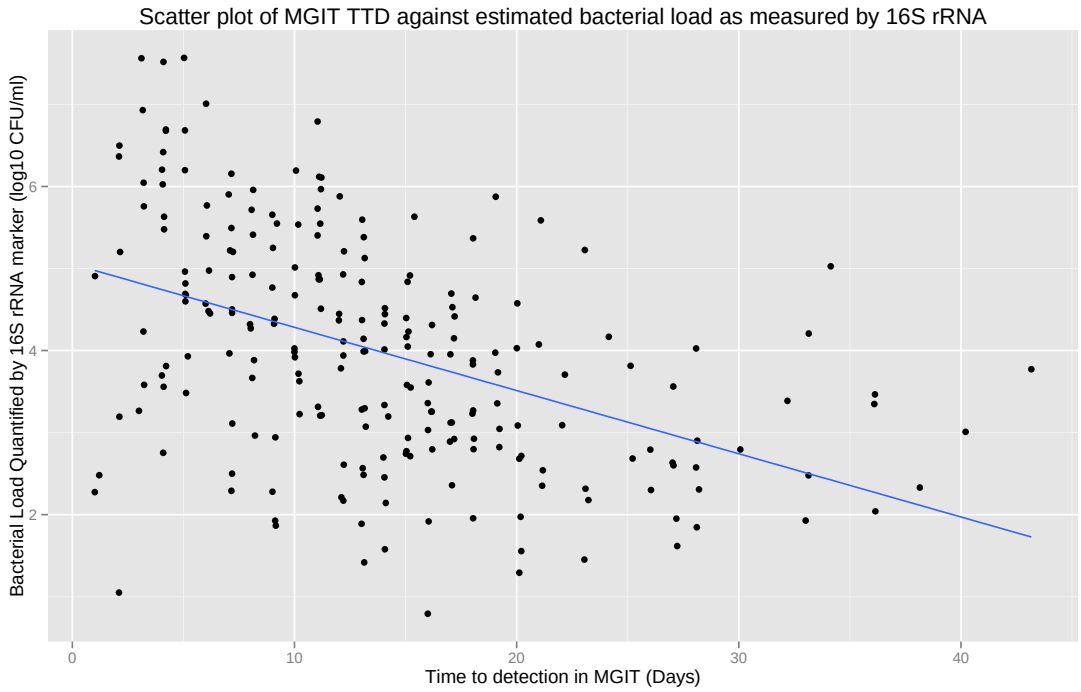

Figure 5.18: Scatterplot of MGIT TTD against bacterial load as measure by 16S rRNA with linear regression represented by a blue line

There was a statistically significant correlation between the quantitative values for MGIT time to detection and 16S rRNA (F-statistic: 58.87 on 1 and 226 DF, p-value: 4.998e-13). However, the adjusted R-squared was very low at 0.2031. The gradient of decline was -2.68.

MGIT TTD against estimated bacterial load as measure by pre-16S rRNA was plotted and linear regression of the data performed.

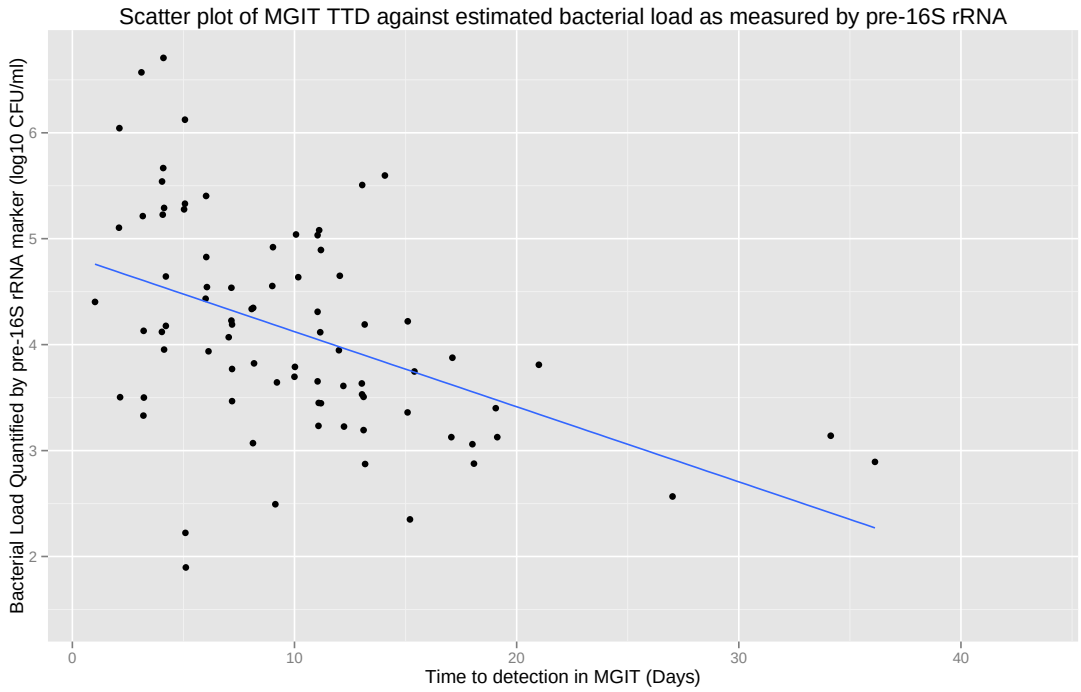

Figure 5.19: Scatterplot of MGIT TTD against bacterial load as measure by pre-16S rRNA with linear regression represented by a blue line

For pre-16S rRNA there was a correlation with TTD inn MGIT, F-statistic: 21.38 on 1 and 79 DF, p-value: 1.448e-05. The adjusted R-squared was 0.203. The gradient of decline was -3.00, much higher than that of 16S rRNA.

MGIT TTD against estimated bacterial load as measured by tm-RNA was plotted with linear regression of the data.

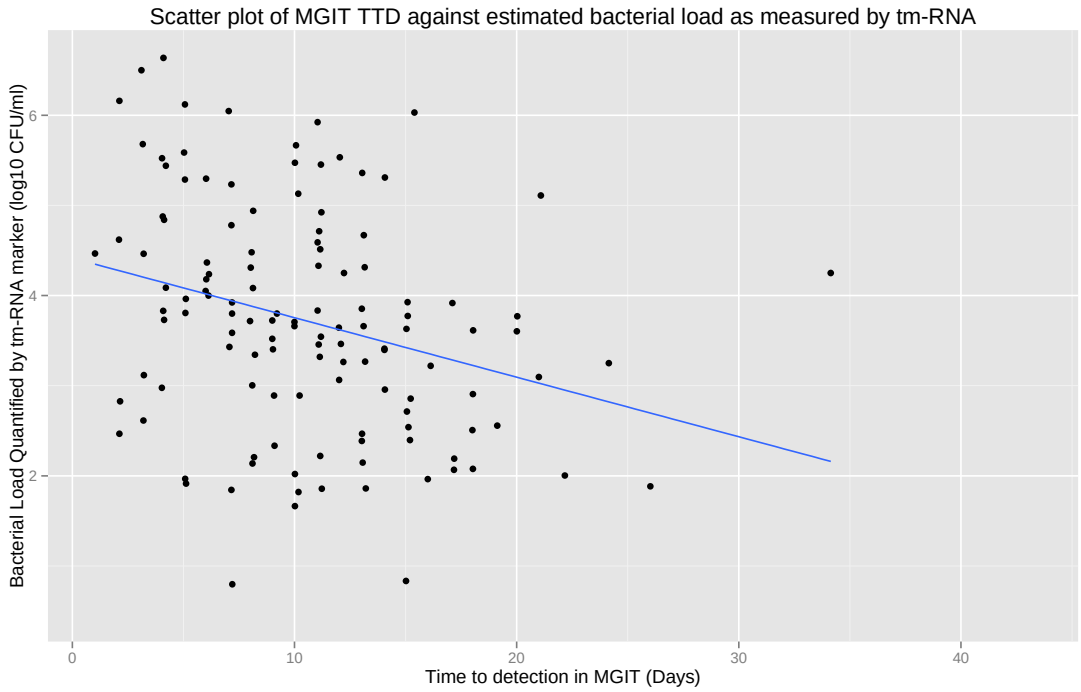

Figure 5.20: Scatterplot of MGIT TTD against bacterial load as measure by tm-RNA with linear regression represented by a blue line

Again there was a statistically significant correlation between tm-RNA and MGIT TTD; F-statistic: 11.49 on 1 and 123 DF, p-value: 0.000943. The gradient of decline was -1.2929. The adjusted R-squared was 0.078.

The estimated bacterial load as measured by 16S rRNA against the estimated bacterial load as measured by pre-16S rRNA was plotted with linear regression displayed as a blue line.

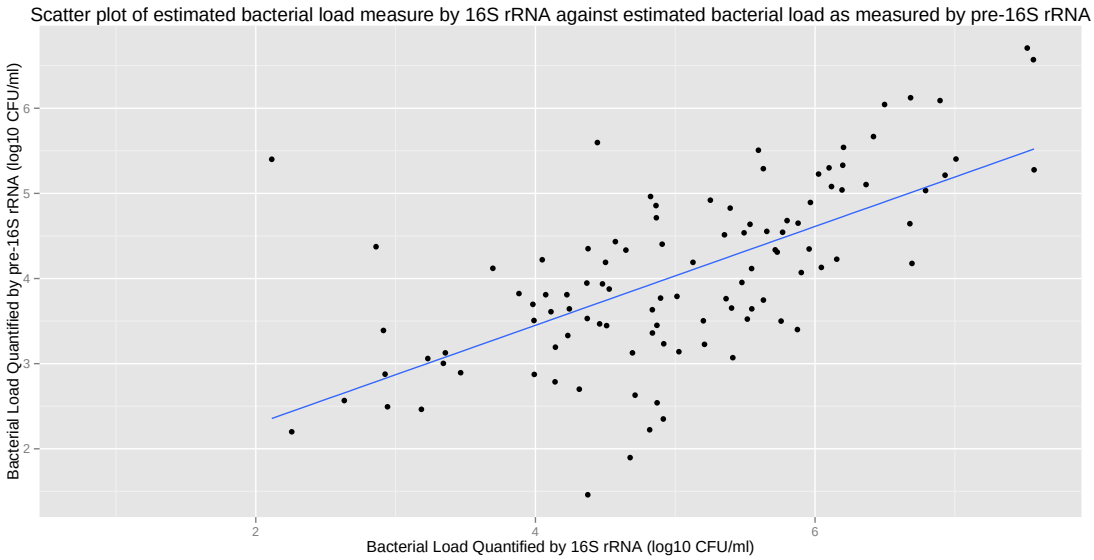

Figure 5.21: Scatterplot of bacterial load as measure by 16S rRNA against bacterial load as measured by pre-16S rRNA with linear regression represented by a blue line

A positive correlation was demonstrated between 16S rRNA and pre-16S rRNA, F-statistic: 73.54 on 1 and 103 DF, p-value: 1.066e-13. The gradient was 0.718. The adjusted R-squared was 0.4109.

The estimated bacterial load as measured by pre-16S rRNA against bacterial load as measured by tm-RNA was plotted with linear regression of the data displayed with a blue line.

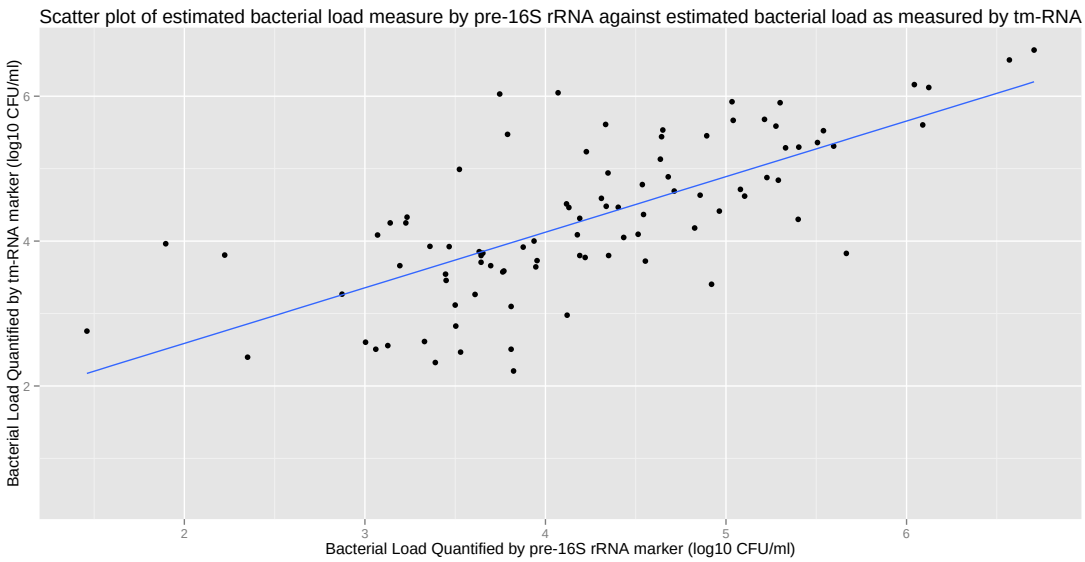

Figure 5.22: Scatterplot of bacterial load as measure by pre-16S rRNA against bacterial load as measured by tm-RNA with linear regression represented by a blue line

There was a positive correlation between pre-16S rRNA and tm-RNA, F-statistic: 88.9 on 1 and 89 DF, p-value: 4.87e-15. The gradient was calculated to be 0.651. The adjusted R-squared was 0.4941.

5.6 Discussion

5.6.1 Statistical Considerations

The data set is large in comparison with other biomarker studies but is still small. First, the sample size makes assessment of normality difficult. The assessments of normality of the data were consistent with literature that has previously described a positive skew of mycobacterial load as measured by MGIT TTD (Perrin et al. 2010).

The correct model for mycobacterial load decline is still undecided. Previous quantitative methods have used bi-exponential models to describe the decline of bacterial loads over the course of treatment (Honeyborne et al. 2011; Gillespie et al. 2002; Davies et al. 2006; Rustomjee et al. 2008).

Due to time constraints linear regression, was used to describe the data rather than demonstrate correlations. Further or more complex statistical analysis such as non-linear mixed models or negative binary regression would have been more helpful if time allowed. The problem with drawing conclusions from the relationship between each marker is that the data points are linked and not independent of one another.

It is important to note that negative results are not integrated into any model describing bacterial load decline. If negative data were set to zero then quantitative markers such as pre-16S rRNA and tm-RNA would have very different gradients of linear regression.

5.6.2 Comparison of results generated for 16S to the literature

Here 16S rRNA was used as a comparator for pre-16S rRNA and tm-RNA. To help give validity to the results described in this chapter it is useful to compare the data generate with already publish data sets.

In 2014, Honeyborne et al. showed 16S rRNA has already shown to correlate with solid culture counts (Honeyborne et al. 2014). The majority of samples from our data set are concordant with the publish literature on 16S rRNA. In figure 5.4 the majority of the samples are positive at two weeks this consistent with results seen in figure 5.23.

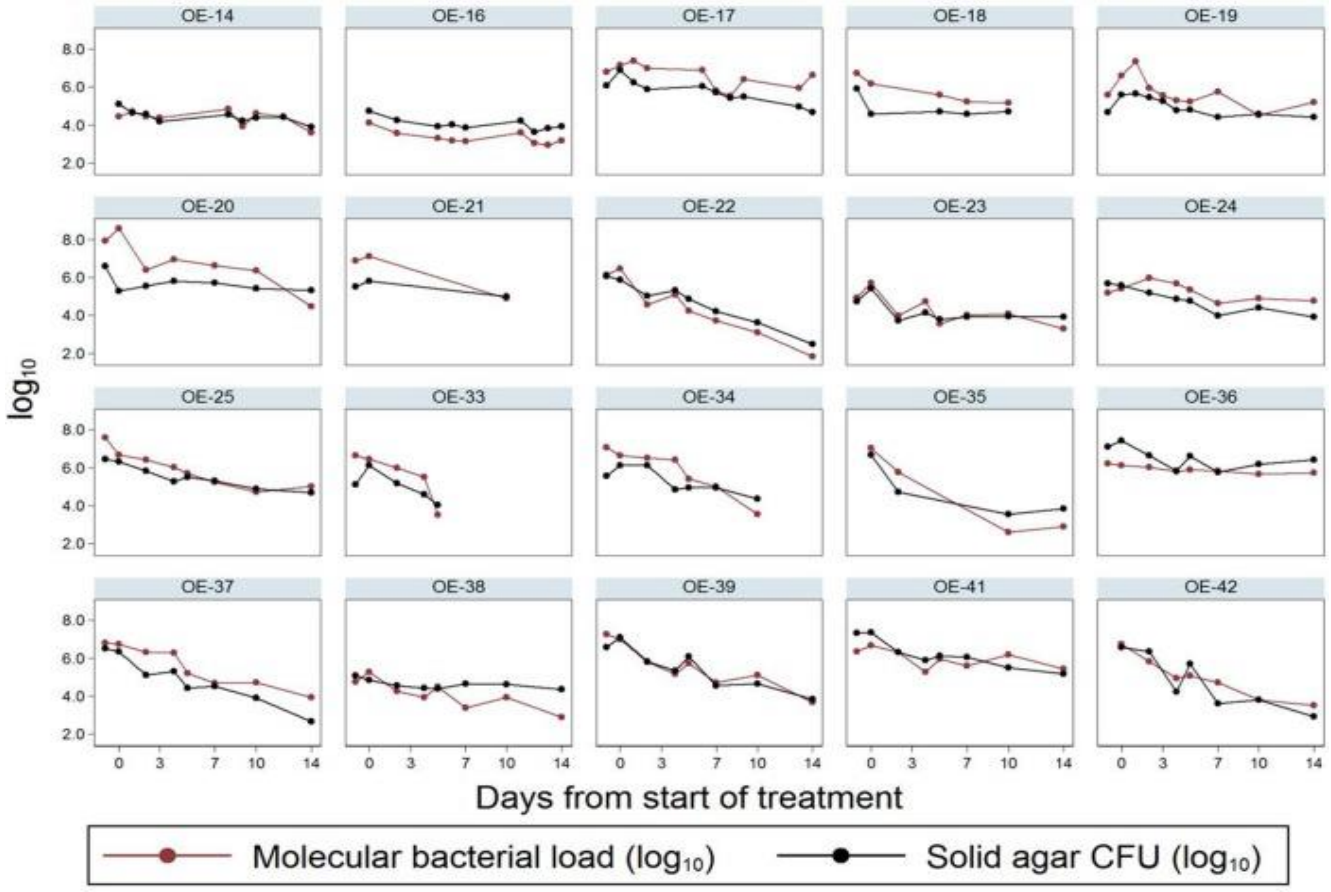

Figure 5.23: Lattice plot taken from Honeyborne et al. showing bacterial loads estimated by 16S rRNA and CFU for the first two weeks of treatment

Figure 5.23 shows only the first two weeks of treatment. The majority of patients are positive at time points. Our sampling rate over the first two weeks was lower but the trend of decline and that the majority of samples being positive are concordant.

5.6.3 Completeness of result vs. culture

For all of the samples processed there were results available for the molecular markers. Contamination rate in MGIT was 9% and 5% in LJ. The time to positivity generated from contaminated samples had to be discarded. This led to a significant amount of MGIT and LJ data being lost to analysis. In clinical practice it can be more important if that the data is only found after the week that the contaminate sample has taken to 'flag' positive.

The loss of data is balanced by the higher sensitivity of MGIT compared to the two novel RNA markers. There are more quantitative data available for analysis particularly at later time points where correlation between treatment successes may be stronger. At present 2 month culture status is the best correlated treatment outcome (Wallis et al. 2015).

5.6.4 Comparing Pre-16S rRNA with 16S rRNA and MGIT TTD

Pre-16S rRNA showed similar distribution to that of 16S rRNA and MGIT. This would suggest that there is a correlation to be found between the data sets.

The estimated bacterial loads were higher for pre-16S rRNA than that of both 16S rRNA and tm-RNA.

The number of positive samples for pre-16S rRNA declines at a similar rate to LJ but much quicker than 16S rRNA and MGIT.

The greater available data for inspection of MGIT and 16S rRNA makes it easier to discern the decline over the first 12 weeks of treatment.

Linear regression of only the available data is interesting, it shows a very different picture from the positive to negative trend . Many patients are not declining or declining slowly. With more data it could be seen if the gradient of decline of individual patients correlated with clinical outcome.

Pre-16S rRNA is only present when cells are actively producing more ribosomes. The more abundant pre-16S rRNA, the more metabolically active the cells are likely to be.

When correlating pre-16S to MGIT TTD the variation in each test is compounded thus increasing the adjusted R2. The R2 was lower for pre-16S rRNA than that of 16S rRNA. Perhaps this is because pre-16S rRNA is a better measure of viable bacilli but

more likely it is because there are fewer positive results later in treatment when the relationship between TTD and RNA is likely changing.

5.6.5 Comparing tm-RNA with 16S rRNA and MGIT TTD

The distribution of the quantitative data for tm-RNA is similar to that of pre-16S rRNA, 16S and MGIT TTD. Again suggesting that there is an underlying correlation to what is being measured.

There were significant number patients positive for tm-RNA positive at the beginning of treatment when compared to pre-16S rRNA. Again the rate of decline was similar to that of LJ. Both MGIT and 16S rRNA were more sensitive at all time points.

5.6.6 Evaluating the binary change of the pre-16S rRNA and tm-RNA data

16S rRNA is a much more stable molecule than pre-16S rRNA and tm-RNA. This is because as well as having a secondary structure 16S rRNA has proteins complexed within. Once the cell becomes non-viable 16S rRNA is more resistant to degradation. In theory this could mean that 16S rRNA is detectable once the cells are non-viable. Both pre-16S rRNA and tm-RNA have less complex secondary structures and are therefore more labile. This can be seen in the data set generated.

The pre-16S rRNA and tm-RNA assays convert to negative very quickly and at a similar rate to that of LJ, figure 5.13.

The similar rates of decline between the two novel markers and LJ may be a promising avenue for predicting treatment outcome because at present 2 month solid culture status is the current best measure of treatment response.

Furthermore, for the evaluation of potential chemotherapy regimens an estimate of early bacterial activity could be gained by the results of pre-16S rRNA and tm-RNA converting to negative.

5.7 Conclusion

The field-testing in this chapter has shown that the remodelled assay with the new *M. marinum* control was able to give reliable results from 520 patient samples. Both pre-16S rRNA and tm-RNA were able to assess the response to treatment. With the limited data set there was a degree of correlation with existing markers such as MGIT TTP, LJ and 16S rRNA. However, no overall conclusions could be drawn without further analysis of the data and with treatment outcomes present.

6 Chapter 6: Final discussion

6.1 Discussion

6.1.1 Molecular vs. culture assays

Molecular methodologies have certain trade offs when compared with conventional methods such as culture. Culture has a high rate of contamination and can be dangerous. The various processing steps of culture methods increase the risk of Laboratory acquired infections. In our study sputum was decontaminated, however, this does not need to occur, as the primers are specific for *M. tuberculosis complex.* It is thought that the bacillary load can be reduced by about 1 $\log_{10}$ CFU/ml.

Although liquid culture gives a result quicker than solid culture it is still required to reach 42 days in order to 'flag' as negative. Here, the pooled median time to positivity was two weeks. This does not compare favourably with RT-qPCR that can give a result in four hours. The speedy turn around time would allow a molecular methodology to accelerate the MAMS or STEP trial methodology described in 3.1.2. Thus, in turn hastening the drug development process.

Costing per test for both methodologies are similar. The cost for combined smear and culture is estimated to be $20 to $40. (Lu et al. 2013) Whereas, the GeneXpert®, the most widely available molecular platform, costs around $20 per test and this has been subsidised by the Bill and Melinda Gates Foundation to $10. (Albert et al. 2016) The difficulty with the molecular techniques is the start up cost associated with molecular platforms as well as developing expertise in molecular methods. Taken together, traditional culture methods are much cheaper but the price of molecular methods would fall if they were more widely used.

6.2 Conclusion

Prior to the start of this work, there was no accepted biomarker for use in monitoring treatment response. This was only a small data set but takes us one step towards this goal. 16S rRNA has been shown to correlate well with currently used mycobacterial methods. The important part of 16S rRNA is that it more accurately reflects the viable bacilli. The purpose of this work was to see if a more accurate measure of viable bacilli could be found and if by measuring other RNA molecules with complex secondary structures could more information be gleaned in monitoring treatment response.

The interpretation of the results gathered remains open until further work is performed. However, pre-16S rRNA and tm-RNA potentially offer a better measure of viable bacilli.

The pre-16S rRNA and tm-RNA developed into working assays in research laboratories. In the field the combination with *phyB* was shown not to be robust enough.

The assays were redeveloped with *M. marinum* internal control to make them robust. With hindsight choosing *M. marinum* was not ideal. The cross reactivity between the two assays meant a 'correct' concentration of *M. marinum* had to be selected. If a different Mycobacterium such as *M. smegmatis* that has no cross detection had been used this would not have to be done.

The data from chapter 5 showed that treatment response could be assessed using pre-16S rRNA and tm-RNA and the *M. marinum* control demonstrated that the results were robust and reliable.

The pre-16S rRNA and tm-RNA assays offered a faster response to treatment than 16S rRNA and far faster than traditional culture techniques. This speed in assessing response could allow the clinician to assess treatment response early during treatment.

6.3 Future work

The future work is always to look at larger data sets. Here, the reason would be to look at the correlation with treatment outcomes. This would be best done in a trial where treatment success is low for example in drug resistance. The pre-16S rRNA and tm-RNA assays would need to be compared with the standard of care that is now MGIT. It would be important to include 16S rRNA and likely LJ.

It would be very interesting to attempt to use tm-RNA and pre-16S rRNA to describe different bacilli populations. The data could be fed into a mathematical model such as the one described by previously (Bowness et al. 2015).

It would be interesting to interrogate the data set with more complex mathematical modelling. Previously, bacterial load decay has been described using a bi-exponential model.(Honeyborne et al. 2011; Gillespie et al. 2002; Davies et al. 2006; Rustomjee et al. 2008)

Another scope of work would be to apply these assays to other disease processes such as NTM disease or patients with chronic bacterial carriage such as CF, bronchiectasis or COPD.

8 References

Agmon, I. et al., 2004. Ribosomal crystallography: a flexible nucleotide anchoring tRNA translocation, facilitates peptide-bond formation, chirality discrimination and antibiotics synergism. *FEBS Letters*, 567(1), pp.20–26.

Ahmad, Z. et al., 2011. Dose-dependent activity of pyrazinamide in animal models of intracellular and extracellular tuberculosis infections. *Antimicrobial agents and chemotherapy*, 55(4), pp.1527–1532.

Albert, H. et al., 2016. Development, roll-out and impact of Xpert MTB/RIF for tuberculosis: what lessons have we learnt and how can we do better? *The European respiratory journal*, 48(2), pp.516–525.

Anon, 1953. Isoniazid in combination with streptomycin or with P.A.S. in the treatment of pulmonary tuberculosis; fifth report to the Medical Research Council by their Tuberculosis Chemotherapy Trials Committee. *British medical journal*, 2(4844), pp.1005–1014.

Anon, 1970. Isoniazid with thiacetazone (thioacetazone) in the treatment of pulmonary tuberculosis in East Africa--second report of fifth investigation. Aco-operative study in East African hospitals, clinics and laboratories with the collaboration of the East African and British Medical Research Councils. *Tubercle*, 51(4), pp.353–358.

Anon, 1948. Streptomycin treatment of tuberculous meningitis. *Lancet (London, England)*, 1(6503), pp.582–596.

Arioli, V. et al., 1967. Rifampicin: a new rifamycin. I. Bacteriological studies. *Arzneimittel-Forschung*, 17(5), pp.523–529.

Azuma, J. et al., 2013. NAT2 genotype guided regimen reduces isoniazid-induced liver injury and early treatment failure in the 6-month four-drug standard treatment of tuberculosis: a randomized controlled trial for pharmacogenetics-based therapy. *European journal of clinical pharmacology*, 69(5), pp.1091–1101.

Azzurri, A. et al., 2006. Serological markers of pulmonary tuberculosis and of response to anti-tuberculosis treatment in a patient population in Guinea. *International journal of immunopathology and pharmacology*, 19(1), pp.199–208.

Bajaj, G., Rattan, A. & Ahmad, P., 1989. Prognostic value of "C" reactive protein in tuberculosis. *Indian pediatrics*, 26(10), pp.1010–1013.

Banada, P.P. et al., 2010. Containment of bioaerosol infection risk by the Xpert MTB/RIF assay and its applicability to point-of-care settings. *Journal of clinical microbiology*, 48(10), pp.3551–3557.

Bark, C.M. et al., 2011. Time to detection of Mycobacterium tuberculosis as an alternative to quantitative cultures. *Tuberculosis (Edinburgh, Scotland)*, 91(3), pp.257–259.

Belanger, A.E. et al., 1996. The embAB genes of Mycobacterium avium encode an

arabinosyl transferase involved in cell wall arabinan biosynthesis that is the target for the antimycobacterial drug ethambutol. *Proceedings of the National Academy of Sciences of the United States of America*, 93(21), pp.11919–11924.

Benson, W.M., Stefko, P.L. & Roe, M.D., 1952. Pharmacologic and toxicologic observations on hydrazine derivatives of isonicotinic acid (rimifon, marsilid). *American review of tuberculosis*, 65(4), pp.376–391.

Bernstein, J. et al., 1952. Chemotherapy of experimental tuberculosis. V. Isonicotinic acid hydrazide (nydrazid) and related compounds. *American review of tuberculosis*, 65(4), pp.357–364.

Besra, G.S. et al., 1995. A new interpretation of the structure of the mycolyl-arabinogalactan complex of Mycobacterium tuberculosis as revealed through characterization of oligoglycosylalditol fragments by fast-atom bombardment mass spectrometry and 1H nuclear magnetic resonance spectroscopy. *Biochemistry*, 34(13), pp.4257–4266.

Bobrowitz, I.D. & Gokulanathan, K.S., 1965. Ethambutol in the retreatment of pulmonary tuberculosis. *Diseases of the chest*, 48(3), pp.239–250.

Boehme, C.C. et al., 2010. Rapid Molecular Detection of Tuberculosis and Rifampin Resistance. *dx.doi.org*, 363(11), pp.1005–1015.

Boeree, M. & Heinrich, N., High-Dose Rifampin, SQ109 and Moxifloxacin for Treating TB: The PanACEA MAMS-TB Trial. In CROI. Seattle.

Boeree, M.J. et al., 2015. A dose-ranging trial to optimize the dose of rifampin in the treatment of tuberculosis. *American journal of respiratory and critical care medicine*, 191(9), pp.1058–1065.

Boeree, M.J. et al., 2017. High-dose rifampicin, moxifloxacin, and SQ109 for treating tuberculosis: a multi-arm, multi-stage randomised controlled trial. *The Lancet. Infectious diseases*, 17(1), pp.39–49.

Bowness, R. et al., 2015. The relationship between Mycobacterium tuberculosis MGIT time to positivity and cfu in sputum samples demonstrates changing bacterial phenotypes potentially reflecting the impact of chemotherapy on critical sub-populations. *The Journal of antimicrobial chemotherapy*, 70(2), pp.448–455.

Britschgi, T.B. & Cangelosi, G.A., 1995. Detection of rifampin-resistant bacteria using DNA probes for precursor rRNA. *Molecular and Cellular Probes*, 9(1), pp.19–24.

CADAR, M.E. & GABOREANU, M., 2014. A LIFE FOR NOBEL PRIZE, REMEMBER GEORGE EMIL PALADE. *… University of Agricultural Sciences …*.

Campbell, E.A. et al., 2001. Structural mechanism for rifampicin inhibition of bacterial rna polymerase. *Cell*, 104(6), pp.901–912.

Cangelosi, G.A. & Brabant, W.H., 1997. Depletion of pre-16S rRNA in starved Escherichia coli cells. *Journal of bacteriology*, 179(14), pp.4457–4463.

Cangelosi, G.A. et al., 1996. Detection of rifampin- and ciprofloxacin-resistant Mycobacterium tuberculosis by using species-specific assays for precursor rRNA. *Antimicrobial agents and chemotherapy*, 40(8), pp.1790–1795.

Cannas, A. et al., 2008. Mycobacterium tuberculosis DNA detection in soluble fraction of urine from pulmonary tuberculosis patients.

Carr, R.E. & Henkind, P., 1962. Ocular Manifestations of Ethambutol: Toxic Amblyopia After Administration of an Experimental Antituberculous Drug. *Archives of ophthalmology*, 67(5), pp.566–571.

Chan, C.H. et al., 1995. Elevated interleukin-2 receptor level in patients with active pulmonary tuberculosis and the changes following anti-tuberculosis chemotherapy. *European Respiratory Journal*, 8(1), pp.70–73.

Daniel, T.M., 2015. *Jean-Antoine Villemin and the infectious nature of tuberculosis*, International Union Against Tuberculosis and Lung Disease.

Davies, G.R. et al., 2006. Use of nonlinear mixed-effects analysis for improved precision of early pharmacodynamic measures in tuberculosis treatment. *Antimicrobial agents and chemotherapy*, 50(9), pp.3154–3156.

de Assunção, T.M. et al., 2014. Real time PCR quantification of viable Mycobacterium tuberculosis from sputum samples treated with propidium monoazide. *Tuberculosis*, 94(4), pp.421–427.

de Steenwinkel, J.E.M., Aarnoutse, R.E., et al., 2013. Optimization of the rifampin dosage to improve the therapeutic efficacy in tuberculosis treatment using a murine model. *American journal of respiratory and critical care medicine*, 187(10), pp.1127–1134.

de Steenwinkel, J.E.M., de Knegt, G.J., et al., 2013. Relapse of tuberculosis versus primary tuberculosis; course, pathogenesis and therapy in mice. *Tuberculosis (Edinburgh, Scotland)*, 93(2), pp.213–221.

Demir, T. et al., 2002. sICAM-1 as a serum marker in the diagnosis and follow-up of treatment of pulmonary tuberculosis.

DESJARDIN, L.E. et al., 2012. Measurement of Sputum Mycobacterium tuberculosis Messenger RNA as a Surrogate for Response to Chemotherapy. *American journal of respiratory and critical care medicine*, 160(1), pp.203–210.

Diacon, A.H. et al., 2010. Time to detection of the growth of Mycobacterium tuberculosis in MGIT 960 for determining the early bactericidal activity of antituberculosis agents. *European journal of clinical microbiology & infectious diseases : official publication of the European Society of Clinical Microbiology*, 29(12), pp.1561–1565.

Dickinson, J.M., Ellard, G.A. & Mitchison, D.A., 1968. Suitability of isoniazid and ethambutol for intermittent administration in the treatment of tuberculosis. *Tubercle*, 49(4), pp.351–366.

Djoba Siawaya, J.F. et al., 2008. Immune parameters as markers of tuberculosis extent of disease and early prediction of anti-tuberculosis chemotherapy response. *Journal of Infection*, 56(5), pp.340–347.

Domagk, G., Offe, H.A. & Siefken, W., 1952. [Additional investigations in experimental chemotherapy of tuberculosis (neoteban)]. *Deutsche medizinische Wochenschrift (1946)*, 77(18), pp.573–578.

Donald, P.R. & van Helden, P.D., 2011. *Antituberculosis Chemotherapy*, Karger Medical

and Scientific Publishers.

Donald, P.R. et al., 2006. Ethambutol dosage for the treatment of children: literature review and recommendations. *The international journal of tuberculosis and lung disease : the official journal of the International Union against Tuberculosis and Lung Disease*, 10(12), pp.1318–1330.

Donald, P.R. et al., 1997. The early bactericidal activity of isoniazid related to its dose size in pulmonary tuberculosis. *American journal of respiratory and critical care medicine*, 156(3 Pt 1), pp.895–900.

Donald, P.R. et al., 2004. The influence of human N-acetyltransferase genotype on the early bactericidal activity of isoniazid. *Clinical infectious diseases : an official publication of the Infectious Diseases Society of America*, 39(10), pp.1425–1430.

Doster, B. et al., 1973. Ethambutol in the initial treatment of pulmonary tuberculosis. U.S. Public Health Service tuberculosis therapy trials. *The American review of respiratory disease*, 107(2), pp.177–190.

Ellard, G.A., 1984. The potential clinical significance of the isoniazid acetylator phenotype in the treatment of pulmonary tuberculosis. *Tubercle*, 65(3), pp.211–227.

Elmendorf, D.F. et al., 1952. The absorption, distribution, excretion, and short-term toxicity of isonicotinic acid hydrazide (nydrazid) in man. *American review of tuberculosis*, 65(4), pp.429–442.

Epstein, M.D. et al., 1998. Time to Detection of Mycobacterium Tuberculosis in Sputum Culture Correlates With Outcome in Patients Receiving Treatment for Pulmonary Tuberculosis. *Chest*, 113(2), pp.379–386.

Erickson, A.E. & Spoerri, P.E., 1946. Syntheses in the pyrazine series; the preparation and properties of the pyrazyl halides. *Journal of the American Chemical Society*, 68, pp.400–402.

Ernst, J.D., 2012. The immunological life cycle of tuberculosis. *Nature reviews. Immunology*, 12(8), pp.581–591.

Escuyer, V.E. et al., 2001. The role of the embA and embB gene products in the biosynthesis of the terminal hexaarabinofuranosyl motif of Mycobacterium smegmatis arabinogalactan. *The Journal of biological chemistry*, 276(52), pp.48854–48862.

Eugen-Olsen, J. et al., 2002. The serum level of soluble urokinase receptor is elevated in tuberculosis patients and predicts mortality during treatment: a community study from Guinea-Bissau.

Forbes, B.A., 2017. Mycobacterial Taxonomy. C. S. Kraft, ed. *Journal of clinical microbiology*, 55(2), pp.380–383.

Fox, W., Ellard, G.A. & Mitchison, D.A., 1999. Studies on the treatment of tuberculosis undertaken by the British Medical Research Council tuberculosis units, 1946-1986, with relevant subsequent publications. *The international journal of tuberculosis and lung disease : the official journal of the International Union against Tuberculosis and Lung Disease*, 3(10 Suppl 2), pp.S231–79.

Fox, W., SUTHERLAND, I. & Daniels, M., 1954. A five-year assessment of patients in a controlled trial of streptomycin in pulmonary tuberculosis; report to the Tuberculosis Chemotherapy Trials Committee of the Medical Research Council. *The Quarterly journal of medicine*, 23(91), pp.347–366.

Friedrich, S.O. et al., 2013. Assessment of the sensitivity and specificity of Xpert MTB/RIF assay as an early sputum biomarker of response to tuberculosis treatment. *The Lancet. Respiratory medicine*, 1(6), pp.462–470.

Furesz, S. et al., 1967. Rifampicin: a new rifamycin. 3. Absorption, distribution, and elimination in man. *Arzneimittel-Forschung*, 17(5), pp.534–537.

Ghora, B.K. & Apirion, D., 1979. Identification of a novel RNA molecule in a new RNA processing mutant of Escherichia coli which contains 5 S rRNA sequences. *The Journal of biological chemistry*, 254(6), pp.1951–1956.

Gillespie, S.H., Gosling, R.D. & Charalambous, B.M., 2002. A reiterative method for calculating the early bactericidal activity of antituberculosis drugs. *American journal of respiratory and critical care medicine*, 166(1), pp.31–35.

Goodridge, A. et al., 2012. Anti-phospholipid antibody levels as biomarker for monitoring tuberculosis treatment response. *Tuberculosis*, 92(3), pp.243–247.

Goutelle, S. et al., 2009. Population modeling and Monte Carlo simulation study of the pharmacokinetics and antituberculosis pharmacodynamics of rifampin in lungs. *Antimicrobial agents and chemotherapy*, 53(7), pp.2974–2981.

Grigg, E.R., 1958. The arcana of tuberculosis with a brief epidemiologic history of the disease in the U.S.A. IV. *American review of tuberculosis*, 78(4), pp.583–603.

GRONDEK, J.F. & CULVER, G.M., 2004. Assembly of the 30S ribosomal subunit: positioning ribosomal protein S13 in the S7 assembly branch. *Rna*, 10(12), pp.1861–1866.

Grosset, J., 1980. Bacteriologic basis of short-course chemotherapy for tuberculosis. *Clinics in chest medicine*, 1(2), pp.231–241.

Grosset, J., 1978. The sterilizing value of rifampicin and pyrazinamide in experimental short-course chemotherapy. *Bulletin of the International Union against Tuberculosis*, 53(1), pp.5–12.

Gumbo, T. et al., 2007. Isoniazid bactericidal activity and resistance emergence: integrating pharmacodynamics and pharmacogenomics to predict efficacy in different ethnic populations. *Antimicrobial agents and chemotherapy*, 51(7), pp.2329–2336.

Gumbo, T. et al., 2009. Pharmacokinetics-pharmacodynamics of pyrazinamide in a novel in vitro model of tuberculosis for sterilizing effect: a paradigm for faster assessment of new antituberculosis drugs. *Antimicrobial agents and chemotherapy*, 53(8), pp.3197–3204.

Gumbo, T., Angulo-Barturen, I. & Ferrer-Bazaga, S., 2015. Pharmacokinetic-pharmacodynamic and dose-response relationships of antituberculosis drugs: recommendations and standards for industry and academia. *The Journal of*

infectious diseases, 211 Suppl 3(suppl 3), pp.S96–S106.

Gutierrez, M.C. et al., 2005. Ancient origin and gene mosaicism of the progenitor of Mycobacterium tuberculosis. *PLoS pathogens*, 1(1), p.e5.

Helb, D. et al., 2010. Rapid detection of Mycobacterium tuberculosis and rifampin resistance by use of on-demand, near-patient technology. *Journal of clinical microbiology*, 48(1), pp.229–237.

Held, W.A. et al., 1974. Assembly mapping of 30 S ribosomal proteins from Escherichia coli. Further studies. *The Journal of biological chemistry*, 249(10), pp.3103–3111.

Hershkovitz, I. et al., 2008. Detection and molecular characterization of 9,000-year-old Mycobacterium tuberculosis from a Neolithic settlement in the Eastern Mediterranean. N. Ahmed, ed. *PloS one*, 3(10), p.e3426.

Hesseling, A.C. et al., 2010. Baseline sputum time to detection predicts month two culture conversion and relapse in non-HIV-infected patients. *The international journal of tuberculosis and lung disease : the official journal of the International Union against Tuberculosis and Lung Disease*, 14(5), pp.560–570.

Honeyborne, I. et al., 2011. Molecular bacterial load assay, a culture-free biomarker for rapid and accurate quantification of sputum Mycobacterium tuberculosis bacillary load during treatment. *Journal of clinical microbiology*, 49(11), pp.3905–3911.

Honeyborne, I. et al., 2014. The molecular bacterial load assay replaces solid culture for measuring early bactericidal response to antituberculosis treatment. *Journal of clinical microbiology*, 52(8), pp.3064–3067.

Hosp, M. et al., 1997. Neopterin, β 2-microglobulin, and acute phase proteins in HIV-1-seropositive and-seronegative Zambian patients with tuberculosis. *Lung*.

Ignatov, D.V. et al., 2015. Dormant non-culturable Mycobacterium tuberculosis retains stable low-abundant mRNA. *BMC genomics*, 16(1), p.954.

Immanuel, C. et al., 2001. Serial evaluation of serum neopterin in HIV seronegative patients treated for tuberculosis.

Jayakumar, A. et al., 2016. Xpert MTB/RIF Assay Shows Faster Clearance of Mycobacterium tuberculosis DNA with Higher Levels of Rifapentine Exposure. G. A. Land, ed. *Journal of clinical microbiology*, 54(12), pp.3028–3033.

Jayaram, R. et al., 2003. Pharmacokinetics-pharmacodynamics of rifampin in an aerosol infection model of tuberculosis. *Antimicrobial agents and chemotherapy*, 47(7), pp.2118–2124.

Jin Hwa Lee, J.H.C., 2003. Changes of Plasma Interleukin-1 Receptor Antagonist, Interleukin-8 and other Serologic Markers during Chemotherapy in Patients with Active Pulmonary Tuberculosis. *The Korean journal of internal medicine*, 18(3), pp.138–145.

Josefsen, M.H. et al., 2010. Rapid quantification of viable Campylobacter bacteria on chicken carcasses, using real-time PCR and propidium monoazide treatment, as a tool for quantitative risk assessment. *Applied and Environmental Microbiology*, 76(15), pp.5097–5104.

King, T.C. & Schlessinger, D., 1983. S1 nuclease mapping analysis of ribosomal RNA processing in wild type and processing deficient Escherichia coli. *The Journal of biological chemistry*, 258(19), pp.12034–12042.

King, T.C., Sirdeskmukh, R. & Schlessinger, D., 1986. Nucleolytic processing of ribonucleic acid transcripts in procaryotes. *Microbiological reviews*, 50(4), pp.428–451.

Kinzig-Schippers, M. et al., 2005. Should we use N-acetyltransferase type 2 genotyping to personalize isoniazid doses? *Antimicrobial agents and chemotherapy*, 49(5), pp.1733–1738.

KoMINE, Y. et al., 1994. A tRNA-like structure is present in 10Sa RNA, a small stable RNA from Escherichia coli. *Proceedings of the National Academy of Sciences of the United States of America*, 91(20), pp.9223–9227.

Kralik, P., Nocker, A. & Pavlik, I., 2010. Mycobacterium avium subsp. paratuberculosis viability determination using F57 quantitative PCR in combination with propidium monoazide treatment. *International journal of food microbiology*, 141, pp.S80–S86.

Kushner, S. & Dalalian, H., 1948. Experimental chemotherapy of tuberculosis; substituted nicotinamides. *The Journal of organic chemistry*, 13(6), pp.834–836.

Lawn, S.D. & Gupta-Wright, A., 2016. Detection of lipoarabinomannan (LAM) in urine is indicative of disseminated TB with renal involvement in patients living with HIV and advanced immunodeficiency: evidence and implications. *Transactions of the Royal Society of Tropical Medicine and Hygiene*, 110(3), pp.180–185.

Leibold, J.E., 1966. The ocular toxicity of ethambutol and its relation to dose. *Annals of the New York Academy of Sciences*, 135(2), pp.904–909.

Lenaerts, A., Barry, C.E. & Dartois, V., 2015. Heterogeneity in tuberculosis pathology, microenvironments and therapeutic responses. *Immunological reviews*, 264(1), pp.288–307.

Li, Z., Pandit, S. & Deutscher, M.P., 1999a. Maturation of 23S ribosomal RNA requires the exoribonuclease RNase T. *Rna*, 5(1), pp.139–146.

Li, Z., Pandit, S. & Deutscher, M.P., 1999b. RNase G (CafA protein) and RNase E are both required for the 5′ maturation of 16S ribosomal RNA. *The EMBO journal*, 18(10), pp.2878–2885.

Long, M.W., Snider, D.E. & Farer, L.S., 1979. U.S. Public Health Service Cooperative trial of three rifampin-isoniazid regimens in treatment of pulmonary tuberculosis. *The American review of respiratory disease*, 119(6), pp.879–894.

Lu, C. et al., 2013. A systematic review of reported cost for smear and culture tests during multidrug-resistant tuberculosis treatment. J. L. Herrmann, ed. *PloS one*, 8(2), p.e56074.

Ma, Z. et al., 2010. Global tuberculosis drug development pipeline: the need and the reality. *Lancet (London, England)*, 375(9731), pp.2100–2109.

Malherbe, S.T. et al., 2016. Persisting positron emission tomography lesion activity and Mycobacterium tuberculosis mRNA after tuberculosis cure. *Nature medicine*,

22(10), pp.1094–1100.

Martinez, V. et al., 2012. 18F-FDG PET/CT in tuberculosis: an early non-invasive marker of therapeutic response. *The international journal of tuberculosis and lung disease : the official journal of the International Union against Tuberculosis and Lung Disease*, 16(9), pp.1180–1185.

McKenzie, D. & Malone, L., 1948. The effect of nicotinic acid amide on experimental tuberculosis of white mice. *The Journal of laboratory and clinical medicine*, 33(10), pp.1249–1253.

Mizushima, S. & Nomura, M., 1970. Assembly Mapping of 30S Ribosomal Proteins from E. coli. *Nature*, 226(5252), pp.1214–1218.

Moore, D.F. et al., 1996. Amplification of rRNA for assessment of treatment response of pulmonary tuberculosis patients during antimicrobial therapy. *Journal of clinical microbiology*, 34(7), pp.1745–1749.

Moore, S.D. & Sauer, R.T., 2005. Ribosome rescue: tmRNA tagging activity and capacity in Escherichia coli. *Molecular microbiology*, 58(2), pp.456–466.

Murray, J.S. et al., 1999. The use of plasma HIV RNA as a study endpoint in efficacy trials of antiretroviral drugs. *AIDS (London, England)*, 13(7), pp.797–804.

Mzinza, D.T. et al., 2015. Kinetics of Mycobacterium tuberculosis-specific IFN-γ responses and sputum bacillary clearance in HIV-infected adults during treatment of pulmonary tuberculosis. *Tuberculosis (Edinburgh, Scotland)*, 95(4), pp.463–469.

Nocker, A., Cheung, C.-Y. & Camper, A.K., 2006. Comparison of propidium monoazide with ethidium monoazide for differentiation of live vs. dead bacteria by selective removal of DNA from dead cells. *Journal of microbiological methods*, 67(2), pp.310–320.

O'Brien, W.A. et al., 1997. Changes in plasma HIV RNA levels and CD4+ lymphocyte counts predict both response to antiretroviral therapy and therapeutic failure. VA Cooperative Study Group on AIDS. *Annals of internal medicine*, 126(12), pp.939–945.

O'Brien, W.A. et al., 1996. Changes in plasma HIV-1 RNA and CD4+ lymphocyte counts and the risk of progression to AIDS. Veterans Affairs Cooperative Study Group on AIDS. *The New England journal of medicine*, 334(7), pp.426–431.

Pallanza, R. et al., 1967. Rifampicin: a new rifamycin. II. Laboratory studies on the antituberculous activity and preliminary clinical observations. *Arzneimittel-Forschung*, 17(5), pp.529–534.

Parkin, D.P. et al., 1997. Trimodality of isoniazid elimination: phenotype and genotype in patients with tuberculosis. *American journal of respiratory and critical care medicine*, 155(5), pp.1717–1722.

Pasipanodya, J. & Gumbo, T., 2011. An oracle: antituberculosis pharmacokinetics-pharmacodynamics, clinical correlation, and clinical trial simulations to predict the future. *Antimicrobial agents and chemotherapy*, 55(1), pp.24–34.

Pasipanodya, J.G. & Gumbo, T., 2010. Clinical and toxicodynamic evidence that high-dose pyrazinamide is not more hepatotoxic than the low doses currently used.

Antimicrobial agents and chemotherapy, 54(7), pp.2847–2854.

Pasipanodya, J.G. et al., 2013. Serum drug concentrations predictive of pulmonary tuberculosis outcomes. *The Journal of infectious diseases*, 208(9), pp.1464–1473.

Pasipanodya, J.G., Srivastava, S. & Gumbo, T., 2012. Meta-analysis of clinical studies supports the pharmacokinetic variability hypothesis for acquired drug resistance and failure of antituberculosis therapy. *Clinical infectious diseases : an official publication of the Infectious Diseases Society of America*, 55(2), pp.169–177.

Perrin, F.M.R. et al., 2007. Biomarkers of treatment response in clinical trials of novel antituberculosis agents. *The Lancet. Infectious diseases*, 7(7), pp.481–490.

Perrin, F.M.R. et al., 2010. Radiological cavitation, sputum mycobacterial load and treatment response in pulmonary tuberculosis. *The international journal of tuberculosis and lung disease : the official journal of the International Union against Tuberculosis and Lung Disease*, 14(12), pp.1596–1602.

Pheiffer, C. et al., 2008. Time to detection of Mycobacterium tuberculosis in BACTEC systems as a viable alternative to colony counting. *The international journal of tuberculosis and lung disease : the official journal of the International Union against Tuberculosis and Lung Disease*, 12(7), pp.792–798.

Philips, J.A. & Ernst, J.D., 2012. Tuberculosis pathogenesis and immunity. *Annual review of pathology*, 7(1), pp.353–384.

Pholwat, S. et al., 2012. Real-time PCR using mycobacteriophage DNA for rapid phenotypic drug susceptibility results for Mycobacterium tuberculosis. *Journal of clinical microbiology*, 50(3), pp.754–761.

Poole, G., Stradling, P. & Worlledge, S., 1971. Potentially serious side effects of high-dose twice-weekly rifampicin. *British medical journal*, 3(5770), pp.343–347.

RATCLIFFE, H.L. & MERRICK, J.V., 1957. Tuberculosis induced by droplet nuclei infection; its developmental pattern in guinea pigs and rats in relation to dietary protein. *The American journal of pathology*, 33(6), pp.1121–1135.

RAY, B.K. & Apirion, D., 1979. Characterization of 10S RNA: a new stable RNA molecule from Escherichia coli. *Molecular and General Genetics MGG*.

Rebollo, M.J. et al., 2006. Blood and urine samples as useful sources for the direct detection of tuberculosis by polymerase chain reaction. *Diagnostic Microbiology and Infectious Disease*, 56(2), pp.141–146.

Refaii, Al, A. & Alix, J.H., 2009. Ribosome biogenesis is temperature-dependent and delayed in Escherichia coli lacking the chaperones DnaK or DnaJ. *Molecular microbiology*, 71(3), pp.748–762.

Ribeiro-Rodrigues, R. et al., 2002. Sputum cytokine levels in patients with pulmonary tuberculosis as early markers of mycobacterial clearance. *Clinical and Diagnostic Laboratory Immunology*, 9(4), pp.818–823.

Rozwarski, D.A. et al., 1998. Modification of the NADH of the isoniazid target (InhA) from Mycobacterium tuberculosis. *Science (New York, N.Y.)*, 279(5347), pp.98–102.

Rudi, K. et al., 2005. Use of ethidium monoazide and PCR in combination for quantification of viable and dead cells in complex samples. *Applied and Environmental Microbiology*, 71(2), pp.1018–1024.

Ruslami, R. et al., 2007. Pharmacokinetics and tolerability of a higher rifampin dose versus the standard dose in pulmonary tuberculosis patients. *Antimicrobial agents and chemotherapy*, 51(7), pp.2546–2551.

Rustomjee, R. et al., 2008. A Phase II study of the sterilising activities of ofloxacin, gatifloxacin and moxifloxacin in pulmonary tuberculosis. *The international journal of tuberculosis and lung disease : the official journal of the International Union against Tuberculosis and Lung Disease*, 12(2), pp.128–138.

Sabiiti, W. et al., 2016. Optimising molecular diagnostic capacity for effective control of tuberculosis in high-burden settings. *The international journal of tuberculosis and lung disease : the official journal of the International Union against Tuberculosis and Lung Disease*, 20(8), pp.1004–1009.

Sahota, T. & Pasqua, Della, O., 2012. Feasibility of a fixed-dose regimen of pyrazinamide and its impact on systemic drug exposure and liver safety in patients with tuberculosis. *Antimicrobial agents and chemotherapy*, 56(11), pp.5442–5449.

Sakula, A., 1979. *Robert Koch (1843--1910): founder of the science of bacteriology and discoverer of the tubercle bacillus. A study of his life and work*,

Scotland, H.P., 2016.

Enhanced Surveillance of Mycobacterial Infections (ESMI) in Scotland: 2016 tuberculosis annual report for Scotland.

Scott, G.M., Murphy, P.G. & Gemidjioglu, M.E., 1990. Predicting deterioration of treated tuberculosis by corticosteroid reserve and C-reactive protein. *Journal of Infection*, 21(1), pp.61–69.

Sechi, L.A. et al., 1997. Detection ofMycobacterium tuberculosisby PCR analysis of urine and other clinical samples from AIDS and non-HIV-infected patients. *Molecular and Cellular Probes*, 11(4), pp.281–285.

Seifart, H.I. et al., 2001. Population screening for isoniazid acetylator phenotype. *Pharmacoepidemiology and drug safety*, 10(2), pp.127–134.

Selikoff, I.J., Robitzek, E.H. & Ornstein, G.G., 1952. Treatment of pulmonary tuberculosis with hydrazide derivatives of isonicotinic acid. *Journal of the American Medical Association*, 150(10), pp.973–980.

Sloan, D.J. et al., 2015. Pharmacodynamic Modeling of Bacillary Elimination Rates and Detection of Bacterial Lipid Bodies in Sputum to Predict and Understand Outcomes in Treatment of Pulmonary Tuberculosis. *Clinical infectious diseases : an official publication of the Infectious Diseases Society of America*, 61(1), pp.1–8.

Smith, T., 1898. A COMPARATIVE STUDY OF BOVINE TUBERCLE BACILLI AND OF HUMAN BACILLI FROM SPUTUM. *The Journal of experimental medicine*, 3(4-5), pp.451–511.

Soejima, T. et al., 2008. Method To Detect Only Live Bacteria during PCR Amplification.

Journal of clinical microbiology, 46(7), pp.2305–2313.

Srivastava, S. et al., 2010. Efflux-pump-derived multiple drug resistance to ethambutol monotherapy in Mycobacterium tuberculosis and the pharmacokinetics and pharmacodynamics of ethambutol. *The Journal of infectious diseases*, 201(8), pp.1225–1231.

Steingart, K.R. et al., 2011. Higher-dose rifampin for the treatment of pulmonary tuberculosis: a systematic review. *The international journal of tuberculosis and lung disease : the official journal of the International Union against Tuberculosis and Lung Disease*, 15(3), pp.305–316.

Sydes, M.R. et al., 2009. Issues in applying multi-arm multi-stage methodology to a clinical trial in prostate cancer: the MRC STAMPEDE trial. *Trials*, 10(1), p.39.

Thomas, J.P. et al., 1961. A new synthetic compound with antituberculous activity in mice: ethambutol (dextro-2,2'-(ethylenediimino)-di-l-butanol). *The American review of respiratory disease*, 83, pp.891–893.

Tissieres, A. & Watson, J.D., 1958. Ribonucleoprotein particles from Escherichia coli. *Nature*.

Tortoli, E., 2012. Phylogeny of the genus Mycobacterium: many doubts, few certainties. *Infection, genetics and evolution : journal of molecular epidemiology and evolutionary genetics in infectious diseases*, 12(4), pp.827–831.

Traub, P. & Nomura, M., 1968. Structure and function of E. coli ribosomes. V. Reconstitution of functionally active 30S ribosomal particles from RNA and proteins. *… of the National Academy of Sciences*.

Tu, G.F. et al., 1995. C-terminal extension of truncated recombinant proteins in Escherichia coli with a 10Sa RNA decapeptide. *The Journal of biological chemistry*, 270(16), pp.9322–9326.

Van der Vliet, G.M. et al., 1994. Assessment of mycobacterial viability by RNA amplification. *Antimicrobial agents and chemotherapy*, 38(9), pp.1959–1965.

van Ingen, J. et al., 2011. Why Do We Use 600 mg of Rifampicin in Tuberculosis Treatment? *Clinical infectious diseases : an official publication of the Infectious Diseases Society of America*, 52(9), pp.e194–9.

Wallis, R.S. et al., 1999. Drug tolerance in Mycobacterium tuberculosis. *Antimicrobial agents and chemotherapy*, 43(11), pp.2600–2606.

Wallis, R.S. et al., 1998. Induction of the Antigen 85 Complex of Mycobacterium tuberculosis in Sputum: A Determinant of Outcome in Pulmonary Tuberculosis Treatment. *The Journal of infectious diseases*, 178(4), pp.1115–1121.

Wallis, R.S. et al., 2012. Predicting the Outcome of Therapy for Pulmonary Tuberculosis. *American journal of respiratory and critical care medicine*, 161(4), pp.1076–1080.

Wallis, R.S., Peppard, T. & Hermann, D., 2015. Month 2 culture status and treatment duration as predictors of recurrence in pulmonary tuberculosis: model validation and update. L. E. Via, ed. *PloS one*, 10(4), p.e0125403.

Weiner, M. et al., 2010. Evaluation of time to detection of Mycobacterium tuberculosis in broth culture as a determinant for end points in treatment trials. *Journal of clinical microbiology*, 48(12), pp.4370–4376.

WELLS, A.Q., 1949. Vaccination with the murine type of tubercle bacillus (vole bacillus). *Lancet (London, England)*, 2(6567), pp.53–55.

Wolinsky, E., Smith, M.M. & Steenken, W., 1956. Isoniazid susceptibility, catalase activity, and guinea pig virulence of recently isolated cultures of tubercle bacilli. *American review of tuberculosis*, 73(5), pp.768–772.

Wood, R. et al., 2012. Lipoarabinomannan in urine during tuberculosis treatment: association with host and pathogen factors and mycobacteriuria. *BMC Infectious Diseases*, 12(1), p.47.

World Health Organization, 2016. Global tuberculosis report 2016.

World Health Organization, 2010. *Treatment of Tuberculosis*, World Health Organization.

Yeager, R.L., Munroe, W.G.C. & Dessau, F.I., 1952. Pyrazinamide (aldinamide) in the treatment of pulmonary tuberculosis. *American review of tuberculosis*, 65(5), pp.523–546.

Yuan, S. et al., 2012. Evaluation of methods for the extraction and purification of DNA from the human microbiome. J. A. Gilbert, ed. *PloS one*, 7(3), p.e33865.

Zhang, M. et al., 2011. Treatment of tuberculosis with rifamycin-containing regimens in immune-deficient mice. *American journal of respiratory and critical care medicine*, 183(9), pp.1254–1261.

Zumla, A., Nahid, P. & Cole, S.T., 2013. Advances in the development of new tuberculosis drugs and treatment regimens. *Nature reviews. Drug discovery*, 12(5), pp.388–404.

Zumla, A.I. et al., 2014. New antituberculosis drugs, regimens, and adjunct therapies: needs, advances, and future prospects. *The Lancet. Infectious diseases*, 14(4), pp.327–340.